



Soluble endoglin and hypercholesterolemia aggravate endothelial and vessel wall dysfunction in mouse aorta



Barbora Vitverova^a, Katerina Blazickova^a, Iveta Najmanova^a, Matej Vicen^a, Radek Hyšpler^b, Eva Dolezelova^a, Ivana Nemeckova^a, Jurjen Duintjer Tebbens^c, Carmelo Bernabeu^d, Miguel Pericacho^e, Petr Nachtigal^{a,*}

^a Department of Biological and Medical Sciences, Faculty of Pharmacy in Hradec Kralove, Charles University, Heyrovského 1203, Hradec Kralove, 500 05, Czech Republic

^b Centrum for Research and Development, University Hospital, Hradec Kralove, Czech Republic

^c Department of Biophysics and Physical Chemistry, Faculty of Pharmacy in Hradec Kralove, Charles University, Heyrovského 1203, Hradec Kralove, 500 05, Czech Republic

^d Center for Biological Research, Spanish National Research Council (CSIC) and Biomedical Research Networking Center on Rare Diseases (CIBERER), 28040, Madrid, Spain

^e Biomedical Research Institute of Salamanca (IBSAL) and Renal and Cardiovascular Physiopathology Unit, Department of Physiology and Pharmacology, University of Salamanca, 37007, Salamanca, Spain

ARTICLE INFO

Article history:

Received 10 November 2017

Received in revised form

6 February 2018

Accepted 7 February 2018

Available online 9 February 2018

Keywords:

Soluble endoglin

Endothelial dysfunction

eNOS

Vascular reactivity

Mice

ABSTRACT

Background and aims: Increased plasma levels of soluble endoglin (sEng) were detected in patients with endothelial dysfunction-related disorders and hypercholesterolemia. In this study, we hypothesized that high levels of sEng accompanied by mild hypercholesterolemia could aggravate endothelial and vessel wall dysfunction and affect endoglin/eNOS signaling in mouse aorta.

Methods: Three-month-old female transgenic mice on CBAXC57BL/6J background, with high levels of sEng (*Sol-Eng*⁺ *high HFD*), and their littermates with low levels of sEng (*Sol-Eng*⁺ *low HFD*), were fed a high fat diet for six months. Plasma samples were used for biochemical, ELISA and Luminex analyses of total cholesterol, sEng and inflammatory markers. Functional parameters of aorta were assessed with wire myograph 620M. Western blot analyses of membrane endoglin/eNOS signaling and endothelial dysfunction/inflammation markers in aorta were performed.

Results: Functional analysis of aorta showed impaired KCl induced vasoconstriction, endothelial-dependent relaxation after the administration of acetylcholine as well as endothelial-independent relaxation induced by sodium nitroprusside in the *Sol-Eng*⁺ *high HFD* group compared to the *Sol-Eng*⁺ *low HFD* group. Ach-induced vasodilation after administration of L-NAME was significantly higher in the *Sol-Eng*⁺ *high HFD* group compared to the *Sol-Eng*⁺ *low HFD* group. The expression of endoglin, p-eNOS/eNOS, pSmad2/3/Smad2/3 signaling pathway was significantly lower in the *Sol-Eng*⁺ *high HFD* group compared to the *Sol-Eng*⁺ *low HFD* group.

Conclusions: The results indicate that long-term hypercholesterolemia combined with high levels of sEng leads to the aggravation of endothelial and vessel wall dysfunction in aorta, with possible alterations of the membrane endoglin/eNOS signaling, suggesting that high levels of soluble endoglin might be considered as a risk factor of cardiovascular diseases.

© 2018 Elsevier B.V. All rights reserved.

1. Introduction

Endoglin (Eng) is a 180-kDa homodimeric transmembrane glycoprotein, predominantly expressed in endothelial cells and

playing a key role in cardiovascular development, angiogenesis, vascular remodeling and homeostasis [1,2]. Eng is a co-receptor of the TGF- β receptor complex that interacts with TGF- β signaling receptors types I and II, and modulates cellular responses to TGF- β [3,4].

A soluble form of endoglin (sEng) is released from membrane bound Eng by proteolytic cleavage of its extracellular domain

* Corresponding author.

E-mail address: petr.nachtigal@faf.cuni.cz (P. Nachtigal).

during endothelial injury or inflammation and subsequently sEng enters the blood circulation [5,6]. Increased levels of sEng in plasma have been detected in patients with cardiovascular-related disorders like atherosclerosis [7,8], hypercholesterolemia [9], hypertension, type II diabetes mellitus [10] and preeclampsia, where sEng levels correlate with disease severity [11]. Because all these pathological conditions are associated with endothelial dysfunction, it was suggested that high levels of sEng could be considered as a biomarker of endothelial dysfunction and cardiovascular-related pathologies [12].

Endothelial dysfunction is considered as the first and key step in the development of atherosclerosis. It is mostly associated with an impairment of endothelial-dependent vasodilation mediated by nitric oxide (NO). The endothelium has a constitutive expression of NO catalyzed by endothelial nitric oxide synthase (eNOS) that is one of the most important factors leading to normal vascular relaxation [13,14]. Decreased expression of membrane Eng was demonstrated to be associated with lower NO-dependent vasodilation and reduced expression of eNOS [15–17]. In addition, it has been reported that Eng affects eNOS expression in endothelial cells via Smad2/3 transcription factors without involvement of TGF- β [18]. In addition, vascular endothelium controls vasodilation respectively vasoconstriction via myosin light chain kinase signaling in smooth muscles [19]. The phosphorylation of myosin light chain (MLC) is the main regulatory mechanism of smooth muscle contraction [20].

It is of interest to mention, that sEng was demonstrated to have potentially opposite effects on vascular endothelium as compared to membrane endoglin, resulting in inhibition of eNOS-dependent vasodilation [11] or higher expression of cell adhesion molecules [21]. Our previous studies in mice were focused on possible effects of sEng in the atherosclerosis prone aorta under the conditions of chow and high fat diet [22,23]. sEng alone did not induce any signs of endothelial dysfunction [23] but combination with hypercholesterolemia resulted in development of pro-inflammatory phenotype. However, this pathological condition was not accompanied by the induction of endothelial dysfunction [22].

Thus, in this study, we used the same transgenic mouse model expressing human sEng (*Sol-Eng*⁺) [24] to reveal whether longer exposure to sEng and hypercholesterolemia will result in functional alteration of aorta. We hypothesized that sEng aggravates endothelial and vessel wall dysfunctions in aorta that are primarily triggered by high fat diet.

2. Materials and methods

2.1. Animals and experimental design

Transgenic mice overexpressing human sEng (*Sol-Eng*⁺) on the CBAx57BL/6J background were generated at the Genetically Modified Organisms Generation Unit (University of Salamanca, Spain), as previously described [24]. Six-month-old female mice with low levels of sEng fed a chow rodent diet (*Sol-Eng*⁺ low chow) were used as control mice for biochemical analysis only. All other experiments were performed with three-month-old female mice with high plasma levels of sEng (*Sol-Eng*⁺ high HFD) (mice with sEng levels higher than 100 ng/mL were considered as *Sol-Eng*⁺ high HFD) and their age matched female transgenic littermates with low levels of sEng (*Sol-Eng*⁺ low HFD) fed a high fat rodent diet containing 1.25% of cholesterol and 40% of fat (Research Diets, Inc., USA) for the following 6 months. The animals were kept in controlled ambient conditions in a temperature-controlled room with a 12h–12h light–dark cycle with constant humidity and had access to tap water *ad libitum*. No weight differences were observed among experimental groups.

All experiments were carried out in accordance with the standards established in the directive of the EU (2010/63/EU) and all procedures were approved by the Ethical Committee for the protection of animals against cruelty at Faculty of Pharmacy, Charles University (Permit Number: 21558/2013–2), and the Bioethics Committee of the University of Salamanca (Permit Number: 006–201400038812). Mice were anesthetized with ketamine/xylazine, and all efforts were made to minimize the suffering of the animals.

2.2. ELISA and luminex assay

Blood samples were obtained from vena cava inferior and plasma levels of human sEng were determined by means of Human Endoglin/CD105 Quantikine ELISA Kit (R&D Systems, MN, USA) according to the manufacturer's instructions. Due to the specificity of the transgenic mouse model, the methodology of human sEng evaluation in plasma had to be adjusted for our studies (300-fold dilution of murine samples compared to typical 4-fold dilution in standard human studies). Plasma levels of intercellular adhesion molecule 1 (ICAM-1), monocyte chemoattractant protein 1 (MCP-1), P-selectin and tumor necrosis factor α (TNF α) were determined by means of Mouse Premixed Multi-Analyte Magnetic Luminex Kit (R&D Systems, MN, USA), according to the manufacturer's protocol. Concentrations were reported as nanograms per milliliter (ng/mL) for human sEng and picograms per milliliter (pg/mL) for ICAM-1, MCP-1, P-selectin and TNF α .

2.3. Biochemical analysis

Total concentration of plasma cholesterol was measured enzymatically by conventional enzymatic diagnostic kits (Lachema, Brno, Czech Republic) and spectrophotometric analysis (cholesterol at 510 nm, ULTROSPECT III, Pharmacia LKB Biotechnology, Uppsala, Sweden). Concentrations were reported as millimolar (mmol/L).

2.4. Immunohistochemistry

Serial sections of heart were cut until the aortic root containing semilunar valves together with aorta appeared. From this point on, serial cross-sections (7 μ m) were cut on a cryostat and placed on gelatin-coated slides. For fluorescence staining of macrophages/monocytes, slides were incubated with rat anti-mouse monoclonal primary antibody macrophages/monocytes (MOMA-2) (Bio-Rad Laboratories, CA, USA) at a dilution of 1:100 in 1% BSA for 1 h in room temperature. Goat anti-rat secondary antibody marked with green fluorochrome DyLight488 (Jackson ImmunoResearch, USA) was used at a dilution of 1:100 in 1% BSA for 30 min at room temperature to detect macrophages. For nuclear counterstaining, blue-fluorescent DAPI nucleic acid staining was used (Invitrogen, Czech Republic).

Photo documentation and image digitizing were performed by using a digital firewire camera Pixelink PL-A642 (Vitana Corporation, Ottawa, Canada) and a VDS Vosskuhler CD-1300QB monochromatic camera (VDS Vosskuhler GmbH, Germany) for fluorescence with image analysis software NIS (Laboratory Imaging, Czech Republic).

2.5. Functional analysis of vascular reactivity

On the day of the experiment, mice were anesthetized i.p. with a mixture of ketamine (100 mg/kg) and xylazine (16 mg/kg) and thoracic aortas were quickly removed, carefully dissected from surrounding tissue and immediately placed in Krebs-Henseleit solution. Connective and adipose tissue in the adventitia was

carefully removed, and the descending aorta was cut into 4 rings each approximately 3 mm long. The aortic rings were transferred to organ-bath chambers of the wire myograph (620M, Danish Myo Technology, Denmark) filled with 5 mL of Krebs-Henseleit solution. The rings were mounted between 2 pins, attached to an isometric force transducer with continuous recording of tension (PowerLab, LabChart, ADI Instruments, Australia) and gassed with 95% O₂ and 5% CO₂. The resting tension was stepwise increased to reach final 10 mN and then rings were incubated to equilibrate for 30 min at 37 °C. The vascular viability was verified by a contractile response to potassium chloride (KCl, 60 mM). After washing, the aortic rings were pre-contracted with increasing concentrations of prostaglandin F₂ alpha (PGF₂α, 0.001–1 μM) to reach approximately 80% of KCl-induced contraction. After reaching a stable plateau phase, the endothelium-dependent relaxation was induced by a cumulative concentration of acetylcholine (Ach, 0.001–1 μM). For the endothelium-independent relaxation, a cumulative concentration-dependent response for sodium nitroprusside (SNP, 0.001–1 μM) was induced. Effect of NO production on vascular reactivity was measured by analyzing the Ach effect in the presence of the nitric oxide synthase inhibitor N (ω)-nitro-L-arginine methyl ester (L-NAME, 300 μM). Between each concentration-response curve, the rings were washed three times with Krebs-Henseleit solution and left to stabilize.

2.6. Western blot analysis

Samples of aortas were homogenized in RIPA lysis buffer (Sigma-Aldrich, St. Louis, USA) supplemented with protease (SERVA Electrophoresis, Germany) and phosphatase (Thermo Fisher Scientific Inc., IL, USA) inhibitors, as described previously [23]. Homogenates (20 μg of total protein) were separated by sodium dodecyl sulfate-polyacrylamide gel electrophoresis, transferred onto PVDF membrane (Millipore, NY, USA), and incubated with appropriate antibodies (Supplemental Table 1). Horseradish peroxidase-conjugated secondary antibodies were from Sigma-Aldrich Co. (St. Louis, USA) as described previously [23]. Membranes were developed using enhanced chemiluminescent reagents (Thermo Fisher Scientific Inc., IL, USA) and exposed to X-Ray films (Foma, Czech Republic). Densitometric quantification of immunoreactive bands was performed by image analysis software NIS (Laboratory Imaging, Prague, Czech Republic). Protein specific signals in each lane were normalized to GAPDH signal.

2.7. Statistical analysis

The statistical analysis was performed by GraphPad Prism 7.0 software (GraphPad Software, Inc., CA, USA). All data are presented as mean ± S.E.M. All multiple comparison data were analyzed using ANOVA with Tukey's multiple comparisons test. Direct group-group comparisons were carried out using non-parametric Mann-Whitney test because D'Agostino & Pearson omnibus normality test failed. *p* values of 0.05 or less were considered statistically significant.

3. Results

3.1. Plasma concentrations of human sEng, inflammatory markers and total cholesterol in Sol-Eng⁺ mice

Mice were fed a high fat diet (HFD) for 6 months and subsequently plasma samples were collected. Six-month-old female mice fed a chow rodent diet were used as control group with reference values of the lipid profile parameters. Biochemical analysis of plasma samples demonstrated significant differences in total

cholesterol concentration (1.84 ± 0.24 vs. 2.94 ± 0.10 mmol/L) between Sol-Eng⁺ low CHOW and Sol-Eng⁺ low HFD mice and between Sol-Eng⁺ high CHOW and Sol-Eng⁺ high HFD mice (1.83 ± 0.15 vs. 2.93 ± 0.10 mmol/L), respectively. Significantly higher concentration of total cholesterol was also observed in Sol-Eng⁺ high HFD mice (3.37 ± 0.23 mmol/L) compared to Sol-Eng⁺ low CHOW mice (1.84 ± 0.24 mmol/L) and in Sol-Eng⁺ high CHOW mice (1.83 ± 0.15 mmol/L) compared to Sol-Eng⁺ low HFD mice (2.93 ± 0.10 mmol/L). On the contrary, no differences were observed between Sol-Eng⁺ low HFD mice (2.93 ± 0.10 mmol/L) and Sol-Eng⁺ high HFD mice (2.93 ± 0.10 mmol/L) or between Sol-Eng⁺ low CHOW mice (1.84 ± 0.24 mmol/L) and Sol-Eng⁺ high CHOW mice (1.83 ± 0.15 mmol/L) (Fig. 1A). As shown in Fig. 1B, ELISA measurements showed that human sEng plasma concentrations were significantly higher in Sol-Eng⁺ high HFD mice (2796.00 ± 264.00 ng/mL) compared to Sol-Eng⁺ low HFD mice (7.40 ± 3.35 ng/mL).

Furthermore, Luminex assay showed no significant differences in levels of inflammatory markers ICAM-1 (4574.00 ± 276.00 vs. 4482.00 ± 664.00 pg/mL) and P-selectin (4434.00 ± 659.00 vs. 3935.00 ± 523.00 pg/mL) between studied groups. On the other hand, MCP-1 levels (88.70 ± 23.40 vs. 45.30 ± 7.67 pg/mL), and TNFα (0.62 ± 0.14 vs. 0.33 ± 0.08 pg/mL) were higher (borderline of statistical significance for MCP [*p* = 0.08] and for TNF-α [*p* = 0.06]) in Sol-Eng⁺ high HFD when compared to Sol-Eng⁺ low HFD female mice, respectively (Fig. 1C–F).

3.2. Impaired vascular reactivity in aortas from Sol-Eng⁺ high HFD mice

KCl, a calcium-sensitizing stimulus leading to increased cytosolic free Ca²⁺ concentration, was used in concentration 60 mM to assess the contractile maximal response. As shown in Fig. 2A, the maximal contraction achieved in response to KCl was significantly lower in Sol-Eng⁺ high HFD compared to Sol-Eng⁺ low HFD mice (2.83 ± 0.20 vs. 3.41 ± 0.20 , respectively). PGF₂α, a receptor-dependent vasoconstrictor, was used for pre-contraction of aortic rings prior to subsequent measurements. The maximal induced contraction after administration of PGF₂α (1 μM) was not significantly different between Sol-Eng⁺ high HFD and Sol-Eng⁺ low HFD mice ($64.70 \pm 9.26\%$ vs. $85.99 \pm 14.18\%$, respectively) (Fig. 2B).

For endothelium-dependent relaxation, the vasodilator response in PGF₂α pre-contracted aortic rings were induced by acetylcholine, a substance that mediates releasing of NO by binding to muscarinic receptors in endothelial cells. Significantly impaired relaxation was measured at 1 μM acetylcholine ($8.71 \pm 2.68\%$ vs. $21.00 \pm 5.11\%$, respectively) in Sol-Eng⁺ high HFD compared to Sol-Eng⁺ low HFD mice (Fig. 2C). Endothelium-independent relaxation induced by SNP, a donor of NO with capability to activate soluble guanylate cyclase in vascular smooth muscle, in PGF₂α pre-contracted aortic rings was significantly impaired at 1 μM SNP ($12.90 \pm 1.96\%$ vs. $23.50 \pm 1.42\%$, respectively) in Sol-Eng⁺ high HFD compared to Sol-Eng⁺ low HFD mice (Fig. 2D) as well. To evaluate whether vasodilation induced by acetylcholine was entirely eNOS-dependent, L-NAME as a direct inhibitor of eNOS was used. The effect of L-NAME on Ach-induced relaxation in PGF₂α pre-constricted vessels reached significantly higher values of vasodilation at 1 μM Ach ($40.90 \pm 15.10\%$ vs. $3.14 \pm 1.30\%$, respectively) in Sol-Eng⁺ high HFD compared to Sol-Eng⁺ low HFD mice (Fig. 2E), suggesting that Ach-induced vasodilation response was accompanied by additional compensatory NO releasing mechanisms. It is of interest to mention that endothelium-dependent relaxation and endothelium-independent relaxation induced by SNP were significantly lower compared to our previous study in mice fed by high fat diet for three months [22] suggesting alteration of endothelial

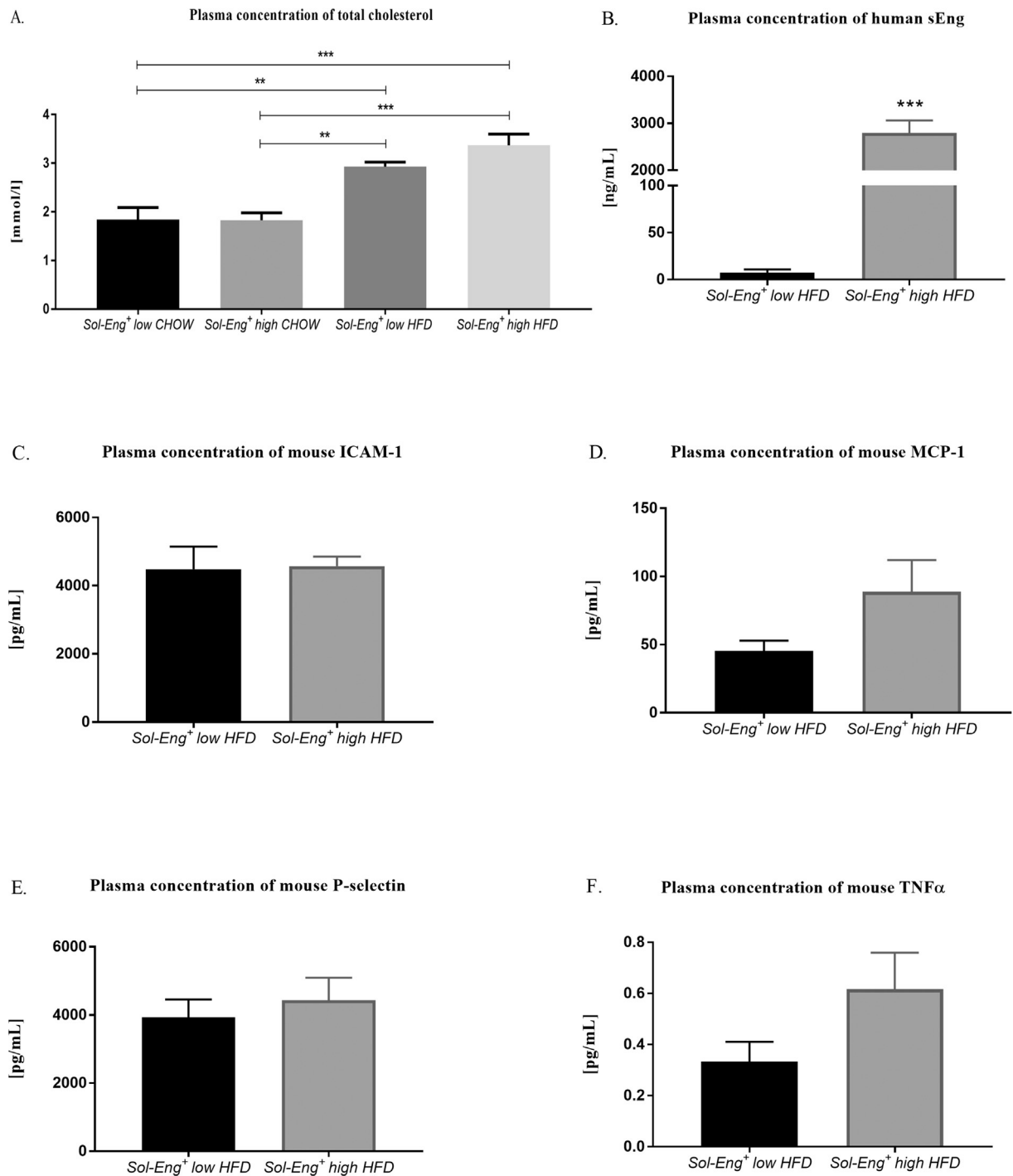


Fig. 1. Total cholesterol, soluble endoglin and inflammatory markers in plasma.

(A) Plasma concentration of total cholesterol in *Sol-Eng⁺ high CHOW* and *Sol-Eng⁺ low CHOW* mice fed a chow rodent diet and in *Sol-Eng⁺ high HFD* and *Sol-Eng⁺ low HFD* mice fed a high fat diet for 6 months. Human (B) sEng, (C) ICAM-1, (D) MCP-1, (E) P-selectin and (F) TNF α in *Sol-Eng⁺ high HFD* and *Sol-Eng⁺ low HFD* mice fed a high fat diet for 6 months. Data are shown as mean \pm S.E.M. Results in Fig. 1A are analyzed by ANOVA, followed by Tukey's multiple comparisons test, ** $p \leq 0.01$, *** $p \leq 0.001$. The following data are analyzed by Mann-Whitney test, *** $p \leq 0.001$. $n = 8$ mice per group.

function by high fat diet in both studied groups in the paper.

3.3. *Sol-Eng⁺ high HFD* mice do not develop pro-inflammatory phenotype in aorta

Western blot analysis of inflammatory markers related to endothelial dysfunction was performed. No significant differences

between *Sol-Eng⁺ high HFD* and *Sol-Eng⁺ low HFD* mice in the expression of VCAM-1 (Fig. 3A), ICAM-1 (Fig. 3B) and P-selectin (Fig. 3C) were observed.

The activation of nuclear factor kappa B (NF- κ B) is reported as a ratio of phosphorylated (active) form expression to the non-phosphorylated form expression. The activation of NF- κ B was not significantly different between *Sol-Eng⁺ high HFD* and *Sol-Eng⁺ low*

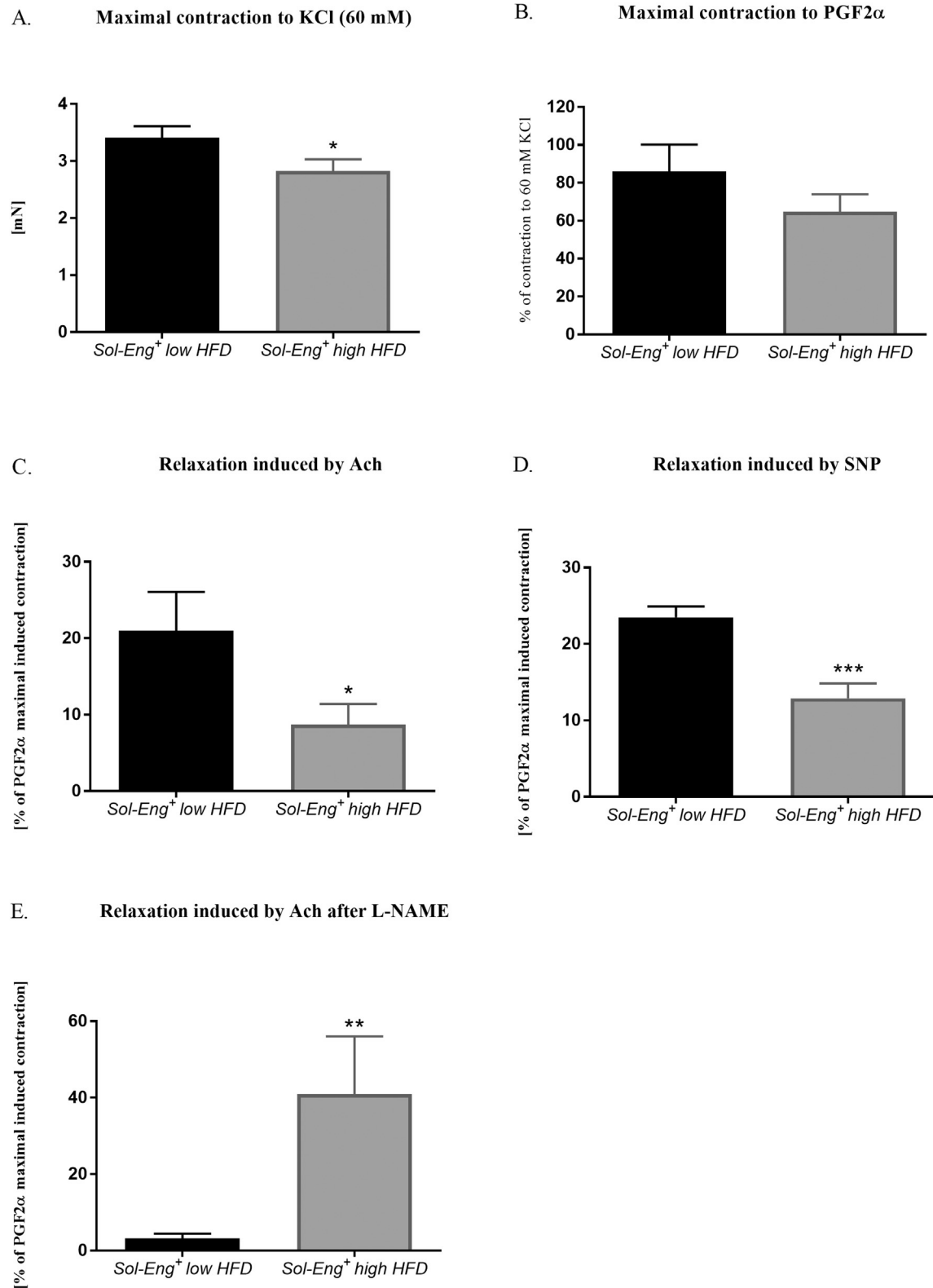


Fig. 2. Functional analysis of vascular reactivity by wire myograph in *Sol-Eng*⁺ high HFD and *Sol-Eng*⁺ low HFD mice.

(A) Maximal contraction to KCl (60 mM). (B) Maximal contraction to PGF2 α (1 μ M). (C) Acetylcholine-induced relaxation (1 μ M) in PGF2 α pre-constricted aortic rings. (D) SNP-induced relaxation (1 μ M) in PGF2 α pre-constricted aortic rings. (E) Inhibitory effect of L-NAME (at 1 μ M Ach) on eNOS-dependent Ach-induced relaxation in PGF2 α pre-constricted aortic rings. Data are shown as mean \pm S.E.M. We used Mann-Whitney U-tests (one-tailed, lower KCl, Ach and SNP means, resp. higher L-NAME means in *Sol-Eng*⁺ low HFD than in *Sol-Eng*⁺ high HFD are considered physically highly improbable), * $p \leq 0.05$, ** $p \leq 0.01$, *** $p \leq 0.001$. $n = 8$ mice per group.

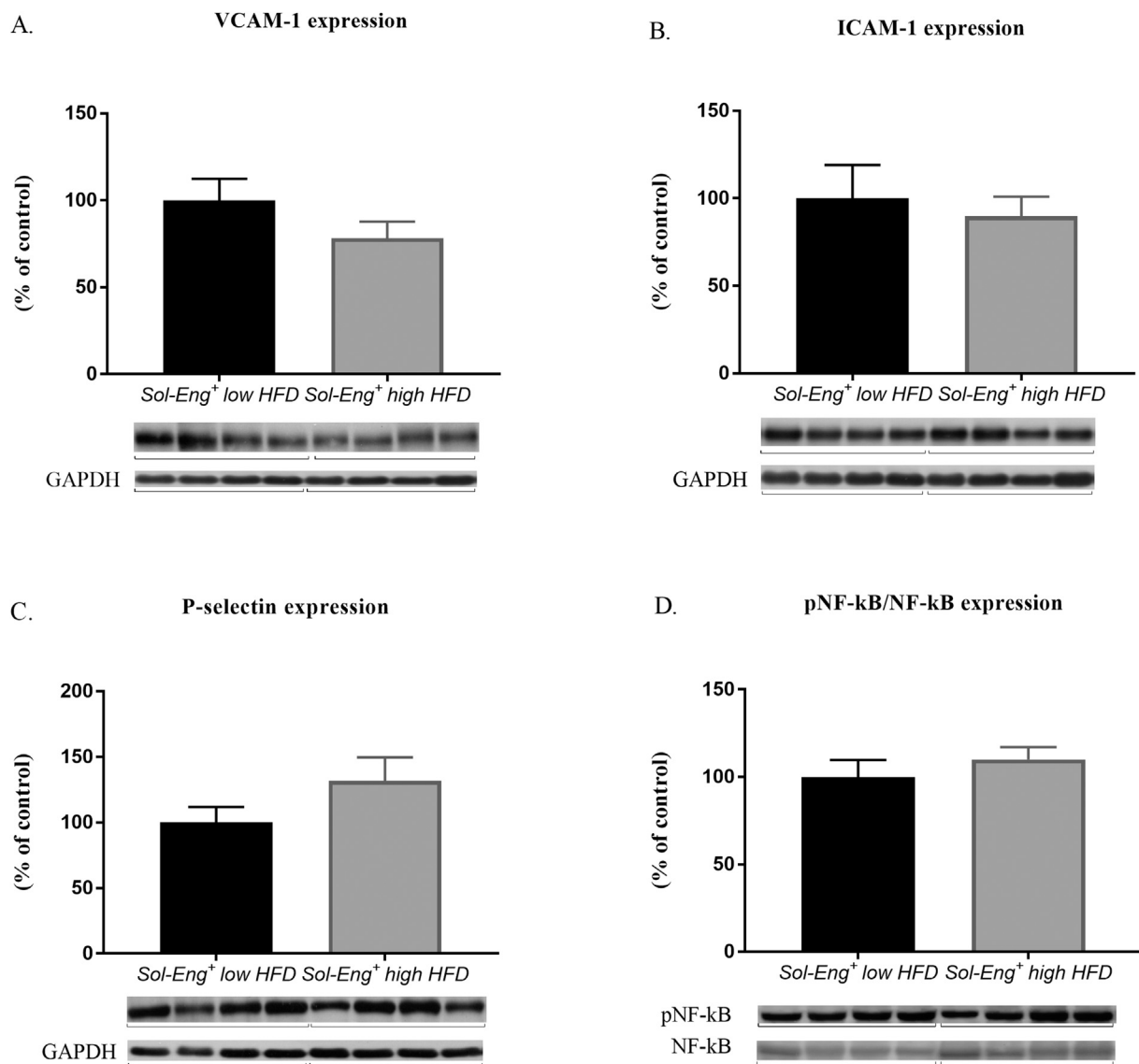


Fig. 3. Expression of inflammatory markers in aorta of *Sol-Eng*⁺ high HFD and *Sol-Eng*⁺ low HFD mice. Expression of (A) VCAM-1, (B) ICAM-1, (C) P-selectin and (D) pNF-κB/NF-κB in total protein extracts from mice aortas. Top panel: densitometric analysis (control = 100%). Densitometric quantification of immunoreactive bands was recalculated to the GAPDH signal. Bottom panel: representative immunoblots. Data are shown as mean ± S.E.M., Mann-Whitney test. n = 5 mice per group.

HFD mice as well (Fig. 3D).

3.4. Endoglin/eNOS signaling is altered in *Sol-Eng*⁺ high HFD mice

Regarding the fact that membrane endoglin signaling via Smad2/3 transcription factor was previously shown to be important in endothelial function, we analyzed the expression of membrane Eng, eNOS and its phosphorylated form *p*-eNOS Ser1177, as well as Smad2/3 and its phosphorylated form.

The expressions of eNOS and *p*-eNOS (Ser1177), Smad2/3 and *p*Smad2/3 are reported as a ratio of the phosphorylated form expression to its non-phosphorylated form expression. Significantly reduced expressions of membrane Eng (to 73%; Fig. 4A), *p*-eNOS Ser1177/e-NOS (to 55%; Fig. 4B) and *p*Smad2/3/Smad2/3 (to 63%; Fig. 4C) were observed in aortas of *Sol-Eng*⁺ high HFD mice compared to *Sol-Eng*⁺ low HFD mice.

3.5. *Sol-Eng*⁺ high HFD mice have impaired vasoconstriction in aorta but no prostacyclin synthase/cyclooxygenase type 2 compensation of altered eNOS-dependent vasodilation

Myosin light chain (MLC) is a major regulatory component in vascular smooth muscle contraction. To determine the phosphorylation (activation) of MLC, expression of phosphorylated MLC on residues threonine 18 and serine 19 (*p*MLC Thr18/Ser19) was assessed, as shown in Fig. 5A. Significantly lower expression of *p*MLC Thr18/19 (by 76%) was demonstrated in aortas of *Sol-Eng*⁺ high HFD mice compared to *Sol-Eng*⁺ low HFD mice.

Expression of prostaglandin I₂ synthase (PTGIS) also known as prostacyclin synthase (Fig. 5B) and cyclooxygenase type 2 (COX-2) (Fig. 5C) was measured to reveal potential compensation mechanisms leading to release of NO under pathological conditions. However, no statistical significant changes were observed in the expressions of either PTGIS or COX-2.

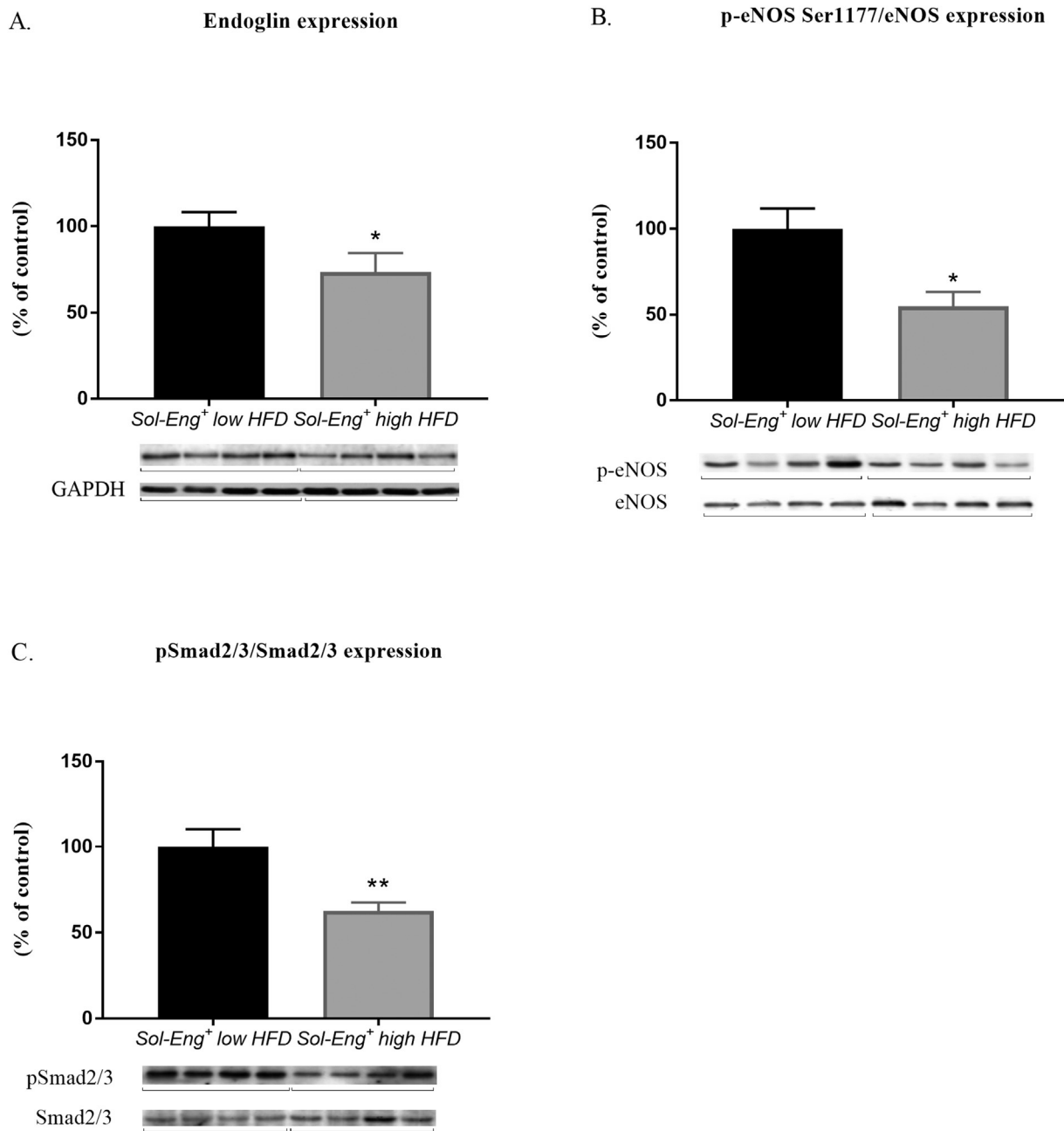


Fig. 4. Expression of membrane endoglin, eNOS and Smads in aortas from *Sol-Eng*⁺ high HFD and *Sol-Eng*⁺ low HFD mice.

Expression of membrane (A) Eng, (B) p-eNOS (Ser1177)/eNOS and (C) pSmad2/3/Smad2/3 in total protein extracts from mouse aortas. Top panel: densitometric analysis (control = 100%). Densitometric quantification of immunoreactive bands was recalculated to the GAPDH signal. Bottom panel: representative immunoblots. Data are shown as mean ± S.E.M., Mann-Whitney test, * $p \leq 0.05$, ** $p \leq 0.01$. $n = 5$ mice per group.

3.6. Immunohistochemical analysis of macrophages in aortic sections

Sixty aortic sections in thirty slides were evaluated per each experimental group. The aortic sections did not develop alteration in histological structure with respect to possible fat accumulation (fatty streaks) or other visible changes in the vessel wall (data not shown). In addition, no infiltration of macrophages in the vessel wall was observed either in *Sol-Eng*⁺ high HFD mice or *Sol-Eng*⁺ low HFD mice. *ApoE*/*LDLR* double knockout mice aortic section was used as a positive control for macrophage staining in aorta (Supplemental Fig. 1).

4. Discussion

Hypercholesterolemia, atherosclerosis, type II diabetes mellitus and hypertension are pathological disorders that were demonstrated to be related to increased levels of sEng, suggesting that sEng could be a potential biomarker of endothelial alteration, which is typical for above mentioned diseases [12]. However, the question is whether sEng might also modulate the function of membrane-bound endothelial endoglin and endothelial function in these pathological conditions, which are usually accompanied by the hypercholesterolemia. Of note, hypercholesterolemia is associated with increased levels of oxysterols, which via LXR nuclear

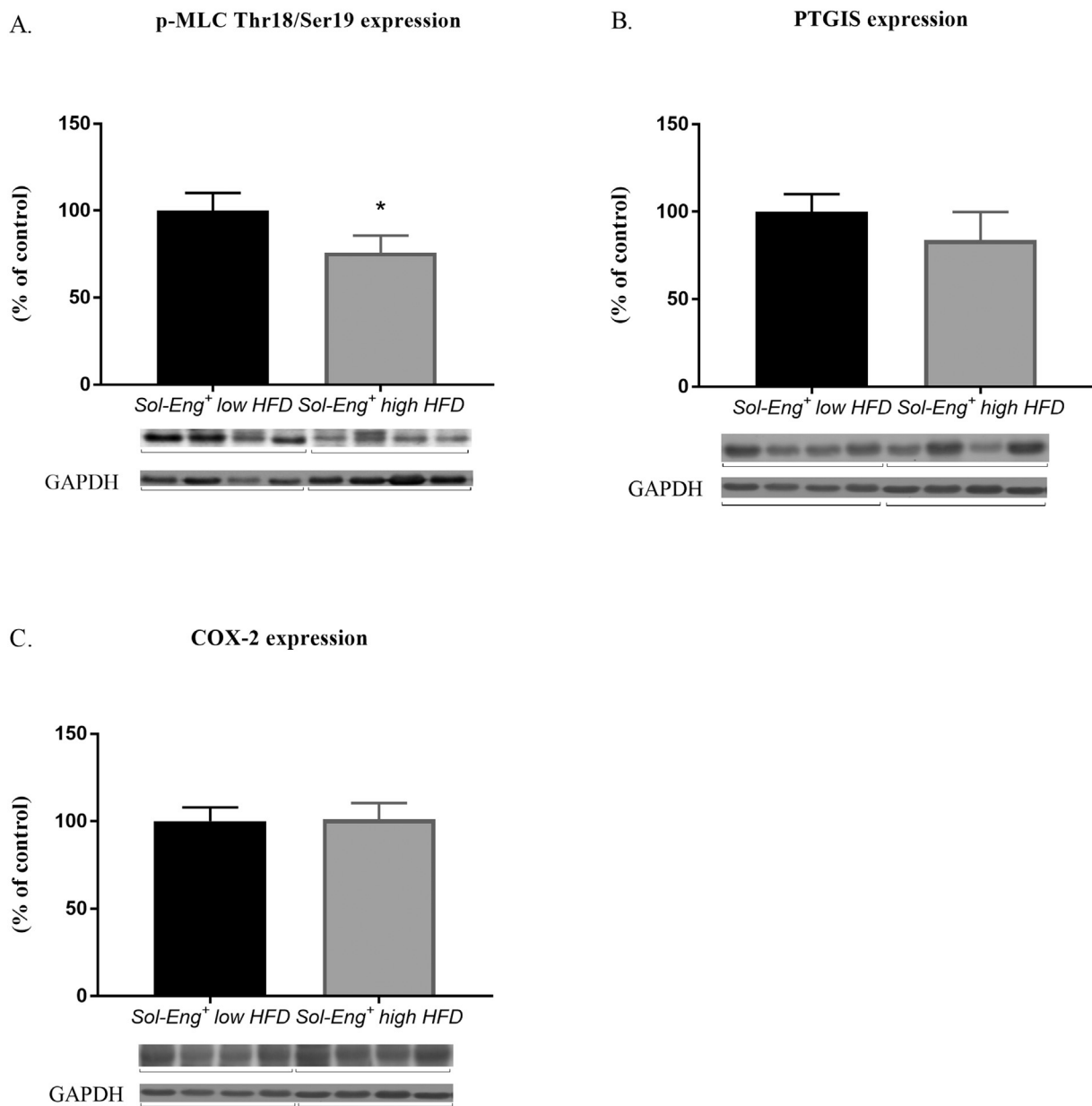


Fig. 5. Expression of markers related to vascular smooth muscle function in aorta of *Sol-Eng*⁺ high HFD and *Sol-Eng*⁺ low HFD mice.

Expression of (A) pMLC Thr18/Ser19, (B) PTGIS and (C) COX-2 in total protein extracts from mouse aortas. Top panel: densitometric analysis (control = 100%). Densitometric quantification of immunoreactive bands was recalculated to the GAPDH signal. Bottom panel: representative immunoblots. Data are shown as mean \pm S.E.M., Mann-Whitney test, * $p < 0.05$. $n = 5$ mice per group.

receptors can upregulate the expression of both membrane-bound and soluble endoglin [24,25]. Here we demonstrate for the first time that long exposure to high sEng levels and mild hypercholesterolemia (induced by high fat diet) result in endothelial and vessel wall dysfunction in aorta and altered membrane endoglin/eNOS signaling.

sEng is chipped from the extracellular domain of the membrane-bound endoglin, which is expressed by endothelial cells and smooth muscle cells in blood vessels [6]. In addition, several papers demonstrated that sEng can directly affect the function of blood vessels. Thus, it has been shown that administration of recombinant sEng led to impaired binding of TGF- β 1 to its receptor and subsequently to an inhibition of eNOS-dependent vasodilation in rat renal microvessels and mesenteric vessels, suggesting

possible hypertensive effects of sEng [11]. It is of interest to point out that mice treated with adenovirus expressing sEng had induction of endothelial dysfunction profile in endothelium of mesenteric venules, which was characterized by higher expression of cell adhesion molecules and impaired vasodilation [21]. As these studies were not actually related to atherosclerosis prone blood vessels, we performed the first study that was targeted to elucidate potential effect of high levels of sEng on aorta [23]. By using transgenic mouse model expressing human sEng (*Sol-Eng*⁺) that shows many symptoms of preeclampsia, such as hypertension, small pup size, proteinuria and renal damage [24], we failed to detect any harmful effect of sEng on aortic function or expression of endothelial dysfunction related markers [23]. These results are in line with a recent paper showing that sEng does not affect TGF- β

signaling alone, but rather together with other TGF- β receptors [26]. To further pursue this line of research, we decided to combine high fat diet with high levels of sEng in order to mimic situation in patients with atherosclerosis, type II diabetes mellitus and hypertension where hypercholesterolemia is very common. The results of Jezkova et al. paper showed that combination with high fat diet induces a pro-inflammatory phenotype in aorta with increased expression of NF- κ B and cell adhesion molecules. Surprisingly, we also found a preservation of aortic function in mice having high sEng plasma levels [22]. Despite these controversial results, we demonstrated that hypercholesterolemia in combination with high plasma levels of sEng deserves further study.

Thus, we hypothesized that long-term exposure to high fat diet in combination with high plasma levels of sEng will result in alteration of aortic function. Indeed, six months feeding with high fat diet resulted in a) impaired endothelium-dependent relaxation induced by acetylcholine (that mediates releasing of NO by binding to muscarinic receptors in endothelial cells), b) impaired endothelium-independent relaxation induced by SNP (a donor of NO with capability to activate soluble guanylate cyclase in vascular smooth muscle cells), c) activated compensatory reaction (measured by L-NAME as direct inhibitor of eNOS), d) reduced contraction induced by KCl and e) reduced phosphorylation of myosin light chain in *Sol-Eng⁺ high HFD* mice. All these functional changes suggest the alteration of both endothelial and vessel wall (smooth muscle cells) function. It is of interest to point out that *Sol-Eng⁺ low HFD* mice showed lower levels of all measured parameters when compared to our previous experiment with mice on chow diet [23] or in mice fed three months with high fat diet [22], suggesting that administration of high fat diet for six months impairs the function of endothelium and vessel wall itself. Thus, we propose that high sEng plasma levels in combination with hypercholesterolemia aggravate already present endothelial and vessel wall dysfunction in aorta.

Indeed, we must emphasize that cholesterol levels were not significantly different between *Sol-Eng⁺ high HFD* and *Sol-Eng⁺ low HFD* mice but significant hypercholesterolemia was present in mice fed high fat diet when compared to mice on chow diet. Moreover, histological and immunohistochemical analysis showed no signs of ongoing atherogenesis on morphological level, therefore all effects and results of this study are related to atherosclerosis-intact aorta. So, the only difference between these groups was in the levels of human sEng. In general, there is a high level of homology between mouse and human sEng (99% sequence overlap, 69% identity) [27,28] and mouse models used by our group showed several times that human sEng can affect mouse endoglin signaling [22,24]. As mentioned above, there are controversial findings on whether sEng interferes with TGF- β signaling [26,29]. However, it was demonstrated that sEng antagonizes the effects of membrane endoglin that is highly expressed by endothelial and smooth muscle cells [30]. In addition, we found that protein levels of mouse membrane endoglin are decreased in *Sol-Eng⁺ high HFD* mice compared to *Sol-Eng⁺ low HFD* mice (Fig. 4A), suggesting a complex and regulatory interplay between the two forms of endoglin. Interestingly, membrane endoglin was shown to be related to a proper function of eNOS and NO-dependent vasodilation [15,18], whereas its reduced expression resulted in an impaired endothelium-dependent vasodilation [15]. In addition, membrane endoglin increases eNOS expression via Smad2/3 transcription factor directly without cooperation with TGF- β 1 [18]. Indeed, Western blot analysis revealed reduced expression of membrane endoglin, phosphorylated Smad2/3 and phosphorylated eNOS Ser1177 in *Sol-Eng⁺ high HFD* mice in this study. Thus, we might propose that sEng aggravates endothelial and vessel wall dysfunction in aorta via interference with membrane endoglin/Smad2/3/eNOS dependent

pathway.

Functional analysis of aorta showed activation of some compensatory reaction in aorta of *Sol-Eng⁺ high HFD* mice (measured by L-NAME as direct inhibitor of eNOS). Indeed, there are several ways that could explain this compensatory reaction including activation of COX-2, PGs, or EDHF [31–33]. However, COX-2 and PTGIS protein expression in aorta did not differ between studied groups in this study. On the other hand, we cannot rule out the involvement of COX-2 and PTGIS activity in the compensation based on the protein expression analysis, therefore no clear conclusion can be drawn from these results. In addition, we must point out that we have not deepened more into this compensatory mechanism as this was not the primary goal of this study. In our view, this is a complex issue and further and independent studies are necessary to address this point, which is out of the scope of the manuscript.

We also focused on potential molecular mechanism related to altered vasoconstriction response in *Sol-Eng⁺ high HFD* mice. Vasodilation and vasoconstriction is regulated via myosin light chain kinase signaling in smooth muscle cells [19]. KCl acts as a calcium sensitizer and membrane depolarization occurs after its administration. KCl activates voltage-dependent calcium channel and this leads to an increased intracellular calcium concentration and subsequently to activation of myosin light chain kinase (MLCK) [34]. MLCK is a Ca²⁺/calmodulin-dependent protein kinase responsible for myosin phosphorylation and the phosphorylation of myosin light chain (MLC) is the main regulatory mechanism of smooth muscle contraction [20]. So, there is a direct relation between activity of MLCK, degree of MLC phosphorylation and therefore ability of smooth muscle contraction [35]. In agreement with this, we showed significantly reduced expression of pMLC Thr18/19 and reduced vasoconstriction in aortas of *Sol-Eng⁺ high HFD* mice compared to *Sol-Eng⁺ low HFD* mice. Thus, we might propose that 6 months HFD feeding and exposure to high levels of soluble endoglin leads to impaired calcium sensitivity/release and subsequently to decreased capability of smooth muscle contraction in *Sol-Eng⁺ high HFD*.

A key aspect of endothelial dysfunction development is the activation of vascular inflammation with increased expression of cell adhesion molecules [36]. Surprisingly, we did not detect any significant differences in the expression of VCAM-1, ICAM-1, P-selectin and pNF- κ B/NF- κ B in both aorta and blood between both studied groups as we showed in our previous paper [22]. One possible explanation why we do not see the differences in VCAM-1, ICAM-1, P-selectin and pNF- κ B/NF- κ B expressions might be in the fact that mice are under long term high fat diet (6 months) in this study and the expression levels of these proteins might be high enough in both groups (especially considering the fact that both groups of mice have aggravated function of endothelium when compared with Jezkova et al. paper). Thus, different age of mice (9 months), different exposure to high fat diet (6 months) and soluble endoglin (9 months) in this study when compared to Jezkova et al. paper (age of mice 6 months, high fat diet 3 months and soluble endoglin 6 months) could be responsible for the different results that we obtained [22]. On the other hand, we measured other pro-inflammatory biomarkers in plasma. We demonstrated increased level of MCP-1 and TNF- α (borderline of statistical significance for MCP-1 [$p = 0.08$] and for TNF- α [$p = 0.06$]) in *Sol-Eng⁺ high HFD* mice suggesting at least partial induced pro-inflammatory reaction in these mice.

It is of interest to mention potential limitation of the study. At this point we cannot answer important question, whether high soluble endoglin levels affect atherogenesis/atherosclerosis in aorta. The group of Lopez-Novoa tried to generate mice with high soluble endoglin on ApoE background, however they failed to

generate viable mice who would have high levels of soluble endoglin (unpublished results). *In vivo* experiments investigating atherogenesis in the mice with high levels of soluble endoglin do not appear yet to be feasible. Moreover, we would like to also point out that we measured blood pressure in the Nemeckova et al. paper [37]. The measurements of arterial pressure by tail-cuff method showed that systolic pressure in male and female Sol-Eng + mice is higher than that of control mice. Higher blood pressure in mice with high soluble endoglin is the key feature of this mouse model established before.

In conclusion, we demonstrated that long-term hypercholesterolemia (induced by high fat diet) combined with high plasma levels of sEng results in the aggravation of endothelial and vessel wall dysfunction in aorta with possible alteration of membrane endoglin/eNOS signaling. Thus, it is necessary to consider sEng as not only a biomarker of cardiovascular diseases, but also as a potential co-inducer of vascular alterations especially in combination with other risk factors of cardiovascular diseases, including hypercholesterolemia.

Conflict of interest

The authors declared they do not have anything to disclose regarding conflict of interest with respect to this manuscript.

Financial support

The work was supported by grants from Czech Science foundation (GACR number GA15-24015S), *Czech Health Research Council* (AZV CR number 17–31754A), the Grant Agency of Charles University in Prague (number 1284214/C, 1158413C and grant SVV/2016/260293), *Ministerio de Economía y Competitividad* of Spain (SAF2013-43421-R to CB *Centro de Investigación Biomédica en Red de Enfermedades Raras* (CIBERER; to CB), and *Instituto de Salud Carlos III* (PI16/00460 and Retic RD16/0009/0025, REDINREN-FEDER). CIBERER and REDINREN are initiatives of the *Instituto de Salud Carlos III* (ISCIII) of Spain supported by FEDER funds from the European Commission.

Author contributions

Barbora Vitverova - designed and performed experiments, wrote the manuscript.

Katerina Blazickova - performed experiments, revised the text of the manuscript.

Iveta Najmanova - performed myograph experiments, revised the text of the manuscript.

Matej Vicen - participated on statistical analysis, revised the text of the manuscript.

Radek Hyšpler - performed biochemical analysis of total cholesterol.

Eva Dolezelova - contributed to data analysis, revised the text of the manuscript.

Ivana Nemeckova - provided cholesterol levels data, revised the text of the manuscript.

Jurjen Duintjer Tebbens - performed statistical analysis.

Carmelo Bernabeu - revised the text of the manuscript.

Miguel Pericacho - revised the text of the manuscript.

Petr Nachtigal - designed experiments, wrote and revised the manuscript.

Acknowledgements

We thank Prof. Lopez-Novoa from University of Salamanca in Spain who kindly provided the unique transgenic mouse model.

Appendix A. Supplementary data


Supplementary data related to this article can be found at <https://doi.org/10.1016/j.atherosclerosis.2018.02.008>.

References

- [1] P.T. Bot, I.E. Hoefler, J.P. Sluijter, et al., Increased expression of the transforming growth factor-beta signaling pathway, endoglin, and early growth response-1 in stable plaques, *Stroke* 40 (2009) 439–447.
- [2] J.M. Lopez-Novoa, C. Bernabeu, The physiological role of endoglin in the cardiovascular system, *Am. J. Physiol. Heart Circ. Physiol.* 299 (2010) H959–H974.
- [3] F.J. Blanco, J.F. Santibanez, M. Guerrero-Esteo, et al., Interaction and functional interplay between endoglin and ALK-1, two components of the endothelial transforming growth factor-beta receptor complex, *J. Cell. Physiol.* 204 (2005) 574–584.
- [4] M. Guerrero-Esteo, T. Sanchez-Elsner, A. Letamendia, C. Bernabeu, Extracellular and cytoplasmic domains of endoglin interact with the transforming growth factor-beta receptors I and II, *J. Biol. Chem.* 277 (2002) 29197–29209.
- [5] E. Gallardo-Vara, F.J. Blanco, M. Roque, et al., Transcription factor KLF6 upregulates expression of metalloprotease MMP14 and subsequent release of soluble endoglin during vascular injury, *Angiogenesis* 19 (2016) 155–171.
- [6] L.J. Hawinkels, P. Kuiper, E. Wiercinska, et al., Matrix metalloproteinase-14 (MT1-MMP)-mediated endoglin shedding inhibits tumor angiogenesis, *Canc. Res.* 70 (2010) 4141–4150.
- [7] A.D. Blann, J.M. Wang, P.B. Wilson, S. Kumar, Serum levels of the TGF-beta receptor are increased in atherosclerosis, *Atherosclerosis* 120 (1996) 221–226.
- [8] Z. Straský, L. Vecerova, J. Rathouska, et al., Cholesterol effects on endoglin and its downstream pathways in ApoE/LDLR double knockout mice, *Circ. J.* 75 (2011) 1747–1755.
- [9] M. Blaha, M. Cermanova, V. Blaha, et al., Elevated serum soluble endoglin (sCD105) decreased during extracorporeal elimination therapy for familial hypercholesterolemia, *Atherosclerosis* 197 (2008) 264–270.
- [10] A.M. Blazquez-Medela, L. Garcia-Ortiz, M.A. Gomez-Marcos, et al., Increased plasma soluble endoglin levels as an indicator of cardiovascular alterations in hypertensive and diabetic patients, *BMC Med.* 8 (2010) 86.
- [11] S. Venkatesha, M. Toporsian, C. Lam, et al., Soluble endoglin contributes to the pathogenesis of preeclampsia, *Nat. Med.* 12 (2006) 642–649.
- [12] J. Rathouska, K. Jezkova, I. Nemeckova, P. Nachtigal, Soluble endoglin, hypercholesterolemia and endothelial dysfunction, *Atherosclerosis* (2015) 383–388.
- [13] J. Davignon, P. Ganz, Role of endothelial dysfunction in atherosclerosis, *Circulation* 109 (2004), III27–32.
- [14] A. Chatterjee, S.M. Black, J.D. Catravas, Endothelial nitric oxide (NO) and its pathophysiological regulation, *Vasc. Pharmacol.* 49 (2008) 134–140.
- [15] M. Jerkic, J.V. Rivas-Elena, M. Prieto, et al., Endoglin regulates nitric oxide-dependent vasodilation, *Faseb. J.* 18 (2004) 609–611.
- [16] M. Jerkic, A. Rodriguez-Barbero, M. Prieto, et al., Reduced angiogenic responses in adult Endoglin heterozygous mice, *Cardiovasc. Res.* 69 (2006) 845–854.
- [17] M. Toporsian, R. Gros, M.G. Kabir, et al., A role for endoglin in coupling eNOS activity and regulating vascular tone revealed in hereditary hemorrhagic telangiectasia, *Circ. Res.* 96 (2005) 684–692.
- [18] J.F. Santibanez, A. Letamendia, F. Perez-Barriocanal, et al., Endoglin increases eNOS expression by modulating Smad2 protein levels and Smad2-dependent TGF-beta signaling, *J. Cell. Physiol.* 210 (2007) 456–468.
- [19] N. Gao, J. Huang, W. He, et al., Signaling through myosin light chain kinase in smooth muscles, *J. Biol. Chem.* 288 (2013) 7596–7605.
- [20] A. Shirazi, K. Iizuka, P. Fadden, et al., Purification and characterization of the mammalian myosin light chain phosphatase holoenzyme. The differential effects of the holoenzyme and its subunits on smooth muscle, *J. Biol. Chem.* 269 (1994) 31598–31606.
- [21] T.E. Walshe, V.S. Dole, A.S. Maharaj, et al., Inhibition of VEGF or TGF- β signaling activates endothelium and increases leukocyte rolling, *Arterioscler. Thromb. Vasc. Biol.* 29 (2009) 1185–1192.
- [22] K. Jezkova, J. Rathouska, I. Nemeckova, et al., High levels of soluble endoglin induce a proinflammatory and oxidative-stress phenotype associated with preserved no-dependent vasodilation in aortas from mice fed a high-fat diet, *J. Vasc. Res.* 53 (2016) 149–162.
- [23] I. Nemeckova, A. Serwadczak, B. Oujó, et al., High soluble endoglin levels do not induce endothelial dysfunction in mouse aorta, *PLoS One* (2015), e0119665.
- [24] A.C. Valbuena-Diez, F.J. Blanco, B. Oujó, et al., Oxysterol-induced soluble endoglin release and its involvement in hypertension, *Circulation* 126 (2012) 2612–2624.
- [25] J. Henry-Berger, K. Mouzat, S. Baron, et al., Endoglin (CD105) expression is regulated by the liver X receptor alpha (NR1H3) in human trophoblast cell line JAR, *Biol. Reprod.* 78 (2008) 968–975.
- [26] Q. Wang, Molecular genetics of coronary artery disease, *Curr. Opin. Cardiol.* 20 (2005) 182–188.
- [27] A. Gougos, M. Letarte, Primary structure of endoglin, an RGD-containing

- glycoprotein of human endothelial cells, *J. Biol. Chem.* 265 (1990) 8361–8364.
- [28] S. St-Jacques, U. Cymerman, N. Pece, M. Letarte, Molecular characterization and in situ localization of murine endoglin reveal that it is a transforming growth factor-beta binding protein of endothelial and stromal cells, *Endocrinology* 134 (1994) 2645–2657.
- [29] A.L. Gregory, G. Xu, V. Sotov, M. Letarte, Review: the enigmatic role of endoglin in the placenta, *Placenta* 35 (Suppl:S93–99) (2014).
- [30] E. Rossi, F. Sanz-Rodriguez, N. Eleno, et al., Endothelial endoglin is involved in inflammation: role in leukocyte adhesion and transmigration, *Blood* 121 (2013) 403–415.
- [31] A. Huang, D. Sun, M.A. Carroll, et al., EDHF mediates flow-induced dilation in skeletal muscle arterioles of female eNOS-KO mice, *Am. J. Physiol. Heart Circ. Physiol.* 280 (2001) H2462–H2469.
- [32] A. Huang, D. Sun, C.J. Smith, et al., In eNOS knockout mice skeletal muscle arteriolar dilation to acetylcholine is mediated by EDHF, *Am. J. Physiol. Heart Circ. Physiol.* 278 (2000) H762–H768.
- [33] B.R. Silva, L. Pernomian, T.D. De Paula, et al., Endothelial nitric oxide synthase and cyclooxygenase are activated by hydrogen peroxide in renal hypertensive rat aorta, *Eur. J. Pharmacol.* 814 (2017) 87–94.
- [34] P.H. Ratz, K.M. Berg, N.H. Urban, A.S. Miner, Regulation of smooth muscle calcium sensitivity: KCl as a calcium-sensitizing stimulus, *Am. J. Physiol. Cell Physiol.* 288 (2005) C769–C783.
- [35] N. Niuro, M. Ikebe, Zipper-interacting protein kinase induces Ca²⁺-free smooth muscle contraction via myosin light chain phosphorylation, *J. Biol. Chem.* 276 (2001) 29567–29574.
- [36] S. Ling, L. Nheu, P.A. Komesaroff, Cell adhesion molecules as pharmaceutical target in atherosclerosis, *Mini Rev. Med. Chem.* 12 (2012) 175–183.
- [37] I. Nemeckova, A. Serwaczak, B. Oujó, et al., High soluble endoglin levels do not induce endothelial dysfunction in mouse aorta, *PLoS One* 10 (2015), e0119665.

High soluble endoglin levels do not induce changes in structural parameters of mouse heart

Jana Rathouska¹ · Petra Fikrova¹ · Alena Mrkvicova² · Katerina Blazickova¹ · Michala Varejkova¹ · Eva Dolezelova¹ · Ivana Nemeckova¹ · Barbora Vitverova¹ · Lenka Peslova¹ · Eunate Gallardo-Vara³ · Miguel Pericacho⁴ · Petr Nachtigal¹ 

Received: 5 January 2017 / Accepted: 31 March 2017 / Published online: 5 April 2017
© Springer Japan 2017

Abstract A soluble form of endoglin (sEng) released into the circulation was suggested to be a direct inducer of endothelial dysfunction, inflammation and contributed to the development of hypertension by interfering with TGF- β signaling in cardiovascular pathologies. In the present study, we assessed the hypothesis that high sEng level-induced hypertension via a possible sEng interference with TGF- β signaling pathways may result in inflammatory, structural or fibrotic changes in hearts of *Sol-Eng*+ mice (mice with high levels of soluble endoglin) fed either chow or high-fat diet. Female *Sol-Eng*+ mice and their age matched littermates with low plasma levels of sEng were fed either chow or high-fat diet (HFD). Heart samples were subsequently analyzed by histology, qRT-PCR and Western blot analysis. In this study, no differences in myocardial morphology/hypertrophy and possible fibrotic changes between *Sol-Eng*+ mice and control mice were detected on both chow and HFD. The presence of sEng did not significantly affect the expression of selected members of TGF- β

signaling (membrane endoglin, TGF β RII, ALK-5, ALK-1, Id-1, PAI-1 and activated Smad proteins-pSmad 1,5 and pSmad 2,3), inflammation, heart remodeling (PDGFb, Col1A1) and endothelial dysfunction (VCAM-1, ICAM-1) in the hearts of *Sol-Eng*+ mice compared to control mice on both chow and high-fat diet. High levels of soluble endoglin did not affect microscopic structure (profibrotic and degenerative cardiomyocyte changes), and specific parts of TGF- β signaling, endothelial function and inflammation in the heart of *Sol-Eng*+ mice fed both chow diet or HFD. However, we cannot rule out a possibility that a long-term chronic exposure (9 months and more) to soluble endoglin alone or combined with other cardiovascular risk factors may contribute to alterations of heart function and structure in *Sol-Eng*+ mice, which is the topic in our lab in ongoing experiments.

Keywords Soluble endoglin · Mice · Heart · Inflammation · TGF- β signaling

✉ Petr Nachtigal
Petr.Nachtigal@faf.cuni.cz

¹ Department of Biological and Medical Sciences, Faculty of Pharmacy in Hradec Kralove, Charles University, Heyrovskeho 1203, 500 05 Hradec Kralove, Czech Republic

² Department of Medical Biochemistry, Faculty of Medicine in Hradec Kralove, Charles University, Simkova 870, 500 38 Hradec Kralove, Czech Republic

³ Center for Biological Research, Spanish National Research Council (CSIC), and Biomedical Research Networking Center on Rare Diseases (CIBERER), 28040 Madrid, Spain

⁴ Department of Physiology and Pharmacology, Renal and Cardiovascular Physiopathology Unit, University of Salamanca, 37007 Salamanca, Spain

Introduction

Soluble form of endoglin (sEng) can be released upon a proteolytic cleavage of the extracellular domain of the membrane-bound endoglin during endothelial injury and inflammation [1, 2]. Increased levels of sEng in blood were reported in patients with hypercholesterolemia [3], type II diabetes mellitus, hypertension [4], preeclampsia [2] and myocardial infarction [5], suggesting that sEng may be considered as a biomarker of cardiovascular-related pathologies.

On the other hand, several authors demonstrated sEng as a direct inducer of endothelial dysfunction in vessels, a subject that has been reviewed in detail recently

[6]. Soluble endoglin was shown to affect eNOS and/or TGF- β signaling (Smad 2,3) in renal and mesenteric arteries [2] and increased expression of inflammatory cell adhesion molecules in venules [7]. However, no data about endothelial dysfunction or inflammation in the heart in the presence of high sEng levels alone and/or in a combination with hypercholesterolemia are available. Therefore, we aimed to evaluate the expression of VCAM-1, ICAM-1 as markers of endothelial dysfunction and vessel inflammation [8] and eNOS as the main enzyme responsible for NO production and maintenance of proper endothelial function [9]. Inflammation and atherosclerosis development in blood vessels are indeed closely related to acute coronary syndromes [10].

Furthermore, high plasmatic levels of sEng also resulted in development of a mild arterial hypertension in mice [11]. Indeed, arterial hypertension represents a possible risk factor for the development of myocardial hypertrophy with the risk of heart remodeling and potential development of fibrotic changes [12]. PDGF β is a member of platelet-derived growth factors affecting cell growth and division and regulating development of various tissues and organs. Apart from its physiological role, PDGF β expression was also connected with vessel inflammation and tissue fibrosis [13], including cardiac fibrosis, where PDGF pathway stimulates fibroblasts to proliferate and transform into myofibroblasts [14]. Moreover, an excess of cardiac collagen type I synthesis and deposition may be involved in the enhancement of myocardial fibrosis that accompanies the development of heart failure in hypertensive heart [15].

In addition, sEng was demonstrated to interfere with TGF- β signaling and membrane endoglin. Membrane endoglin affects two specific signaling pathways TGF β RII/ALK-1/Smad 1,5,8/Id-1 and TGF β RII/ALK-5/Smad 2,3/PAI-1 regulating cell proliferation, migration and angiogenesis [16]. Moreover, sEng was shown to affect BMP-9/ALK-1/Smad 1,5,8 signaling directly, antagonizing tissue endoglin effects, which limits TGF- β 1 signaling and type I collagen synthesis in cardiac fibroblasts [2, 17, 18]. More recently, conditional knock-out of ALK-1 was associated with the development of high-output heart failure [19]. However, sEng effects on TGF- β signaling in healthy hearts have not been studied so far.

Transgenic mice with high levels of human sEng (*Sol-Eng*+) suffer from symptoms of preeclampsia, such as hypertension, renal damage and proteinuria, and may serve as an appropriate animal model to study possible effects of high sEng levels on cardiovascular system [11, 20, 21]. Our previous paper showed that combination of high-fat diet and high levels of soluble endoglin resulted in pro-inflammatory and oxidative stress changes in mouse

aorta [22] suggesting that combination of these two factors might induce pathological changes in cardiovascular system.

In this study, we used these mice and assessed the hypothesis that high sEng levels modulate TGF- β signaling pathways resulting in inflammatory, structural or fibrotic changes in the heart of *Sol-Eng*+ mice when either sEng operating as a single factor or in a combination with a mild hypercholesterolemia.

Materials and methods

Animals and study design

Female mice with the overexpression of human sEng (*Sol-Eng*+) on the CBAxC57BL/6J background were generated at the Genetically Modified Organisms Generation Unit (University of Salamanca, Spain), as described previously [11]. In a chow diet study, 4- to 6-month-old *Sol-Eng*+ mice with high plasma levels of sEng (*Sol-Eng*+ chow group, 6 animals) and their age matched transgenic littermates with low plasma levels of sEng (control chow group, 7 animals) were used for the experiment. In a high-fat diet study, 6-month-old *Sol-Eng*+ mice with high plasma levels of sEng (*Sol-Eng*+ HFD group, 5 animals) and their age matched transgenic littermates with low plasma levels of sEng (control HFD group, 6 animals) fed a high-fat rodent diet containing 1.25% of cholesterol and 40% of fat (D12108C Research Diets, New Brunswick, NJ, USA) for the following 3 months were used for the experiment. The animals were housed under a 12-h light cycle at constant temperature and humidity and had free access to tap water and a standard laboratory pellet diet.

All experiments were performed in accordance with the directive of the EEC (86/609/EEC), and the use of animals was approved by the Ethical Committee for the protection of animals against cruelty of the Faculty of Pharmacy in Hradec Kralove, Charles University in Prague (Permit Number: 21558/2013-2), and the Bioethics Committee of the University of Salamanca (Permit Number: 006-201400038812).

All surgery procedures were carried out under ketamine/xylazine or fluorane anesthesia, and all efforts were made to minimize the suffering of the animals.

Quantitative real-time RT-PCR

Total RNA was isolated from all heart tissue samples (myocardium of heart ventricles) using TRI reagent (Sigma-Aldrich, St. Louis, USA) according to the manufacturer's protocol and directly converted into cDNA via a High-Capacity cDNA reverse transcription kit

(Life Technologies, Foster City, USA). 20 ng cDNA were loaded into one reaction and experiments were performed in triplicate. TaqMan[®] Gene Expression Master Mix and pre-designed TaqMan[®] Gene Expression Assay kits for the following genes: endoglin (Mm00468256_m1), NOS3 (Mm-00435217_m1), TGF β 1 (Mm01178820_m1), PDGF β (Mm00440677_m1), Col1A1 (Mm00801666_g1), NQO1 (Mm01253561_m1), VCAM-1 (Mm01320970_m1), ICAM-1 (Mm00516023_m1), ALK-1/Acvr11 (Mm00437432_m1), ALK-5/TGF β R1 (Mm00436964_m1), TGF β R2 (Mm03024091_m1), PAI-1/serpine1 (Mm00435858_m1), Id-1 (Mm00775963_g1), Myh7 (Mm00600555_m1) and Gapdh mouse endogenous control/housekeeping gene (Mm99999915_g1) were provided by Life Technologies (Foster City, USA). Analysis was performed using QuantStudio[™] 6. Glyceraldehyde 3-phosphate dehydrogenase (Gapdh) was used as reference for normalizing the data. The time–temperature profile used was: 95 °C for 10 min; 40 cycles: 95 °C for 15 s, 60 °C for 1 min. The relative normalized quantity was calculated using delta–delta Ct method as described [23].

Western blot analysis

Samples of hearts (myocardium of heart ventricles) from all female mice were homogenized in RIPA lysis buffer (Sigma-Aldrich, St. Louis, USA) containing proteases and phosphatases inhibitors, as described previously [20]. Proteins (20 μ g of total protein) were separated by SDS-PAGE, transferred to a PVDF membrane (Millipore, NY, USA) and incubated with appropriate antibodies (Table 1). Horseradish peroxidase-conjugated secondary antibodies were from Sigma-Aldrich Co. (St. Louis, USA) as described [20]. Membranes were developed using enhanced chemiluminescent reagents (Thermo Fisher Scientific Inc., IL, USA) and exposed to X-ray films (Foma, Czech Republic). Quantification of immunoreactive bands on the exposed films was performed by NIS imaging software (Laboratory Imaging, Prague, Czech Republic). The equal loading of proteins onto the gel was confirmed by immunodetection of GAPDH.

Histology of heart tissue sections

Specimens of the heart (myocardium of heart ventricles) from all female mice were fixed in 4% paraformaldehyde (pH 7.35) and paraffin embedded for histological evaluation. 40 sections (thickness 7 μ m) from each animal and each experimental group were taken for each histological analysis. Hematoxylin–eosin staining and Goldner's green trichrome staining (for the detection of collagen)

Table 1 Primary and secondary antibodies used in Western blot

Protein	Source	Dilution	Secondary antibody dilution
ALK-5	Sigma	1:500	1:4000
COX-2	Proteintech	1:500	1:5000
Endoglin	Santa Cruz	1:200	1:4000
eNOS	Santa Cruz	1:200	1:2000
GAPDH	Sigma	1:10000	1:20000
ICAM-1	Santa Cruz	1:500	1:2000
Id-1	Abcam	1:1000	1:2000
p-eNOS Ser1177	Santa Cruz	1:500	1:2000
pSmad 1,5	Cell Signaling	1:1000	1:2000
pSmad 2,3	Cell Signaling	1:1000	1:2000
VCAM-1	R&D systems	1:500	1:5000
VEGF	Abcam	1:1000	1:2000

were performed to reveal possible microscopic changes in the heart.

Statistical analysis

The statistical analysis was performed by GraphPad Prism 6.0 software (GraphPad Software, Inc., CA, USA). All data are presented as mean \pm SEM. Direct group–group comparisons in heart rate and heart weight evaluations were carried out using unpaired *t* test. Direct group–group comparisons in quantitative real-time RT-PCR and Western blot analysis were carried out using Mann–Whitney test. *P* values of 0.05 or less were considered statistically significant.

Results

Plasma human-soluble endoglin levels in *Sol-Eng+* and control mice fed either chow or high fat diet

The values of plasma sEng levels in *Sol-Eng+* and control female mice fed chow diet (2477 \pm 110.3 vs. 54.68 \pm 16.64 ng/ml, respectively) [20], as well as in female mice fed a high-fat diet (3480 \pm 501 ng/ml vs. undetectable levels, respectively) [22], have been reported in our previous papers.

Effect of high-soluble endoglin levels on TGF- β signaling components in mouse heart at the level of mRNA in mice fed either chow diet or high-fat diet

Quantitative real-time RT-PCR provided an overview of sEng effects on the mRNA levels of some components of TGF- β signaling pathways (TGF β R2/ALK-1/

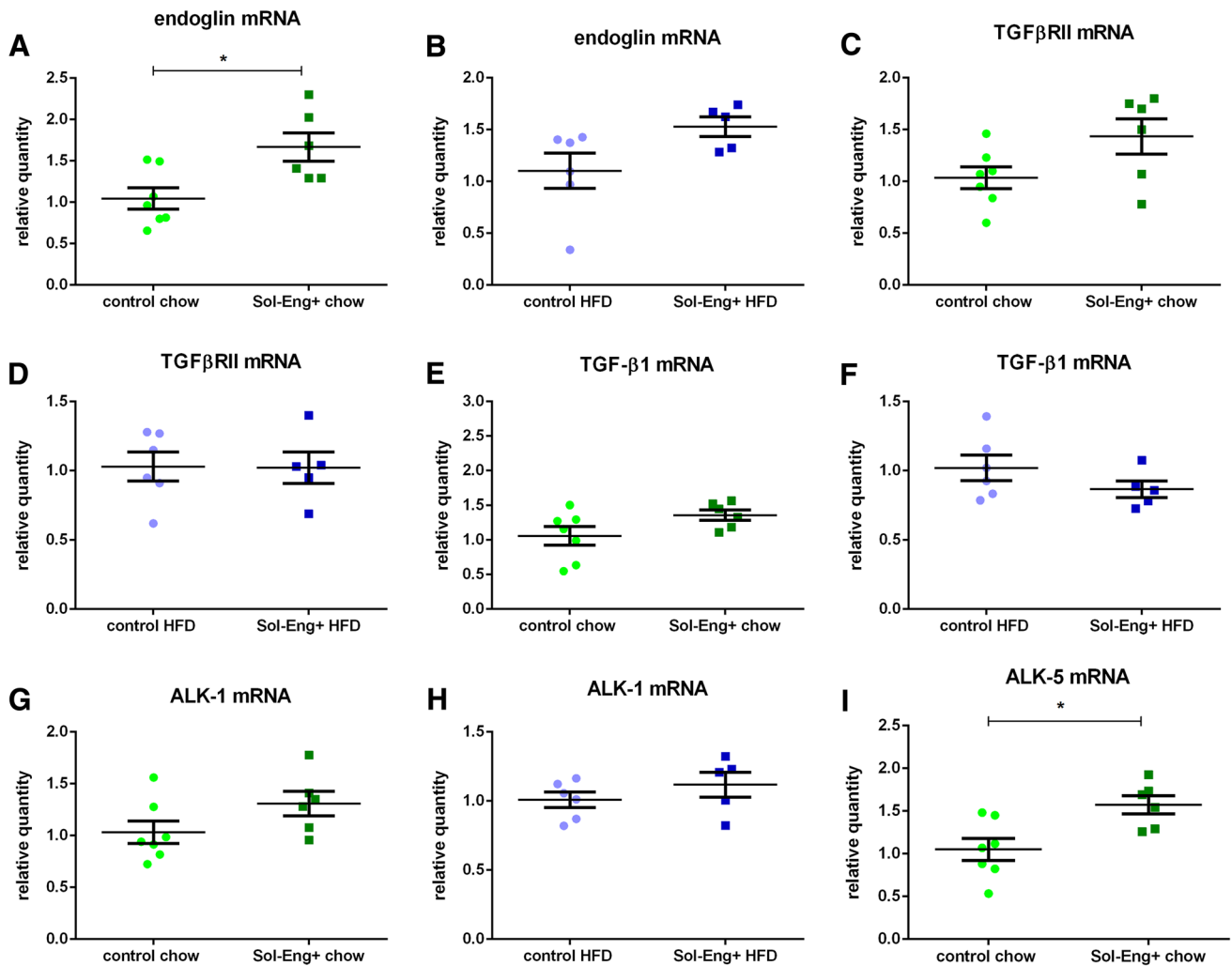


Fig. 1 Gene expression of some components of TGF- β signaling pathways in the hearts of *Sol-Eng+* and control mice fed either chow diet or high-fat diet. Relative gene expression of endoglin (a), TGF β RII (c), TGF- β 1 (e), ALK-1 (g), ALK-5 (i), Id-1 (k) and serpine1 (m) between control chow and *Sol-Eng+* chow mice and

relative gene expression of endoglin (b), TGF β RII (d), TGF- β 1 (f), ALK-1 (h), ALK-5 (j), Id-1 (l) and serpine1 (n) between control HFD and *Sol-Eng+* HFD mice. Error line segment indicating mean \pm SEM, Mann-Whitney test. * $p \leq 0.05$, ** $p \leq 0.01$

Id-1 and TGF β RII/ALK-5/PAI-1) in the heart. A significant upregulation of endoglin (Fig. 1a), ALK-5 (Fig. 1i) and Id-1 (Fig. 1k) mRNA expression in *Sol-Eng+* chow mice compared to control chow mice was observed. On the other hand, no significant differences in TGF β RII (Fig. 1c), TGF- β 1 (Fig. 1e), ALK-1 (Fig. 1g) and PAI-1 (marked as serpine1, Fig. 1m) mRNA levels were found between control chow and *Sol-Eng+* chow mice. In the groups of mice fed high-fat diet, only a significant upregulation of Id-1 (Fig. 1l) mRNA expression in control HFD mice compared to *Sol-Eng+* HFD mice was observed. No significant differences in endoglin (Fig. 1b), TGF β RII (Fig. 1d), TGF- β 1 (Fig. 1f), ALK-1 (Fig. 1h), ALK-5 (Fig. 1j) and PAI-1 (marked as serpine1, Fig. 1n) mRNA

levels were found between control HFD and *Sol-Eng+* HFD mice.

Effect of high-soluble endoglin levels on markers of inflammation, oxidative stress and heart remodeling at the level of mRNA in mice fed either chow diet or high-fat diet

Quantitative real-time RT-PCR also provided data related to inflammation (VCAM-1 Fig. 2a, b and ICAM-1 Fig. 2c, d), oxidative stress (NOS3 Fig. 2e, f and NQO1 Fig. 2g, h) and heart remodeling (PDGF β Fig. 2i, j, Col1A1 Fig. 2k, l and Myh7 Fig. 2m, n) in groups of mice fed chow diet or high-fat diet, respectively. Both

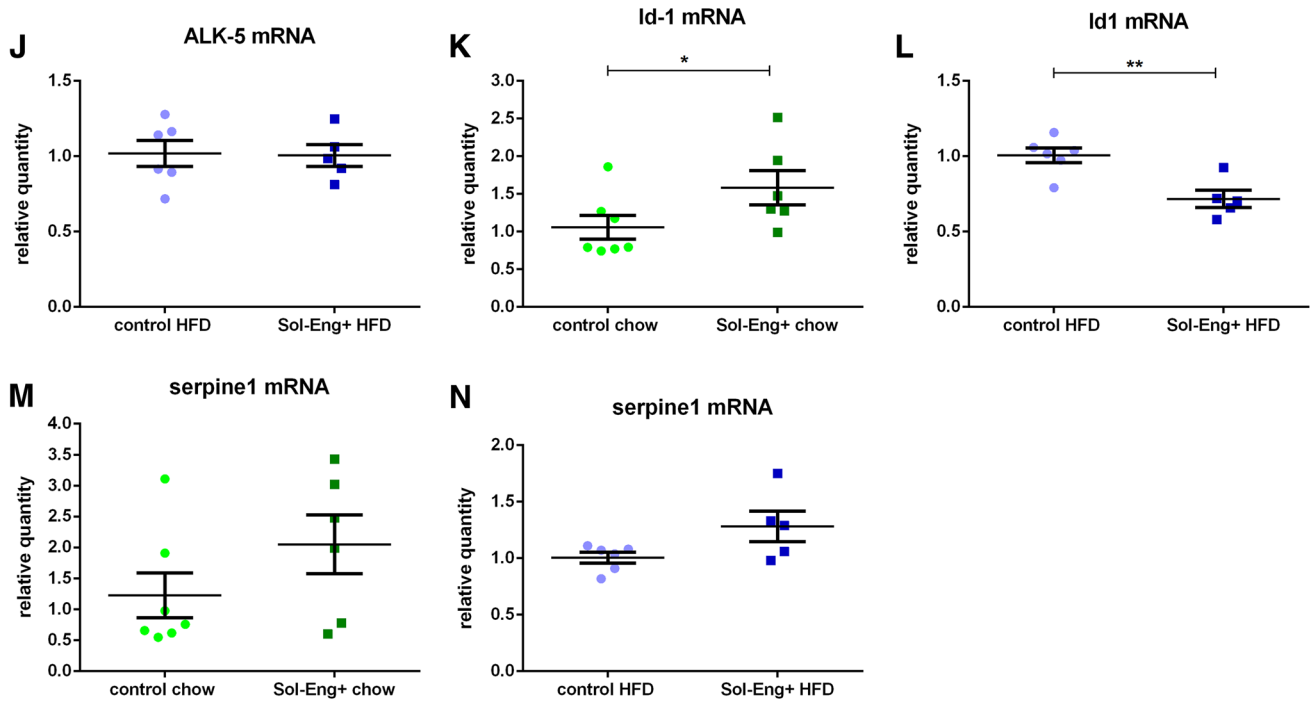


Fig. 1 continued

adhesion molecules, VCAM-1 (Fig. 2a) and ICAM-1 (Fig. 2c), were significantly upregulated in *Sol-Eng+* chow mice compared to control chow mice at the level of mRNA. However, the rest of the markers did not differ significantly between control chow and *Sol-Eng+* chow mice. No differences in mRNA expressions of any of the marker were also found between control HFD and *Sol-Eng+* HFD mice.

Soluble endoglin does not affect the morphological structure of the heart in mice fed either chow diet or high-fat diet

Hematoxylin–eosin and green trichrome staining were used to evaluate possible alterations or microscopic changes in the hearts of control and *Sol-Eng+* mice fed either chow or high-fat diet. 40 sections (thickness 7 μ m) from each mouse were used for the evaluation of histological changes in the left ventricle. Hematoxylin–eosin staining showed no differences in the heart (myocardium) structure between control and *Sol-Eng+* mice on both diets. No changes in the nuclei staining, cardiomyocytes structure or inflammatory infiltrate were detected in all groups (Fig. 3). Green trichrome staining did not reveal fibrotic changes in any of the studied hearts from all groups (data not shown). In general, there were no signs of pathological changes in the hearts of all mice.

Effect of high-soluble endoglin levels on markers of endothelial dysfunction in the hearts of mice fed either chow diet or high-fat diet

Western blot analysis of endothelial dysfunction-related markers did not reveal any significant differences in the expression of eNOS (Fig. 4a, b), its active phosphorylated form peNOS (Ser 1177) (Fig. 4c, d) and VEGF (Fig. 4e, f) between control and *Sol-Eng+* mice on either chow diet or high-fat diet, respectively.

High-soluble endoglin levels do not upregulate pro-inflammatory proteins in the hearts of mice fed either chow diet or high-fat diet

Western blot analysis did not confirm the qRT-PCR significant results with respect to the differential expression of VCAM-1 and ICAM-1 between control chow and *Sol-Eng+* chow mice. The protein expression of VCAM-1 (Fig. 5a) and ICAM-1 (Fig. 5c) did not significantly differ between control chow and *Sol-Eng+* chow mice. COX-2 protein expression (Fig. 5e) was not significantly different between control chow and *Sol-Eng+* chow mice as well. Similarly, none of the protein expression of VCAM-1 (Fig. 5b), ICAM-1 (Fig. 5d) and COX-2 (Fig. 5f) was significantly different between control HFD and *Sol-Eng+* HFD mice.

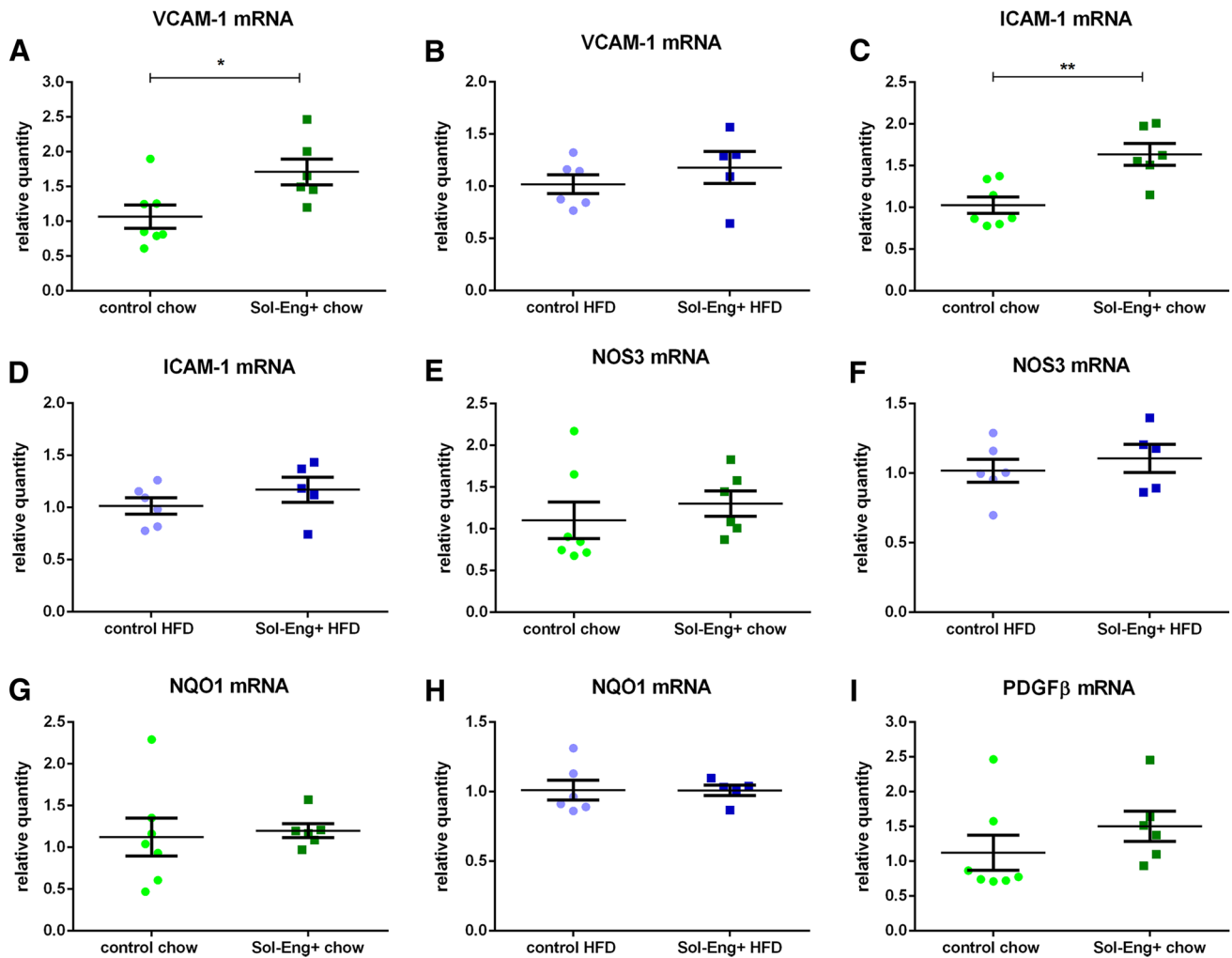


Fig. 2 Gene expression of inflammatory, oxidative stress and heart remodeling markers in the hearts of *Sol-Eng+* and control mice fed either chow diet or high-fat diet. Relative gene expression of VCAM-1 (a), ICAM-1 (c), NOS3 (e), NQO1 (g), PDGFβ (i), Col1A1 (k) and Myh7 (m) between control chow and *Sol-Eng+* chow mice

and relative gene expression of VCAM-1 (b), ICAM-1 (d), NOS3 (f), NQO1 (h), PDGFβ (j), Col1A1 (l) and Myh7 (n) between control HFD and *Sol-Eng+* HFD mice. Error line segment indicating mean ± SEM, Mann–Whitney test. * $p \leq 0.05$, ** $p \leq 0.01$

High-soluble endoglin levels do not induce upregulation of Id-1, ALK-5, pSmad 1,5 and pSmad 2,3 at the protein level in mice fed either chow diet or high-fat diet

Western blot analysis was also performed to confirm the significant upregulation of Id-1, ALK-5 and endoglin in *Sol-Eng+* chow mice compared to control chow mice and the significant downregulation of Id-1 in *Sol-Eng+* HFD mice compared to control HFD mice at the mRNA level. Subsequently, the evaluation of activated transcription factors pSmad 1,5 and pSmad 2,3 was done. Protein evaluation of Id-1 (Fig. 6a), ALK-5 (Fig. 6b) did not show any

significant differences between *Sol-Eng+* chow and control chow mice. Protein expression of the membrane-bound mouse endoglin turned out below detection limit in both groups of mice (data not shown). Similarly, protein evaluation of Id-1 (Fig. 6c) did not show any significant difference between *Sol-Eng+* HFD and control HFD mice. Protein expression of pSmad 1,5 did not show any significant difference between *Sol-Eng+* chow and control chow mice (Fig. 6d), as well as between *Sol-Eng+* HFD and control HFD mice (Fig. 6e). Similarly, protein expression of pSmad 2,3 did not show any significant difference between *Sol-Eng+* chow and control chow mice (Fig. 6f), as well as between *Sol-Eng+* HFD and control HFD mice (Fig. 6g).

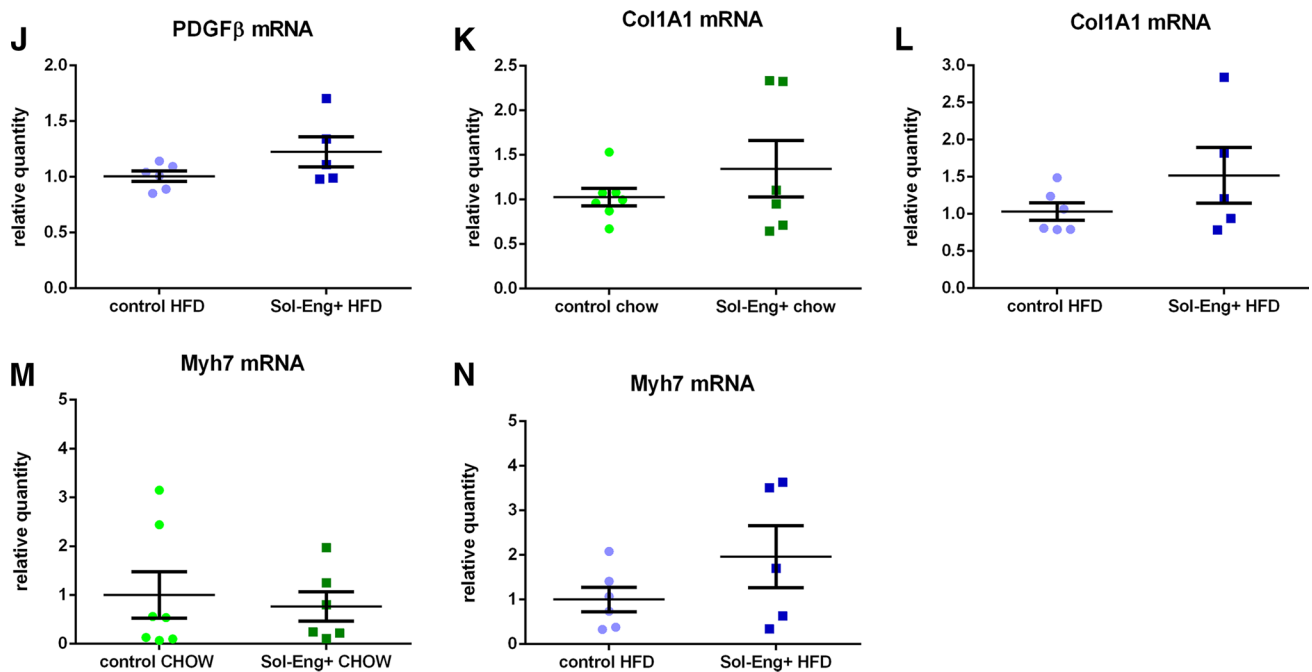


Fig. 2 continued

Discussion

Recently published data suggest that sEng may actively promote cardiovascular pathologies. In this line, administration of recombinant sEng to rats interfered with TGF- β 1 binding to TGF- β receptor II and reduced Smad2/3 signaling, which resulted in an inhibition of eNOS-dependent vasodilatation in isolated rat renal microvessels and mesenteric vessels [2]. In another study, Walshe et al. demonstrated that sEng neutralizes TGF- β and VEGF effects, which results in a subsequent increase of P-selectin expression and leukocyte rolling to endothelium, elevated levels of soluble E-selectin and soluble VCAM-1 and impaired vasodilatation [7]. It was also proposed that sEng antagonizes the function of membrane endoglin. Thus, Rossi et al. showed that sEng modulates leukocyte and smooth muscle cell adhesion to endothelium by interfering with membrane endoglin [24, 25].

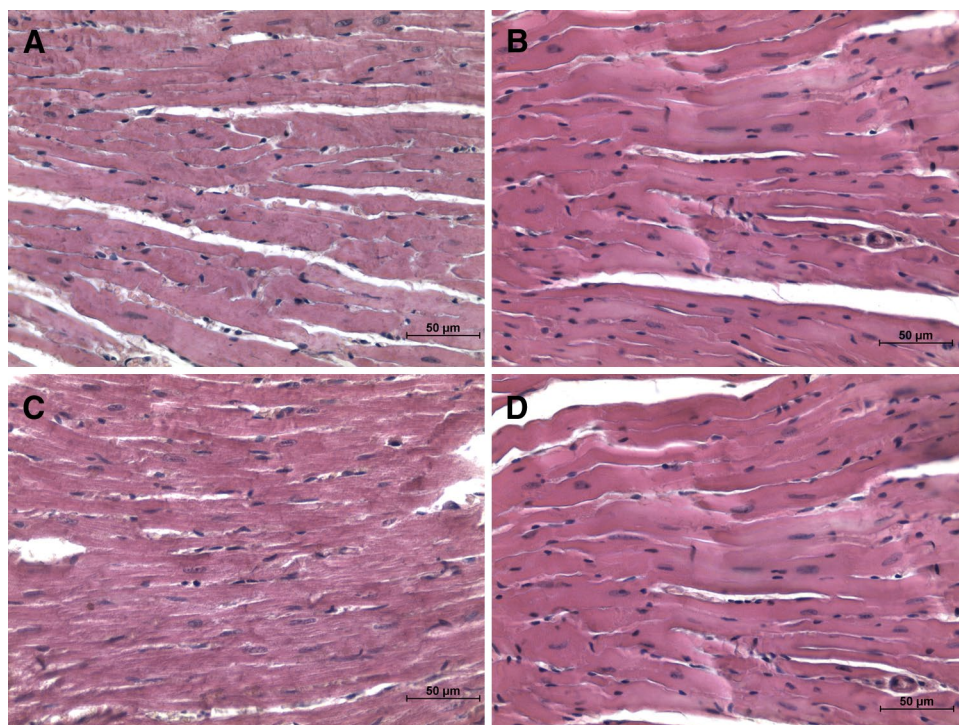
Taken together, sEng seems to induce signs of endothelial dysfunction and inflammation in different parts of the vascular bed, suggesting that it might be considered as a risk factor of cardiovascular diseases. Indeed, mice overexpressing human sEng have higher systolic blood pressure when compared to wild-type littermates, although the precise mechanism of hypertension development is unknown [11]. Endothelial dysfunction and arterial hypertension represent risk factors alteration of heart (e.g. hypertrophy, fibrosis and heart failure) [26]. Therefore, we hypothesized that high levels of sEng may induce pathological changes

in the heart due to induced hypertension, endothelial dysfunction in heart vessels and/or by interfering with TGF- β 1 signaling in mice on chow and high-fat diet.

A transgenic mouse expressing high levels of human sEng is a well-defined animal model used in previous studies [11, 20]. In our previous studies in transgenic mice fed either chow [20] or high-fat diet [22], neither high levels of sEng alone, nor a combination of hyperlipidemia (caused by a high-fat diet) together with high sEng levels affected any morphological or structural parameters in vessel (aorta) in male mice. The changes were detected only in female aortas. Therefore, we performed this study of mouse myocardium only in females. Thus, in this study, we used the same groups of female mice (not male mice) as described previously [20, 22], this time focusing on heart samples.

In the first part of this study, we focused on mice fed by chow diet. The results of our study showed no difference in myocardial morphology/hypertrophy and possible fibrotic changes between *Sol-Eng+* mice and control mice was detected. Furthermore, we assessed possible molecular changes in the heart. Soluble endoglin was reported to interfere with TGF- β signaling (Smad 2/3) [2]. In addition, sEng was shown to scavenge the ligand BMP-9 and thus affect ALK-1/Smad 1,5,8 signaling [17]. At the level of heart pathology, sEng was demonstrated to interfere with TGF- β 1/collagen signaling leading in suppression of collagen I formation [18] and even reduction of fibrosis in the area of myocardial infarction scar [27]. Therefore, we expected that the proposed sEng interaction with TGF- β signaling

Fig. 3 Representative microphotographs of hematoxylin–eosin staining of the hearts from control and *Sol-Eng*+ mice fed either chow diet or high-fat diet. No differences between hearts (myocardium) from control chow mice (**a**), *Sol-Eng*+ chow mice (**b**), control HFD mice (**c**) and *Sol-Eng*+ HFD mice (**d**) were visible in nuclei and cardiomyocytes structure. No inflammatory infiltration was visible as well. Bar 50 μ m



might be also detected in the heart in this study. However, no significant effects of high sEng levels on any member of TGF- β signaling was shown for membrane endoglin, TGF β RII, ALK-5, ALK-1, Id-1, PAI-1 and activated Smad proteins (pSmad 1,5 and pSmad 2,3), suggesting that high levels of sEng do not affect TGF- β signaling, at least with respect to studied markers in the heart of these mice.

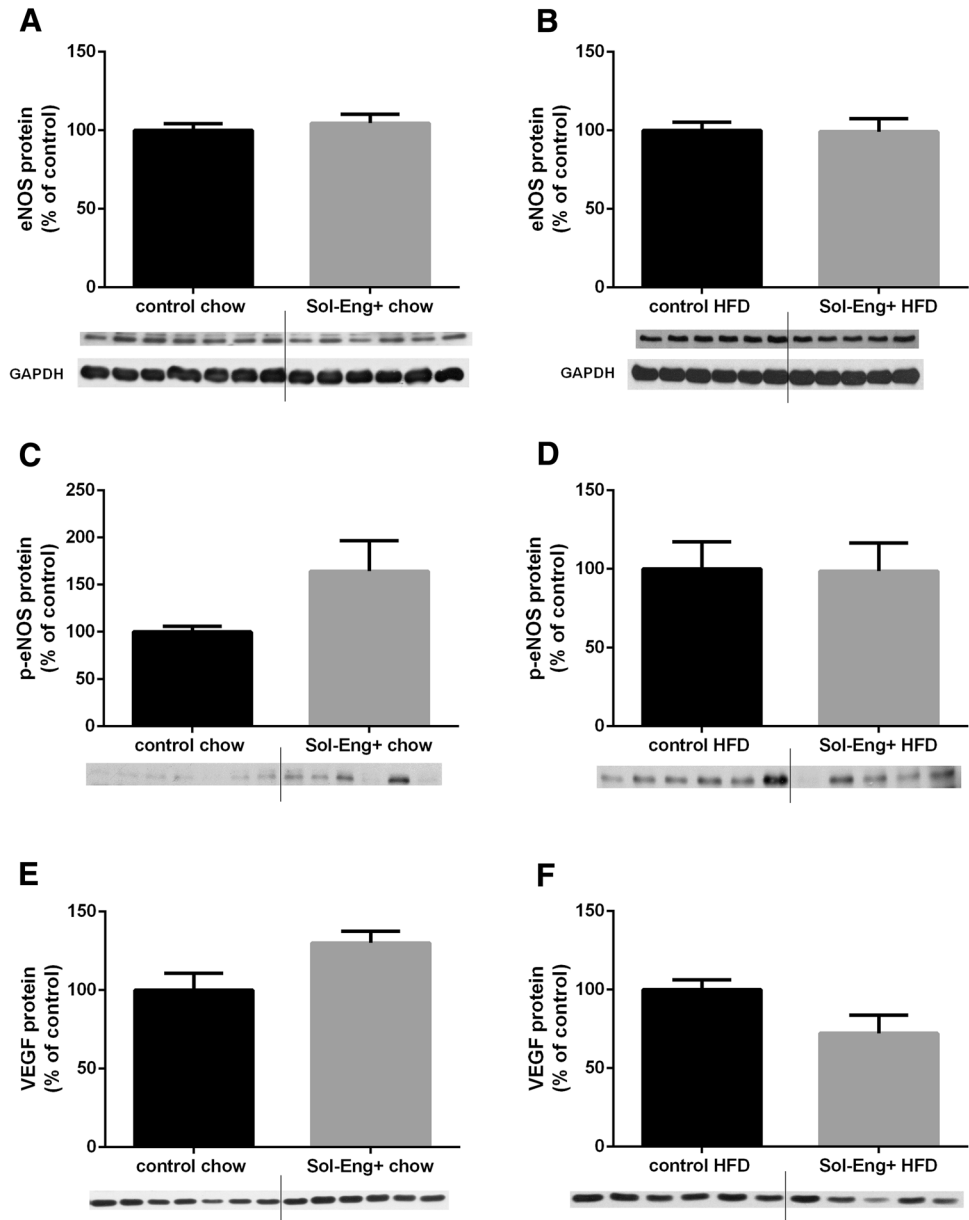
As mentioned above, sEng was shown to induce inflammation and signs of endothelial dysfunction in various parts of the vascular bed [2, 7]. We aimed to evaluate whether any similar effects were also evident in the heart. In this study, we did not reveal any inflammatory changes (the mild ICAM-1 and VCAM-1 mRNA upregulation in *Sol-Eng*+ chow mice were not confirmed at the protein level) in *Sol-Eng*+ mice fed chow diet compared to their relevant control group. Even any endothelial function-related markers, possibly represented by changes of eNOS, peNOS, VEGF and oxidative stress markers were not detected in *Sol-Eng*+ mice fed chow diet when compared to the relevant control group.

Taken together, the results of a “chow diet part” of this study show that high levels of sEng do not induce any functional or morphological changes in the heart. These data are in agreement with results of Nemeckova et al. showing that high plasma sEng levels did not cause any alterations in aortic vascular function, inflammation status or endothelial dysfunction markers in aortas from *Sol-Eng*+ mice [20].

High levels of sEng were associated with hypercholesterolemia in both humans and mice [6]. Thus, we aimed to simulate this condition, in a “high-fat diet part” of this study. We hypothesized that high levels of sEng combined with hypercholesterolemia might act as a double risk factor on cardiovascular system. It should be noted that the term high-fat diet is commonly used for various types of diets that are used in mice experiments. We used high-fat rodent diet with 1.25% cholesterol and 40% of fat. Administration of this high-fat diet in a combination with high levels of sEng induced a mild hypercholesterolemia (3 mmol/l) in these animals, which was accompanied by induction of inflammation and oxidative stress in aortas of *Sol-Eng*+ female mice in our recent paper [22].

Thus, we used the same mice to evaluate whether the combination of sEng levels and hypercholesterolemia affects the expressions of the same markers in the heart we studied in mice on chow diet. Surprisingly, the administration of high-fat diet (combined with high-soluble endoglin levels) did not result in significant differences in either myocardial morphology, profibrotic changes or inflammatory infiltration in both control and *Sol-Eng*+ mice. In addition, no significant changes in the expression of the same proteins studied in mice on chow diet (TGF- β signaling, endothelial dysfunction, inflammation, oxidative stress) between control and *Sol-Eng*+ mice were detected. These data suggest that even the presence of

Fig. 4 Expression of endothelial function-related markers in the hearts of mice fed either chow diet or high-fat diet. Expression of eNOS (a, b), active phosphorylated form peNOS (c, d) and VEGF (e, f) in total protein extracts from mice hearts. *Top* densitometric analysis (control = 100%). *Bottom* representative immunoblots. Data are shown as mean \pm SEM, Mann–Whitney test

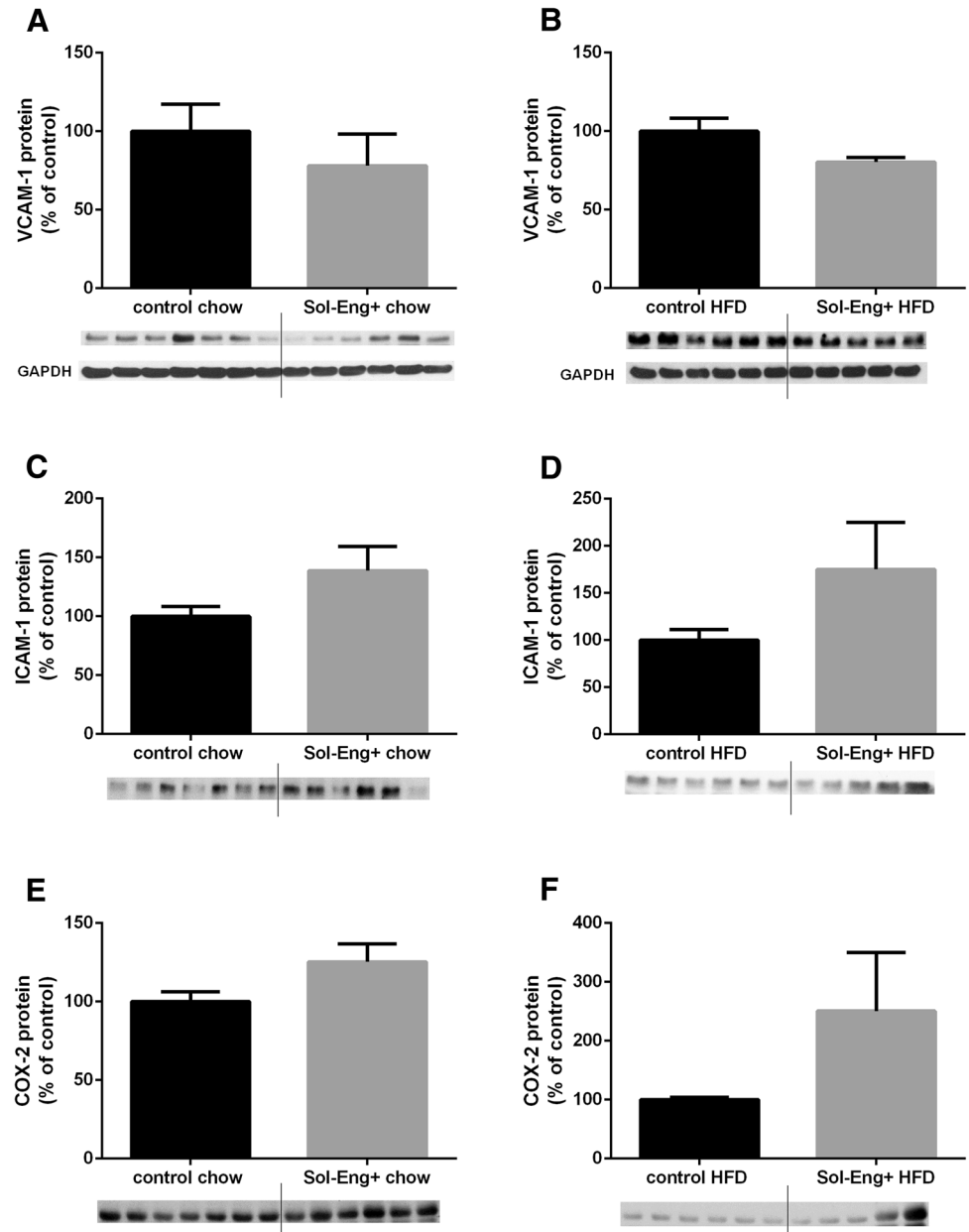


high-fat diet (mild hypercholesterolemia) does not potentiate the effects of sEng levels on the heart despite significant pro-inflammatory and oxidative effects demonstrated in aorta [22].

In conclusion, high levels of soluble endoglin do not affect microscopic structure (profibrotic and degenerative cardiomyocyte changes), and specific parts of TGF- β signaling, endothelial function and inflammation in the heart

of *Sol-Eng+* mice fed chow diet. Despite the fact that an increase in soluble endoglin was often related to another cardiovascular risk factor (hypercholesterolemia), no changes in studied markers were also found in the hearts of mice fed high-fat diet. However, we cannot rule out a possibility that a long-term chronic exposure (9 months and more) to soluble endoglin alone or combined with other cardiovascular risk factors may contribute to alterations of

Fig. 5 Expression of pro-inflammatory proteins in the hearts of mice fed either chow diet or high-fat diet. Expression of VCAM-1 (a, b), ICAM-1 (c, d) and COX-2 (e, f) in total protein extracts from mice hearts. *Top* densitometric analysis (control = 100%). *Bottom* representative immunoblots. Data are shown as mean \pm SEM, Mann–Whitney test



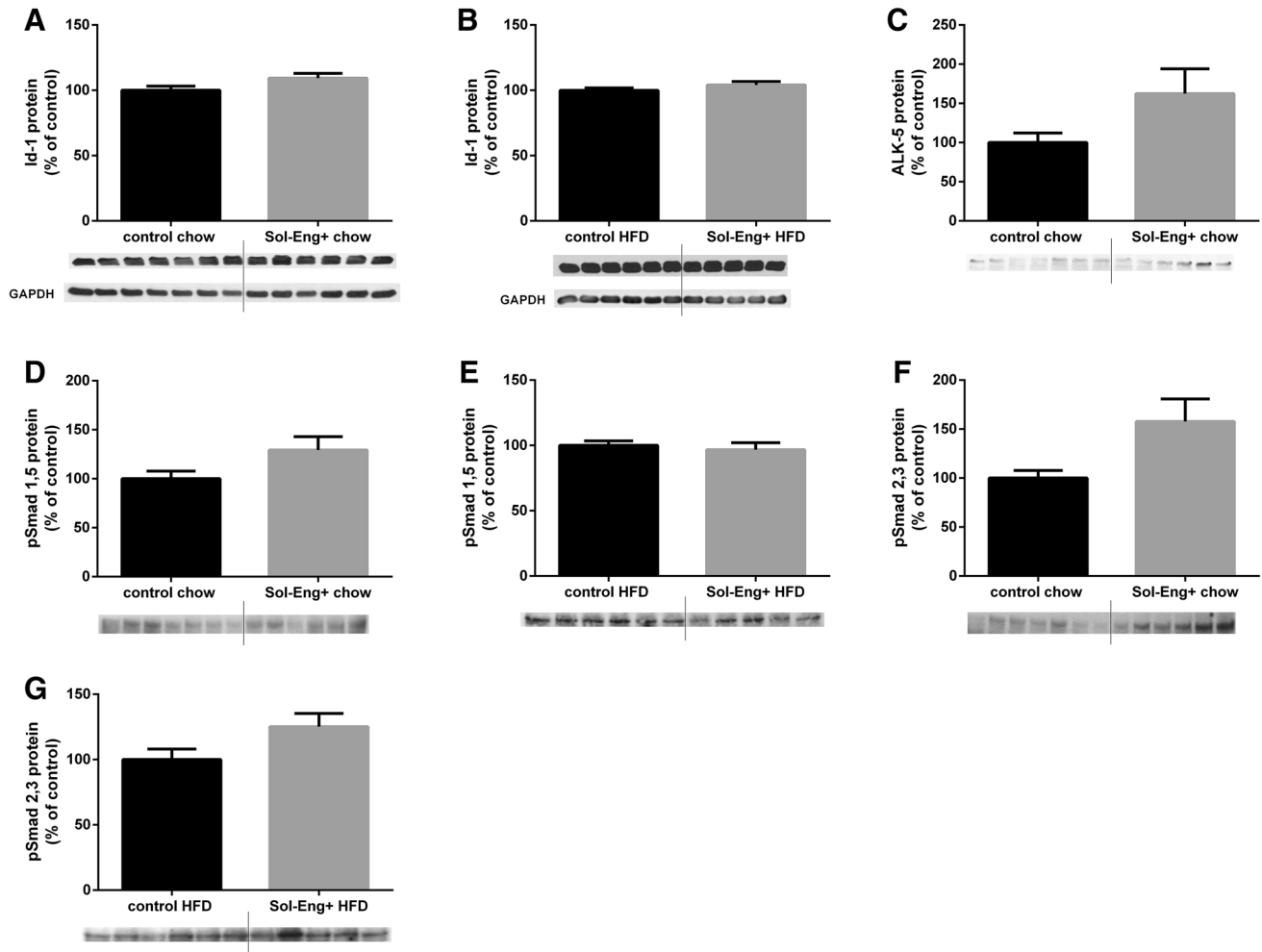


Fig. 6 Protein expression of Id-1, ALK-5, pSmad 1,5 and pSmad 2,3 in the hearts of mice fed either chow diet or high-fat diet. Expression of Id-1 (a, b), ALK-5 (c), pSmad 1,5 (d, e) and pSmad 2,3 (f, g)

in total protein extracts from mice hearts. *Top* densitometric analysis (control = 100%). *Bottom* representative immunoblots. Data are shown as mean \pm SEM, Mann–Whitney test

heart function and structure in *Sol-Eng+* mice, which is the topic in our lab in ongoing experiments.

Acknowledgements The work was supported by grants from Czech Science Foundation GACR number GA15-24015S, the Grant Agency of Charles University in Prague Number 1284214/C, and Grant SVV/2017/260414, Ministerio de Economía y Competitividad of Spain (SAF2013-43421-R to CB and SAF2013-45784-R to JML-N), Junta de Castilla y León (GR100 to JML-N), Centro de Investigación Biomédica en Red de Enfermedades Raras (CIBERER; to CB) and Red de Investigación Cooperativa en Enfermedades Renales (RD12/0021/0032; REDINREN, JML-N). CIBERER and REDINREN are initiatives of the Instituto de Salud Carlos III (ISCIII) of Spain supported by FEDER funds. The Cardiovascular Phenotyping Unit of the University of Salamanca was acquired with the support of the European Regional Development Funds (FEDER). We would like to give a special thanks to prof. Jose Miguel Lopez-Novoa and prof. Carmelo Bernabeu for the critical revision of the manuscript.

Compliance with ethical standards

Conflict of interest The authors declare that they have no competing interests.

References

- Gallardo-Vara E, Blanco FJ, Roque M, Friedman SL, Suzuki T, Botella LM, Bernabeu C (2016) Transcription factor KLF6 upregulates expression of metalloprotease MMP14 and subsequent release of soluble endoglin during vascular injury. *Angiogenesis* 19:155–171
- Venkatesha S, Toporsian M, Lam C, Hanai J, Mammoto T, Kim YM, Bdoolah Y, Lim KH, Yuan HT, Libermann TA, Stillman IE, Roberts D, D'Amore PA, Epstein FH, Sellke FW, Romero R, Sukhatme VP, Letarte M, Karumanchi SA (2006) Soluble

- endoglin contributes to the pathogenesis of preeclampsia. *Nat Med* 12:642–649
3. Blann AD, Wang JM, Wilson PB, Kumar S (1996) Serum levels of the TGF-beta receptor are increased in atherosclerosis. *Atherosclerosis* 120:221–226
 4. Blazquez-Medela AM, Garcia-Ortiz L, Gomez-Marcos MA, Recio-Rodriguez JI, Sanchez-Rodriguez A, Lopez-Novoa JM, Martinez-Salgado C (2010) Increased plasma soluble endoglin levels as an indicator of cardiovascular alterations in hypertensive and diabetic patients. *BMC Med* 8:86
 5. Cruz-Gonzalez I, Pabon P, Rodriguez-Barbero A, Martin-Moreiras J, Pericacho M, Sanchez PL, Ramirez V, Sanchez-Ledesma M, Martin-Herrero F, Jimenez-Candil J, Maree AO, Sanchez-Rodriguez A, Martin-Luengo C, Lopez-Novoa JM (2008) Identification of serum endoglin as a novel prognostic marker after acute myocardial infarction. *J Cell Mol Med* 12:955–961
 6. Rathouska J, Jezkova K, Nemeckova I, Nachtigal P (2015) Soluble endoglin, hypercholesterolemia and endothelial dysfunction. *Atherosclerosis* 243:383–388
 7. Walshe TE, Dole VS, Maharaj AS, Patten IS, Wagner DD, D'Amore PA (2009) Inhibition of VEGF or TGF- β signaling activates endothelium and increases leukocyte rolling. *Arterioscler Thromb Vasc Biol* 29:1185–1192
 8. Ling S, Nheu L, Komesaroff PA (2012) Cell adhesion molecules as pharmaceutical target in atherosclerosis. *Mini Rev Med Chem* 12:175–183
 9. Garcia-Prieto CF, Hernandez-Nuno F, Rio DD, Ruiz-Hurtado G, Aranguiz I, Ruiz-Gayo M, Somoza B, Fernandez-Alfonso MS (2015) High-fat diet induces endothelial dysfunction through a down-regulation of the endothelial AMPK-PI3K-Akt-eNOS pathway. *Mol Nutr Food Res* 59:520–532
 10. Darabi F, Aghaei M, Movahedian A, Elahifar A, Pourmoghadas A, Sarrafzadegan N (2016) Association of serum microRNA-21 levels with Visfatin, inflammation, and acute coronary syndromes. *Heart Vessels*. doi:10.1007/s00380-016-0913-z
 11. Valbuena-Diez AC, Blanco FJ, Oujó B, Langa C, Gonzalez-Nunez M, Llano E, Pendas AM, Diaz M, Castrillo A, Lopez-Novoa JM, Bernabeu C (2012) Oxysterol-induced soluble endoglin release and its involvement in hypertension. *Circulation* 126:2612–2624
 12. Medvedev NV, Gorshukova NK (2013) Pathogenetic significance of interstitial fibrosis in development myocardial dysfunction and chronic heart failure in elderly patients with arterial hypertension. *Adv Gerontol* 26:130–136
 13. Andrae J, Gallini R, Betsholtz C (2008) Role of platelet-derived growth factors in physiology and medicine. *Genes Dev* 22:1276–1312
 14. Fan B, Ma L, Li Q, Wang L, Zhou J, Wu J (2014) Role of PDGFs/PDGFRs signaling pathway in myocardial fibrosis of DOCA/salt hypertensive rats. *Int J Clin Exp Pathol* 7:16–27
 15. Querejeta R, Lopez B, Gonzalez A, Sanchez E, Larman M, Martinez Ubago JL, Diez J (2004) Increased collagen type I synthesis in patients with heart failure of hypertensive origin: relation to myocardial fibrosis. *Circulation* 110:1263–1268
 16. Lopez-Novoa JM, Bernabeu C (2010) The physiological role of endoglin in the cardiovascular system. *Am J Physiol Heart Circ Physiol* 299:H959–H974
 17. Gregory AL, Xu G, Sotov V, Letarte M (2014) Review: the enigmatic role of endoglin in the placenta. *Placenta* 35(Suppl):S93–S99
 18. Kapur NK, Wilson S, Yunis AA, Qiao X, Mackey E, Paruchuri V, Baker C, Aronovitz MJ, Karumanchi SA, Letarte M, Kass DA, Mendelsohn ME, Karas RH (2012) Reduced endoglin activity limits cardiac fibrosis and improves survival in heart failure. *Circulation* 125:2728–2738
 19. Morine KJ, Qiao X, Paruchuri V, Aronovitz MJ, Mackey EE, Buiten L, Levine J, Ughreja K, Nepali P, Blanton RM, Karas RH, Oh SP, Kapur NK (2017) Conditional knockout of activin like kinase-1 (ALK-1) leads to heart failure without maladaptive remodeling. *Heart Vessels*. doi:10.1007/s00380-017-0955-x
 20. Nemeckova I, Serwaczak A, Oujó B, Jezkova K, Rathouska J, Fikrova P, Varejkova M, Bernabeu C, Lopez-Novoa JM, Chlopicki S, Nachtigal P (2015) High soluble endoglin levels do not induce endothelial dysfunction in mouse aorta. *PLoS One* 10:e0119665
 21. Oujó B, Perez-Barriocanal F, Bernabeu C, Lopez-Novoa JM (2013) Membrane and soluble forms of endoglin in preeclampsia. *Curr Mol Med* 13:1345–1357
 22. Jezkova K, Rathouska J, Nemeckova I, Fikrova P, Dolezelova E, Varejkova M, Vitverova B, Tysonova K, Serwaczak A, Buczek E, Bernabeu C, Lopez-Novoa JM, Chlopicki S, Nachtigal P (2016) High levels of soluble endoglin induce a proinflammatory and oxidative-stress phenotype associated with preserved NO-dependent vasodilatation in aortas from mice fed a high-fat diet. *J Vasc Res* 53:149–162
 23. Livak KJ, Schmittgen TD (2001) Analysis of relative gene expression data using real-time quantitative PCR and the 2^{-Delta Delta C(T)} Method. *Methods* 25:402–408
 24. Rossi E, Sanz-Rodriguez F, Eleno N, Duwell A, Blanco FJ, Langa C, Botella LM, Cabanas C, Lopez-Novoa JM, Bernabeu C (2013) Endothelial endoglin is involved in inflammation: role in leukocyte adhesion and transmigration. *Blood* 121:403–415
 25. Rossi E, Smadja DM, Boscolo E, Langa C, Arevalo MA, Pericacho M, Gamella-Pozuelo L, Kauskot A, Botella LM, Gaussem P, Bischoff J, Lopez-Novoa JM, Bernabeu C (2016) Endoglin regulates mural cell adhesion in the circulatory system. *Cell Mol Life Sci* 73:1715–1739
 26. Frohlich ED (2000) Ischemia and fibrosis: the risk mechanisms of hypertensive heart disease. *Braz J Med Biol Res* 33:693–700
 27. Tseliou E, Reich H, de Couto G, Terrovitis J, Sun B, Liu W, Marban E (2014) Cardiospheres reverse adverse remodeling in chronic rat myocardial infarction: roles of soluble endoglin and Tgf-beta signaling. *Basic Res Cardiol* 109:443

Regulation and role of endoglin in cholesterol-induced endothelial and vascular dysfunction *in vivo* and *in vitro*

Matej Vicen,^{*,1} Barbora Vitverova,^{*,1} Radim Havelek,[†] Katerina Blazickova,^{*} Miloslav Machacek,[‡] Jana Rathouska,^{*} Iveta Najmanová,^{*} Eva Dolezelova,^{*} Alena Prasnicka,^{*} Magdalena Sternak,[§] Carmelo Bernabeu,^{¶,||} and Petr Nachtigal^{*,2}

^{*}Department of Biological and Medical Sciences, [†]Department of Biochemical Sciences, Faculty of Pharmacy in Hradec Kralove, and

[‡]Department of Medical Biochemistry, Faculty of Medicine in Hradec Kralove, Charles University, Hradec Kralove, Czech Republic;

[§]Jagiellonian Centre for Experimental Therapeutics (JCET), Bobrzynskiego, Krakow, Poland; and [¶]Center for Biological Research, Spanish National Research Council (CSIC) and ^{||}Biomedical Research Networking Center on Rare Diseases (CIBERER), Madrid, Spain

ABSTRACT: Our objective was to investigate the effect of cholesterol [hypercholesterolemia and 7-ketocholesterol (7K)] on endoglin (Eng) expression and regulation with respect to endothelial or vascular dysfunction *in vivo* and *in vitro*. *In vivo* experiments were performed in 2-mo-old atherosclerosis-prone apolipoprotein E-deficient/LDL receptor-deficient (ApoE^{-/-}/LDLR^{-/-}) female mice and their wild-type C57BL/6J littermates. In *in vitro* experiments, human aortic endothelial cells (HAECs) were treated with 7K. ApoE^{-/-}/LDLR^{-/-} mice developed hypercholesterolemia accompanied by increased circulating levels of P-selectin and Eng and a disruption of NO metabolism. Functional analysis of the aorta demonstrated impaired vascular reactivity, and Western blot analysis revealed down-regulation of membrane Eng/Smad2/3/eNOS signaling in ApoE^{-/-}/LDLR^{-/-} mice. 7K increased Eng expression *via* Krüppel-like factor 6 (KLF6), liver X nuclear receptor, and NF-κB in HAECs. 7K-induced Eng expression was prevented by the treatment with 2-hydroxypropyl-β-cyclodextrin; 8-[[5-chloro-2-(4-methylpiperazin-1-yl) pyridine-4-carbonyl] amino]-1-(4-fluorophenyl)-4, 5-dihydrobenzo[g]indazole-3-carboxamide; or by KLF6 silencing. 7K induced increased adhesion and transmigration of monocytic human leukemia promonocytic cell line cells and was prevented by Eng silencing. We concluded that hypercholesterolemia altered Eng expression and signaling, followed by endothelial or vascular dysfunction before formation of atherosclerotic lesions in ApoE^{-/-}/LDLR^{-/-} mice. By contrast, 7K increased Eng expression and induced inflammation in HAECs, which was followed by an increased adhesion and transmigration of monocytes *via* endothelium, which was prevented by Eng inhibition. Thus, we propose a relevant role for Eng in endothelial or vascular dysfunction or inflammation when exposed to cholesterol.—Vicen, M., Vitverova, B., Havelek, R., Blazickova, K., Machacek, M., Rathouska, J., Najmanová, I., Dolezelova, E., Prasnicka, A., Sternak, M., Bernabeu, C., Nachtigal, P. Regulation and role of endoglin in cholesterol-induced endothelial and vascular dysfunction *in vivo* and *in vitro*. FASEB J. 33, 6099–6114 (2019). www.fasebj.org

KEY WORDS: hypercholesterolemia · oxysterols · endothelial cells · mice

Endoglin (Eng), also known as CD105 and TGF-β receptor III, is a homodimeric transmembrane glycoprotein that is predominantly expressed in arterial endothelial cells (1). It is an important regulator of TGF-β signaling in different physiologic and pathologic conditions. Moreover, a soluble Eng (sEng) is released into the blood circulation after

ABBREVIATIONS: 7K, 7-ketocholesterol; Ach, acetylcholine; ApoE^{-/-}/LDLR^{-/-}, apolipoprotein E-deficient/LDL receptor-deficient; EGM-2, endothelial growth medium 2; Eng, endoglin; FBS, fetal bovine serum; GAPDH, glyceraldehyde 3-phosphate dehydrogenase; HAEC, human aortic endothelial cell; HIF-1α, hypoxia-inducible factor 1α; HO-1, heme oxygenase-1; ICAM-1, intercellular cell adhesion molecule 1; KCl, potassium chloride; KLF6, Krüppel-like factor 6; L-NAME, Nω-nitro-L-arginine methyl ester; LXR, liver X nuclear receptor; MLC, myosin light chain; MMP-14, matrix metalloproteinase-14; NO₃⁻, nitrate; NR1H3, LXRα variant 1 member 3 gene; oxLDL, oxidized LDL; PE, phenylephrine; p-eNOS, phosphorylated eNOS; PHA-408, 8-[[5-chloro-2-(4-methylpiperazin-1-yl) pyridine-4-carbonyl] amino]-1-(4-fluorophenyl)-4,5-dihydrobenzo[g]indazole-3-carboxamide; pMLC Thr18/Ser19, phosphorylated MLC on residues threonine 18 and serine 19; pSmad2/3, phosphorylated Smad2/3; RELA, NF-κB phosphorylated on carbon 65; sEng, soluble Eng; SNP, sodium nitroprusside; THP-1, human acute monocytic leukemia cell line; WT, wild type

¹ These authors contributed equally to this work.

² Correspondence: Department of Biological and Medical Sciences, Faculty of Pharmacy in Hradec Kralove, Charles University, Heyrovského 1203, Hradec Kralove 500 05, Czech Republic. E-mail: petr.nachtigal@faf.cuni.cz

doi: 10.1096/fj.201802245R

proteolytic cleavage of the juxtamembrane region of membrane-bound Eng (2) in various pathologic conditions with potential involvement of matrix metalloproteinase-14 (MMP-14) as the major Eng shedding protease (3).

Membrane Eng expression is regulated by various transcription factors including Krüppel-like factor 6 (KLF6) (member of the zinc finger Krüppel-like factor family ubiquitously expressed in human tissues) (4), NF- κ B phosphorylated on carbon 65 (RELA) hypoxia-inducible factor 1 α (HIF-1 α) (inflammatory and oxidative stress pathway factors) (5–7), and liver X nuclear receptor (LXR; cholesterol metabolism related factor and oxysterol receptor) (8). In addition, it has been shown that Eng is involved in Smad2/3 phosphorylation (signaling), which results in regulation of expression and proper function of eNOS in endothelial cells and demonstrates a relationship between Eng and NO-dependent vasodilation (9, 10). Thus, Eng might be considered as a vasoprotective or endothelium protective agent. On the other hand, membrane Eng and sEng were proposed to be ligands for leukocyte integrins. It was suggested that Eng might participate in integrin-mediated inflammatory infiltration of leukocytes (11) and platelet adhesion to endothelium (12).

Hypercholesterolemia and/or increased levels of oxidized LDL (oxLDL) are crucial inducers of development of endothelial dysfunction, which is followed by atherogenesis as shown in experimental animal models as well as in humans (13). Cholesterol in blood especially the one accumulated in arterial intima can be modified by different mechanisms resulting in formation of oxysterols. LDL particles contain predominantly oxysterols of non-enzymatic origins. Among these, 7-ketocholesterol (7K) is a typical representative (14), and it is one of the most common oxysterols present in healthy human plasma (15). In addition, it was demonstrated that 7K promotes inflammation (16) and foam cell formation (17).

We previously demonstrated that Eng expression is detected only in endothelial cells in the aorta in a mouse model of atherosclerosis (1). Moreover, membrane Eng expression was reduced in advanced atherosclerotic plaques, whereas sEng levels were increased (18, 19). In addition, membrane Eng expression was decreased and sEng levels were increased when HUVECs were exposed to inflammatory stimulation by TNF- α for 24 h (20). Interestingly, membrane Eng and sEng were shown to participate in inflammatory infiltration of leukocytes both *in vivo* and *in vitro* (11, 21). These data suggest a complex regulated expression and function of Eng during endothelial dysfunction and inflammation, which are key early steps of atherogenesis.

The above-mentioned data clearly show discrepancies in the potential role Eng plays in *in vivo* studies simulating atherogenesis (macrocirculation) and *in vitro* studies focusing on different blood vessels (microcirculation).

Thus, in this paper, we aimed to combine the *in vivo* and *in vitro* approaches and focus on regulation of Eng expression and Eng-related signaling in aortic endothelial cells [mouse aorta and human aortic endothelial cells (HAECs)] under the “cholesterol attack” in order to elucidate the role of Eng in endothelial function or dysfunction.

Therefore, in the first part of this study, we hypothesized that hypercholesterolemia alters Eng expression and signaling with respect to endothelial function in aorta before formation of any atherosclerotic changes in wild-type (WT) C57BL/6J and hypercholesterolemic atherosclerosis-prone apolipoprotein E-deficient /LDL receptor-deficient (ApoE^{-/-}/LDLR^{-/-}) mice. In the second part, using HAECs, we hypothesized that 7K (mimicking hypercholesterolemia) affects membrane Eng expression and its involvement in monocyte adhesion and transmigration *in vitro*.

The results of this manuscript showed for the first time 3 main outcomes: 1) Hypercholesterolemia altered Eng expression and signaling followed by endothelial or vascular dysfunction before the formation of atherosclerotic changes in aorta (previous papers showed alteration of Eng expression and signaling but without functional consequences and in aorta with advanced atherosclerotic lesions); 2) 7K (simulating ox-LDL effects in *in vivo* experiments)-induced increase in Eng expression was regulated by simultaneous activation of 3 transcription factors, including KLF6, RELA (NF- κ B), and LXR α variant 1 member 3 gene (NR1H3); and 3) Eng might be involved in cholesterol-induced adhesion and transmigration of monocytes *via* endothelium.

MATERIALS AND METHODS

Animals and experimental design

ApoE^{-/-}/LDLR^{-/-} female mice ($n = 7$ in each group), the model initially described by Ishibashi *et al.* (22) and extensively characterized in previous studies (23, 24), were used in the current study at the age of 2 mo. C57BL/6J (WT) female mice ($n = 7$ in each group) were used for comparison and were obtained from the Jackson Laboratory (Bar Harbor, ME, USA). It is of interest to mention that in our hands female mice are easier to breed than male mice. All our previous studies with ApoE^{-/-}/LDLR^{-/-} mice were performed with female mice for consistency and comparative purposes. The animals were kept in controlled ambient conditions in a temperature-controlled room with a 12-h light/dark cycle with constant humidity and had access to tap water and standard chow diet *ad libitum*. WT and ApoE^{-/-}/LDLR^{-/-} mice were not cohoused in the same cages. At the age of 8 wk, mice were euthanized under general anesthesia induced by a combination of xylazine (10 mg/kg, i.p.) and ketamine (100 mg/kg, i.p.), and blood, urine, and aorta samples were harvested for further analysis.

All experiments were carried out in accordance with the standards established in the directive of the European Union (2010/63/EU), and all procedures were approved by the Ethical Committee for the Protection of Animals Against Cruelty at Faculty of Pharmacy, Charles University (Permit: 21558/2013-2).

Cell culture

HAECs are primary cells from pooled donors purchased from Lonza (Basel, Switzerland). HAECs were cultured on Petri dishes (TPP, Trasadingen, Switzerland) coated with gelatin (MilliporeSigma, Burlington, MA, USA) in endothelial growth medium (EGM-2; Lonza) with adequate supplements (Lonza) and 10% fetal bovine serum (FBS; MilliporeSigma) at 37°C and 5% CO₂. Gelatin acts as an extracellular matrix and helps HAECs to attach to the bottom of Petri dishes. All experiments were performed with HAECs passage 5 (cumulative population doubling

9–10). To avoid cell-cell contact inhibition, HAECs were passaged or premedicated after reaching of 80–90% confluence.

The human acute monocytic leukemia cell line (THP-1), with features of monocytes derived from blood plasma, was kindly provided by Soňa Čejková (Institute for Clinical and Experimental Medicine, Prague, Czech Republic) and used to study the effects of 7K. THP-1 cells were cultured in Rosewell Park Memorial Institute (RPMI) 1640 medium (Thermo Fisher Scientific, Waltham, MA, USA) and supplemented with penicillin-streptomycin (MilliporeSigma), glutamine (Glutamax; Thermo Fisher Scientific) and 10% FBS in nonadhesive flasks (SPL Life Sciences, Gyeonggi-do, South Korea). Cell density was maintained at a concentration of 0.1–0.9 million cells per milliliter of medium. For amplification, cells were split 1:3 after reaching a density of 0.8–0.9 million cells per milliliter.

Chemicals

7K, 2-hydroxypropyl β -cyclodextrin, 8-[[5-chloro-2-(4-methylpiperazin-1-yl)pyridine-4-carbonyl]amino]-1-(4-fluorophenyl)-4,5-dihydrobenzo[g]indazole-3-carboxamide (PHA-408), and *N,N'*-bis-[4-(4,5-dihydro-1H-imidazol-2-yl)phenyl]-3,3'-*p*-phenylenebis-acrylamide dihydrochloride were purchased from MilliporeSigma. Solutions of 7K were prepared just before cell premedication at 10 μ g/ml using 100 μ l ethanol (Penta, Prague, Czech Republic) as cosolvent to dissolve 1 mg of oxysterol in culture medium. The same amount of ethanol was added to control samples. Stock solution of PHA-408 was prepared using DMSO (MilliporeSigma) 25 μ l/125 μ g. Treatments were done with a medium containing 10% FBS. To analyze acute effects of oxysterols, we used doses of 5 and 10 μ g/ml. Dosage was selected according to preliminary dose and time-dependent experiments (unpublished results) and a previously published paper by Yamagata *et al.* (25). We used 2-hydroxypropyl β -cyclodextrin (for the inhibition of NR1H3/LXR) and PHA-408 (for the inhibition of NF- κ B) at a final concentration of 10 mM and 10 μ M, respectively.

Biochemical analysis

Total concentration of plasma cholesterol was measured enzymatically by conventional enzymatic diagnostic kits (Lachema, Brno, Czech Republic) and spectrophotometric analysis (cholesterol at 510 nm, Ultrospec III; Pfizer, New York City, NY, USA).

Luminex assay

Blood samples from mice were obtained from vena cava inferior and plasma levels of mouse sEng, and soluble P-selectin were determined by means of a Mouse Premixed Multi-Analyte Magnetic Luminex Kit (R&D Systems, Minneapolis, MN, USA), according to the manufacturer's protocol.

Measurement of plasma and urinary concentration of nitrate

The concentration of nitrate (NO_3^-) in plasma and urine was measured by an ENO-20 NO_x Analyzer (Eicom, Kyoto, Japan). The analysis is based on a liquid chromatography method with post-column derivatization using Griess reagent. NO_3^- was separated from other substances in matrices on a NO-PAK column (4.6 \times 50 mm; Eicom). Then, NO_3^- was reduced to nitrite using a cadmium-copper column (NO-RED; Eicom). Subsequently, nitrite was mixed with Griess reagent to form a purple azo dye in reaction coil placed in a column oven at 35°C. The absorbance of derivatives was measured at 540 nm. The flow rate of the mobile phase (carrier solution) was 330 μ l/min. The Griess

reagent (Reactor A and B Solution 1:1, v/v) was delivered by a pump at a flow rate of 110 μ l/min. Plasma samples were precipitated with methanol at a ratio of 1:1 (v/v), centrifuged at 10,000 *g* for 10 min, and the resulting supernatant was analyzed. To measure urinary NO_3^- concentration, urine samples were diluted 5-fold and analyzed directly (26, 27).

Functional analysis of vascular reactivity *ex vivo*

Aortic rings underwent cleaning, mounting, and measuring processes as previously described by Vitverova *et al.* (28). The change of contractile substance is the only difference from the previous protocol. Aortic rings were precontracted with increasing concentrations of phenylephrine (PE; 0.01–10 μ M).

Western blot analysis

The procedure was performed as previously reported by Nemeckova *et al.* (29). For the list of antibodies please see Table 1.

Elisa

HAECs were treated with 5 or 10 μ g/ml of 7K for 12 h and culture supernatants were collected and analyzed by ELISA assay (DNG00 Human Eng/CD105 Quantitative ELISA Kit; R&D Systems). Concentration of sEng was determined according to the manufacturer's protocol.

Real-time quantitative PCR

HAECs were treated with 5 or 10 μ g/ml of 7K for 12 h. The mRNA expression of glyceraldehyde 3-phosphate dehydrogenase (*GAPDH*; Hs02758991_g1), membrane Eng (Hs00923996_m1), *NR1H3* (Hs00172885_m1), *KLF6* (Hs00810569_m1), *RELA* (Hs00153294_m1), *eNOS* (Hs00167166_m1), and intercellular cell adhesion molecule 1 (*ICAM-1*; Hs00164932_m1) (all provided by Thermo Fisher Scientific) was evaluated using real-time quantitative PCR. *KLF6* and Eng silencing and treatment with either 2-hydroxypropyl- β -cyclodextrin or PHA-408 were followed by evaluation by means of the same set of genes. Tri reagent (MilliporeSigma) was used for isolation of RNA from HAECs. RNA was directly converted to cDNA using a cDNA Reverse Transcription Kit (Thermo Fisher Scientific). TaqMan Gene Expression Master Mix (Thermo Fisher Scientific) and predesigned TaqMan primers were used for amplification reaction 20 ng of cDNA. The relative expression ratio was calculated as previously described by Zemankova *et al.* (20). *GAPDH* was used as a reference for normalizing the data.

Immunofluorescence flow cytometry

After reaching 80–90% confluence, cells [WT, transfected or not with scrambled RNA (scRNA), *KLF6* or Eng small interfering RNA (siRNA)] were exposed to 7K (5 or 10 μ g/ml) for 12 h with or without 2-hydroxypropyl- β -cyclodextrin (11 h before experiment) or PHA-408 (12 h 10 min before experiment). Protein expression was evaluated by immunofluorescence flow cytometry analysis.

Direct flow cytometry was used for the detection of ICAM-1 and P/E-selectins on the cell surface. Cells were rinsed with PBS (prepared from tablets; MilliporeSigma) after 12 h of premedication, detached with trypsin (Biosera, Nuaille, France) and incubated with primary fluorescent-labeled mouse monoclonal

antibody against human ICAM-1 (R&D Systems) or P/E-selectins (R&D Systems).

Indirect flow cytometry was used for the detection of membrane Eng. Cells were rinsed with PBS after 12 h of premedication, detached with trypsin, and incubated with primary mouse monoclonal antibody against human Eng (P4A4; Developmental Studies Hybridoma Bank, The University of Iowa, Iowa, IA, USA). After 1 h incubation, cells were rinsed with PBS and incubated with secondary goat anti-mouse fluorescent-labeled antibody (Alexa 488; Thermo Fisher Scientific).

Intracellular flow cytometry was used for detection of phosphorylated Smad2/3 (pSmad2/3). Cells were rinsed with PBS and detached with trypsin. Subsequently, cells were fixed with 2% paraformaldehyde and permeabilized with 90% methanol before experiment. After the fixation and permeabilization period, the primary rabbit anti-human pAb (Cell Signaling Technology, Danvers, MA, USA) and fluorescent-labeled secondary chicken anti-rabbit antibody (Thermo Fisher Scientific) were used.

Determination of protein expression was performed on Cell Lab Quanta SC Flow Cytometer (Beckman Coulter, Brea, CA, USA). Results are presented as relative expression index, calculated as percentage of positive cells multiplied by the mean fluorescence intensity (30).

Cell transfections

HAECs were cultured on 6-well plates (KLF6 silencing; MilliporeSigma) or Petri dishes (Eng silencing; 60 cm², VWR) using EGM-2 with supplements until 80% confluence. Cells were rinsed with PBS and transfected in serum and antibiotic-free medium with silencing Krüppel-like factor 6 (siKLF6) (SC-38021; Santa Cruz Biotechnology, Dallas, TX, USA), silencing endoglin (siENG) (s4679 and s4677; Thermo Fisher Scientific), or scrambled RNA (SIC001-1; MilliporeSigma) mixed in Opti-MEM (Thermo Fisher Scientific) with Lipofectamin 3000 (siKLF6; Thermo Fisher Scientific) or RNAiMax (siENG; Thermo Fisher Scientific). The final siRNA concentration used for transfections was 16.34 nM/ml. After 5 h of incubation in a medium containing transfection reagents, it was replaced with complete EGM-2 containing 10% FBS. Thirty-six hours after transfection, cells were used for experiments according to the manufacturer's guidelines.

Immunofluorescence microscopy in chamber slides

HAECs were cultured on chamber slides (Eppendorf, Hamburg, Germany). After reaching 80–90% confluence, cells were treated with 10 µg/ml 7K, alone or in combination with 10 µM PHA-408, for 4 h. Cells were fixed and permeabilized with ice-cold acetone for 10 min. After blockage with 5% bovine serum albumin and 0.1% glycine in PBS, cells were incubated with primary rabbit anti-human antibody against RELA (NF-κB p65; Santa Cruz Biotechnology) overnight at 4°C. The next morning, cells were rinsed with PBS (MilliporeSigma) and incubated with secondary chicken anti-rabbit antibody (Thermo Fisher Scientific).

eNOS, phosphorylated eNOS (p-eNOS), and heme oxygenase-1 (HO-1) expression was quantified after 2.5 (p-eNOS), 6 (HO-1), or 12 (eNOS) h treatment with 5 or 10 µg/ml of 7K. After fixation, permeabilization, and blocking, cells were incubated with primary rabbit anti-human antibody against eNOS or p-eNOS (both from Santa Cruz Biotechnology) or with primary mouse anti-human antibody against HO-1 (Abcam, Cambridge, MA, USA) overnight at 4°C. The next morning, cells were rinsed with PBS (MilliporeSigma) and incubated with secondary chicken anti-rabbit antibody (Thermo Fisher Scientific) (eNOS, p-eNOS) or secondary goat anti-mouse antibody (Thermo Fisher Scientific) (HO-1). After rinsing with PBS, cells were incubated with DAPI (Thermo Fisher Scientific) for nuclear staining for 5 min. Chamber slides were

mounted using a solution of 1,4-diazabicyclo[2.2.2]octane (Dabco; MilliporeSigma) prepared with polyvinyl alcohol (MilliporeSigma), Tris-HCl (Serva, Heidelberg, Germany), and distilled water. Photomicrographs were obtained using confocal laser scanning microscope system (Nikon A1+; Nikon, Tokyo, Japan) and NIS Elements AR 4.02 software (Laboratory Imaging, Prague, Czech Republic). Six focal planes were imaged to cover the whole volume of the specimen in the field of view using ×20 objective lens and 405 and 488 nm lasers together with DAPI and FITC emission filters, respectively. Pinhole was set at 14 µm and laser power was kept as low as possible to prevent any photodamage to the specimen.

Cell adhesion assays

HAECs were cultured in EGM-2 on Petri dishes until 80–90% confluency and exposed, or not, to 10 µg/ml 7K for 12 h. THP-1 cells were added to HAECs; after 1 h coincubation, dishes were rinsed using PBS and nonadherent cells were removed. HAECs with adherent THP-1 cells were dissociated using acutase (Thermo Fisher Scientific). The cell mixture was stained on membrane Eng as previously mentioned and analyzed using a flow cytometer and Kaluza software. The method of negative cell sorting was used for detection and counting of the cells. For adhesion experiments on transfected cells, positive sorting of THP-1 monocytes labeled with Vybrant-Dio (3 µl/ml 30 min before addition to HAECs) in combination with the inhibitor of exocytosis *N,N'*-bis-[4-(4,5-dihydro-1H-imidazol-2-yl)phenyl]-3,3'-*p*-phenylene-bis-acrylamide dihydrochloride (15 µM 1 h before addition to HAECs) was used.

Cell transmigration assays

Monolayers of HAECs created from normal or transfected cells on the membrane of a transwell insert were used to mimic the endothelium of an aorta. HAECs were cultured on membranes of polycarbonate cell culture inserts in multidishes with 3-µm pore size (Nunc, Thermo Fisher Scientific) until 100% confluency. Then, complete EGM-2 (control, siENG group) or EGM-2 with 10 µg/ml 7K (siENG + 7K group) was added into the lower compartment. Approximately 100,000 of actively proliferating THP-1 cells were added into the upper compartment; after 12 h of incubation, transmigrated cells were counted in 100 µl of medium from the lower compartment using a flow cytometer (Beckman Coulter) and Kaluza analysis software.

Statistical analysis

The statistical analysis was performed by Prism 7.0 software and Outlier calculator (both from GraphPad Software, La Jolla, CA, USA). All data are presented as means ± SEM. All multiple comparisons were analyzed using ANOVA with a Kruskal-Wallis test and Dunnett's multiple comparisons test. Direct group-group comparisons were carried out using Mann-Whitney test. A value of $P \leq 0.05$ was the minimum requirement for a statistically significant difference.

RESULTS

ApoE^{-/-}/LDLR^{-/-} mice have elevated cholesterol levels, sEng levels, and inflammatory biomarkers in plasma

Biochemical and immunologic analyses of cholesterol, sEng, and inflammatory biomarkers were performed. We found significantly increased total cholesterol levels (1.53 ± 0.10 vs. 19.0 ± 1.57 mM) between WT and

ApoE^{-/-}/LDLR^{-/-} mice (Fig. 1A). In parallel with increased total cholesterol concentration, plasma levels of sEng were significantly higher in ApoE^{-/-}/LDLR^{-/-} (4817 ± 341 pg/ml) compared to WT mice (3010 ± 309 pg/ml) (Fig. 1B). Luminex analysis also showed elevated plasma concentration of P-selectin in the blood of ApoE^{-/-}/LDLR^{-/-} (60,013 ± 1747 pg/ml) compared to WT mice (38,548 ± 3321 pg/ml) (Fig. 1C).

We examined plasma and urinary levels of NO₃⁻ as a marker of NO metabolism. Determination of NO₃⁻

plasma concentration showed significant differences between ApoE^{-/-}/LDLR^{-/-} and WT mice (34.3 ± 3.10 vs. 65.3 ± 5.25 μM), respectively (Fig. 1D). Urinary NO₃⁻ excretion was also significantly decreased in ApoE^{-/-}/LDLR^{-/-} (524 ± 80.0 μM) compared to WT mice (2288 ± 206 μM) (Fig. 1E). As expected, ApoE^{-/-}/LDLR^{-/-} mice demonstrated a significant decrease in urine creatinine-normalized concentration of NO₃⁻ compared to WT mice (1.63 ± 0.30 vs. 3.74 ± 0.27 μM/μmol), respectively (Fig. 1F).

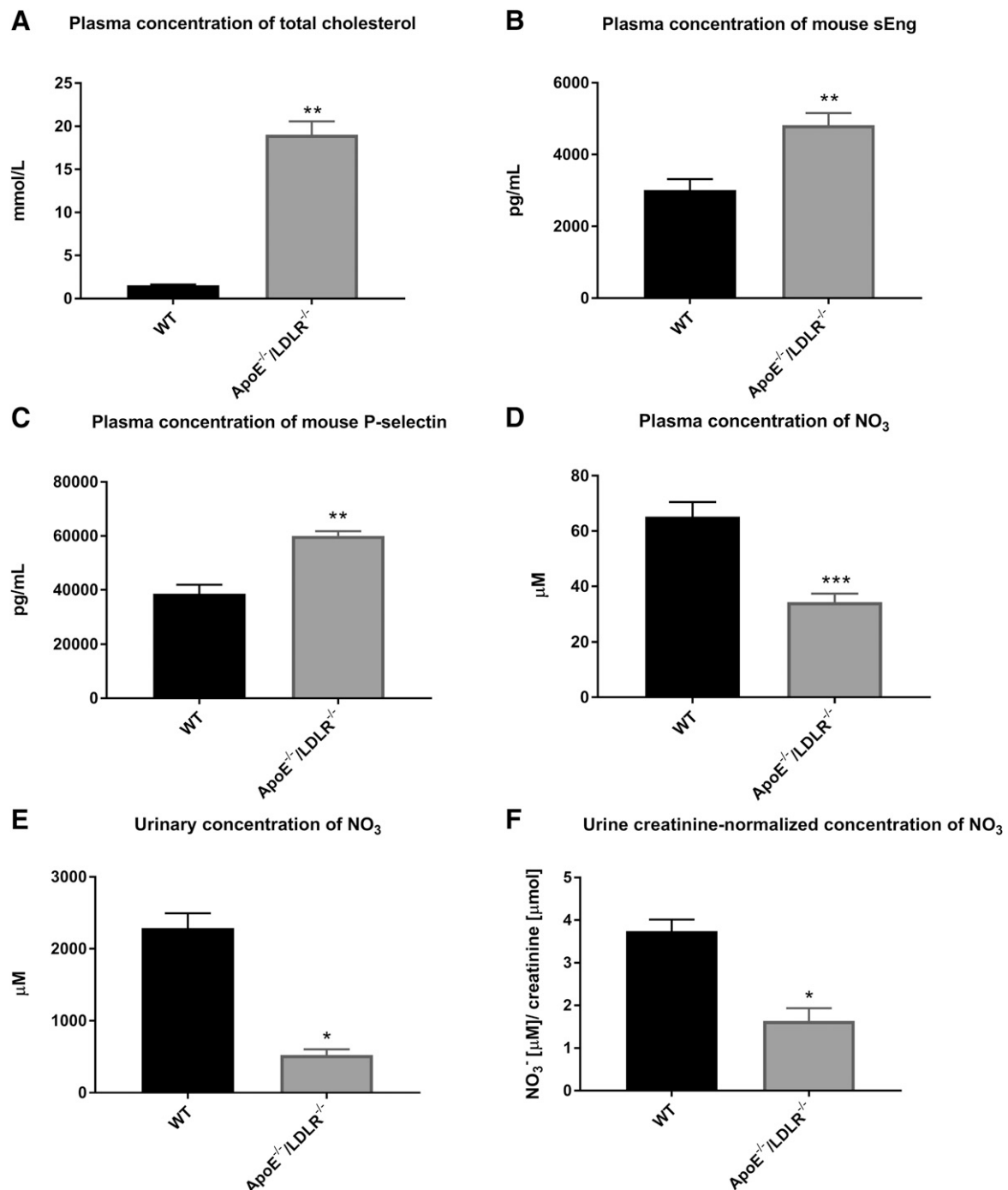


Figure 1. Biochemical and Luminex analyses of plasma. Plasma concentration of total cholesterol (A), mouse sEng (B), P-selectin (C), NO₃⁻ in plasma (D), NO₃⁻ in urine (E), and urine creatinine-normalized concentration of NO₃⁻ (F) in ApoE^{-/-}/LDLR^{-/-} and WT mice. Data are shown as means ± SEM, Mann-Whitney test (*n* = 7 mice/group). **P* ≤ 0.05, ***P* ≤ 0.01, ****P* ≤ 0.001.

Impaired vascular and endothelial function *ex vivo* in ApoE^{-/-}/LDLR^{-/-} mice

Vascular reactivity is primarily evaluated by administration of potassium chloride (KCl) that is able to evoke receptor-independent contraction based on membrane depolarization with subsequent increased cytosolic concentration of Ca²⁺ ions (31). We used KCl in concentration 60 mM to assess the maximal contractile response. As shown in Fig. 2A, the maximal contraction achieved in response to KCl was not significantly different between ApoE^{-/-}/LDLR^{-/-} and WT mice (3.56 ± 0.21 vs. 3.78 ± 0.35 mN). Next, increasing concentrations of PE (0.01–10 μM), an α-adrenergic vasoconstrictor, was used for precontraction of aortic rings prior to the next measurements. The maximal induced contraction after administration of PE (10 μM) showed no significant differences between ApoE^{-/-}/LDLR^{-/-} and WT mice (35.1 ± 5.70 vs. 27.4 ± 4.48%) (Fig. 2B).

Endothelium-dependent relaxation induced by cumulative concentrations of acetylcholine (ACh; 0.001–0.1 μM) was measured in PE precontracted aortic rings. ACh mediates relaxation *via* activation of muscarinic receptors type III that are responsible for synthesis of NO. We found that the maximal induced relaxation was not significantly different between ApoE^{-/-}/LDLR^{-/-} and WT mice (98.7 ± 13.6 vs. 97.1 ± 11.0% at 0.1 μM ACh) (Fig. 2C). For endothelium-independent relaxation, the vasodilator response in PE precontracted aortic rings was induced by cumulative concentrations of sodium nitroprusside (SNP; 0.001–0.1 μM), a direct NO donor. The maximal relaxation induced by SNP was significantly impaired in ApoE^{-/-}/LDLR^{-/-} compared to WT mice (31.1 ± 9.02 vs. 72.8 ± 8.43% at 0.1 μM SNP) (Fig. 2D). To determine the contribution of other sources of NO, different from the NO generated from L-arginine/eNOS cascade, N (ω)-nitro-L-arginine methyl ester (L-NAME; 300 μM) as a direct inhibitor of eNOS was used (23, 28). The effect of L-NAME on the maximal ACh-induced relaxation in PE precontracted aortic rings reached significantly increased values in ApoE^{-/-}/LDLR^{-/-} (10.5 ± 4.82%) compared to WT mice (2.44 ± 0.86%) (Fig. 2E).

Eng/Smad2/3/eNOS signaling is impaired in aortas of ApoE^{-/-}/LDLR^{-/-} mice

Because Eng regulates protein expression and function of eNOS (9, 10) and is involved in eNOS expression *via* Smad2/3 transcription factors (32), we examined the protein levels of membrane Eng, eNOS, and its active phosphorylated form p-eNOS Ser1177, as well as pSmad2/3 in mice aortas. Significantly reduced expression of membrane Eng (to 12%; Fig. 3A), eNOS (to 59%; Fig. 3B), p-eNOS Ser1177 (to 38%; Fig. 3C), and pSmad2/3 (to 71%; Fig. 3D) were observed in aortas of ApoE^{-/-}/LDLR^{-/-} mice when compared to WT mice. Next, we determined the protein level of MMP-14 previously reported to be involved in sEng shedding in preeclampsia (33). Interestingly, ApoE^{-/-}/LDLR^{-/-} mice displayed a significantly reduced expression of MMP-14 (to 20%; Fig. 3E) compared to WT mice.

Expression of HO-1, a carbon monoxide-releasing molecule, was measured to evaluate a possible involvement of this protein in the vasodilatory mechanism leading to an interaction with soluble guanylate cyclase and subsequently to higher NO release (34). In line with this, we observed a significantly lower expression of HO-1 (to 42%; Fig. 3F) in aortas of ApoE^{-/-}/LDLR^{-/-} mice compared to WT mice.

Myosin light chain (MLC) is a major regulatory component in vascular smooth muscle reactivity. To determine the activation status of MLC, expression of phosphorylated MLC on residues threonine 18 and serine 19 (pMLC Thr18/Ser19) was assessed. As shown in Fig. 3G, significantly lower expression of pMLC Thr18/Ser19 (to 67%) was demonstrated in aortas of ApoE^{-/-}/LDLR^{-/-} mice compared to WT mice.

7K increases Eng expression and induces endothelial dysfunction in HAECs

To assess whether the oxidized cholesterol contributes to the decrease in Eng expression of hypercholesterolemic mice, HAECs were incubated with 5 or 10 μg/ml of 7K. Significant increase in both Eng mRNA (131 ± 8.73 and 138 ± 5.77% of control, respectively; Fig. 4A) and protein (14,123 ± 1424 and 16,127 ± 1240, respectively, compared to control 6853 ± 465) levels was found after 12 h incubation (Fig. 4B). In addition, a significant dose-dependent increase in Eng protein levels was demonstrated by immunofluorescence flow cytometry as illustrated by means of representative histograms (Fig. 4C). It is of interest to mention that increase in membrane Eng protein levels after treatment with 7K was not followed by an increase in sEng levels (243 ± 37.7 and 279 ± 54.0 pg/ml, respectively, compared to control 334 ± 11.4 pg/ml) (Fig. 4D). Nevertheless, pSmad2/3 was significantly increased after 7K premedication (95.8 ± 18 and 77.5 ± 16.5 respectively compared to control 29 ± 2.8) (Fig. 4E).

Endothelial dysfunction in vascular endothelium is characterized by increased expression of proinflammatory cell adhesion molecules, including ICAM-1 and P/E-selectins. Therefore, we analyzed whether oxysterol treatment affects the expression of these proinflammatory markers. Treatment with 7K for 12 h significantly increased ICAM-1 mRNA expression (148 ± 5.70 and 262 ± 20.5% at 5 and 10 μg/ml of 7K, respectively; Fig. 4F). To confirm the hypothesis that 7K treatment can induce an endothelial dysfunction-like phenotype in HAECs, flow cytometry analysis of ICAM-1, and P/E-selectins protein levels was carried out. Protein levels of ICAM-1 were significantly increased at 2 different doses (5 and 10 μg/ml) of 7K (438 ± 23.3 and 715 ± 98.6, respectively, compared to control 78.7 ± 11.3; Fig. 4G, H). Similarly, protein levels of P/E-selectins were increased after treatment with 10 μg/ml 7K (97.7 ± 9.2 vs. 45.2 ± 4.22) but not at 5 μg/ml of 7K (Fig. 4I, J). Expression of HO-1 was significantly decreased after 7K treatment (1923 ± 22.8 and 1810 ± 18.1, respectively), compared to control values (2957 ± 29.6) (Fig. 4K).

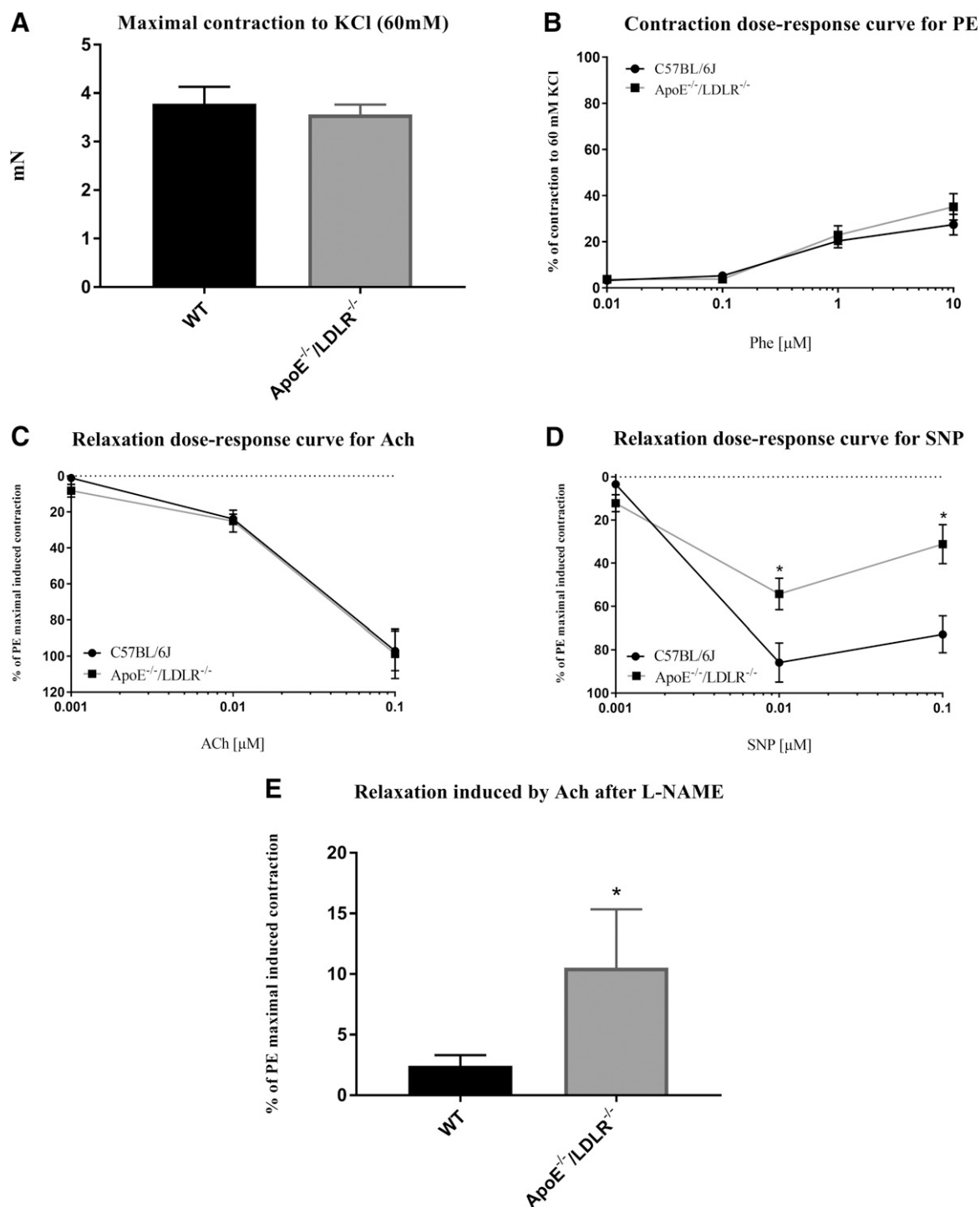


Figure 2. Vasomotor function evaluation of aorta. Maximal contraction to KCl (60 mM) (A), PE-induced contraction (B), Ach-induced relaxation in PE-precontracted aortic rings (C), SNP-induced relaxation in PE precontracted aortic rings (D), and inhibitory effect of L-NAME on eNOS-dependent, Ach-induced relaxation in PE-precontracted aortic rings (E) in ApoE^{-/-}/LDLR^{-/-} and WT mice. Data are shown as means \pm SEM, Mann-Whitney test ($n = 7$ mice/group). * $P \leq 0.05$.

Activation of eNOS signaling was detected at the mRNA level of eNOS (121.7 ± 4.9 and $176.8 \pm 7.3\%$ of control, respectively; Fig. 4L), and protein levels of eNOS (2412 ± 38 and 2195 ± 38.6 , respectively, compared to control 1120 ± 38 ; Fig. 4M) and p-eNOS (2548 ± 11.4 and 2565 ± 20 , respectively, compared to control 2075 ± 14.4 ; Fig. 4N). Representative confocal microscopy photomicrographs are displayed in Fig. 4O.

7K induces the expression of transcription factors involved in Eng regulation

It has been demonstrated that Eng expression is regulated by the activity of different transcription factors, including KLF6 (4, 35), RELA (p65 NF- κ B)-HIF-1 (6, 7), and LXR (NR1H3) (8, 36). In agreement with these findings, we found that the expression of the genes encoding these

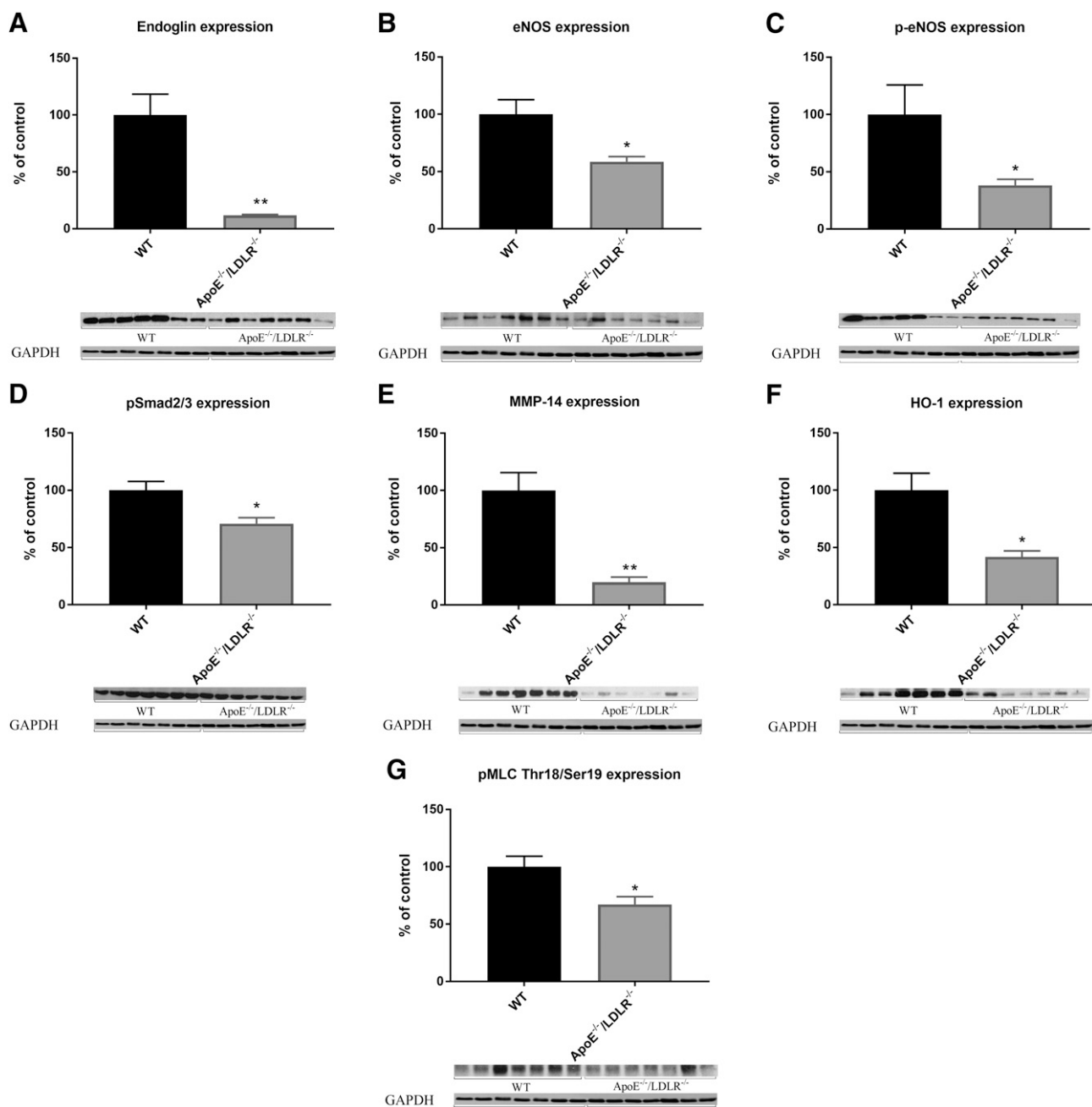


Figure 3. Western blot analysis of aortas from ApoE^{-/-}/LDLR^{-/-} and WT mice. The expression of membrane Eng (A), eNOS (B), p-eNOS-Ser1177 (C), pSmad2/3 (D), MMP-14 (E), HO-1 (F), and pMLC Thr18/Ser19 (G) in total protein extracts from mice aortas. Top: densitometric analysis (control = 100%). Equal loading of samples was confirmed by immunodetection of GAPDH. Bottom: representative immunoblots. Data are shown as means \pm SEM, Mann-Whitney test ($n = 7$ mice/group). * $P \leq 0.05$, ** $P \leq 0.01$.

proteins was significantly increased after premedication with 10 μ g/ml 7K ($127 \pm 6.40\%$ for KLF6; $143 \pm 4.64\%$ for RELA; and $133 \pm 6.44\%$ for NR1H3) (Fig. 5A–C).

KLF6 silencing, cyclodextrins, or RELA (NF- κ B) inhibition prevent 7K-induced up-regulation of Eng expression

Because of the increased expression of KLF6 after 12 h premedication with 7K in HAECs (Fig. 5A), we investigated further the role of KLF6 in 7K-induced Eng

expression. For this purpose, we used HAECs where the 7K-induced KLF6 mRNA increase was inhibited upon transfection with KLF6-specific siRNA (98.9 ± 2.99 vs. $128 \pm 6.43\%$, Fig. 6A). Parallel transfection experiments showed that siKLF6 mRNA was able to prevent 7K-mediated increase in both Eng mRNA (115 ± 2.96 vs. $139 \pm 5.80\%$, Fig. 6B) and Eng protein (107 ± 24.8 vs. $235 \pm 18.1\%$) levels (Fig. 6C, D).

In order to elucidate the role of LXR (NR1H3) in 7K-induced Eng expression, we used 2-hydroxypropyl- β -cyclodextrin, which was able to significantly abolish the

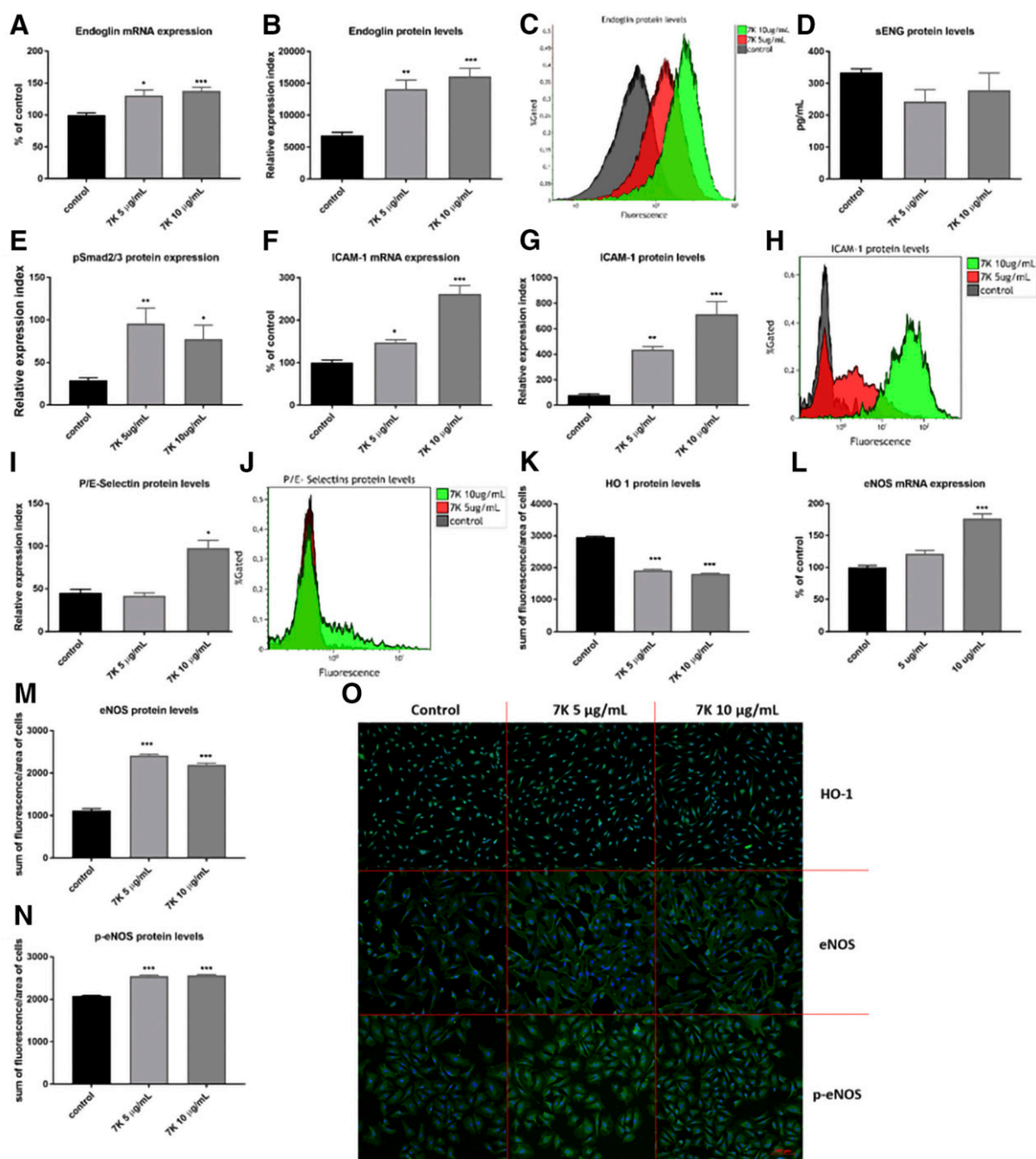


Figure 4. Effect of oxysterol on the expression of Eng, pSmad2/3, ICAM-1, P/E-selectins, HO-1, eNOS, and p-eNOS in HAECs. A) Untreated HAECs (control) and premedicated HAECs for 12 h with 5 or 10 µg/ml 7K were analyzed for mRNA and protein expression, as indicated. Eng mRNA expression. B, C) Eng protein levels. D) sENG protein levels. E–H) pSmad2/3 protein levels (E), ICAM-1 mRNA expression (F), protein levels (G, H). I, J) P/E-selectins protein levels. K–M) HO-1 protein levels (K), eNOS mRNA expression (L), and protein levels (M). N) p-eNOS protein levels. O) HO-1, eNOS, and p-eNOS protein levels were calculated from confocal microscopy photomicrographs as described in Materials and Methods. DAPI (blue): nuclei; Alexa Fluor 488 (green): HO-1/eNOS/p-eNOS, respectively. Scale bar, 100 µm. Data are shown as means ± SEM, ANOVA with Kruskal-Wallis test followed Dunn’s multiple comparisons test ($n = 5–208$ measurements from 3 independent cell stocks). * $P \leq 0.05$, ** $P \leq 0.01$, *** $P \leq 0.001$.

7K-induced gene expression of NR1H3 (LXR) (71.3 ± 2.07 vs. $129 \pm 6.22\%$, Fig. 6E). In the same set of experiments, we found that 2-hydroxypropyl-β-cyclodextrin significantly decreased Eng gene expression (116 ± 6.10 vs. $138 \pm 5.78\%$, Fig. 6F) and Eng protein levels (87.0 ± 4.80 vs. $235 \pm 18.1\%$, Fig. 6G, H) compared to the group premedicated

with 7K alone. Our results suggest that this cyclodextrin prevents 7K-induced increase in Eng expression.

RELA (NF-κB p65) is important for canonical pathway of inflammation (37) and production of HIF-1α (6, 7), which, in turn, regulates Eng expression (6). We interfered with RELA (NF-κB) expression by using the IκB

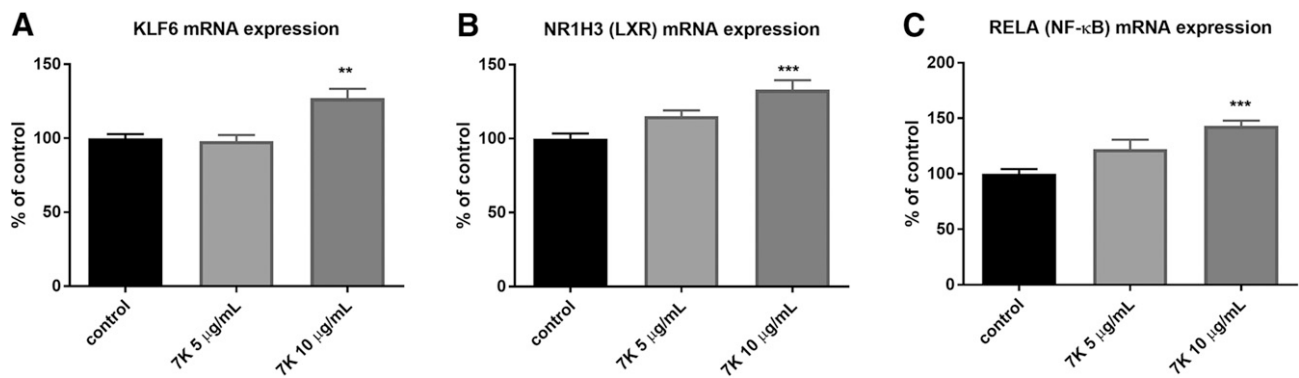


Figure 5. Effect of 7K on mRNA levels of transcription factors that regulate Eng expression. mRNA expression of KLF6 (A), NR1H3 (LXR) (B), and RELA (NF-κB) (C) in control group and groups premedicated for 12 h with 5 or 10 μg/ml 7K, as indicated. Data are shown as means ± SEM, ANOVA with Kruskal-Wallis test followed Dunn's multiple comparisons test ($n = 18-24$ measurements from 3 independent cell stocks). ** $P \leq 0.01$, *** $P \leq 0.001$.

kinase-2 inhibitor PHA-408, which decreases translocation of NF-κB to nucleus (38). We found that PHA-408 decreases 7K-induced mRNA expression of RELA (NF-κB) (88.9 ± 3.65 vs. $145 \pm 4.68\%$, Fig. 6I), as well as the 7K-induced increase in Eng mRNA expression (109 ± 6.12 vs. $138 \pm 5.79\%$, Fig. 6J) and protein levels (121 ± 9.02 vs. $235 \pm 18.1\%$) (Fig. 6K, L).

Eng is involved in 7K-induced adhesion and transmigration of THP-1 monocytes through HAECs monolayers

THP-1 was used to study the effect of 7K combined with Eng silencing on the cell permeability across the monolayer formed by HAECs in transwell inserts. Flow cytometry analysis was used to determine the number of adherent and transmigrated THP-1 cells through the endothelial monolayer, whereas inhibition of Eng expression in HAECs served to elucidate its role in adhesion and transmigration. Eng silencing with siRNA resulted in significant reduction of both mRNA (6.63 ± 0.14 and $6.12 \pm 0.37\%$ in the presence of 7K, compared to control; Fig. 7A) and protein (177 ± 7.76 and 168 ± 9.29 in the presence of 7K, compared to control 1705 ± 117 Fig. 7B, C) levels of Eng, and this reduction was not affected upon treatment with 7K. Adhesion studies showed that incubation with 7K increased the number of adherent THP-1 cells on endothelial monolayers ($136 \pm 6.79\%$ compared to control group), whereas silencing of Eng in HAECs led to a decreased number of adherent cells, both in the absence ($47.9 \pm 2.23\%$) or in the presence of 7K ($53.4 \pm 0.31\%$) (Fig. 7D). Similarly, incubation with 7K showed a markedly increased transmigration of THP-1 cells across HAECs ($242 \pm 15.0\%$), whereas Eng silencing significantly reduced the number of transmigrated cells both in the absence ($27.4 \pm 2.78\%$) or in the presence of 7K ($40.9 \pm 4.14\%$), suggesting an important role for membrane endothelial Eng in monocyte transmigration (Fig. 7E).

DISCUSSION

Changes of Eng expression in endothelium reflect potential pathologic conditions in the cardiovascular system.

Our previous papers suggest that hypercholesterolemia and progression of atherosclerosis are related to the reduced expression of Eng in mice aorta (19, 39). Moreover, it was demonstrated that membrane Eng/Smad2/3 signaling affects eNOS expression and stability (32), and reduced Eng expression results in impaired eNOS-dependent vasodilatation (9, 10). Recently, we showed that a combination of high soluble Eng levels and mild hypercholesterolemia results in aggravation of the vascular function in the aorta, with alterations of the Eng/Smad2/3/eNOS signaling (28). Taken together, we might propose that alteration in Eng expression is related to potential development or progression of endothelial dysfunction, suggesting that Eng acts as a protective agent in endothelium.

At variance with the vasoprotective role of Eng, Rossi *et al.* (11) showed a regulatory role for Eng in trans-endothelial leukocyte trafficking. These proinflammatory effects of Eng suggest that Eng could also have a proatherogenic role. However, it is of interest to mention that the *in vivo* experiments in the above-mentioned study were focused on Eng effects in the microcirculation. In addition, these experiments were performed in a short time frame (hours), which points out to acute experimental conditions. This is a completely different experimental setting when compared to those studies where the long-term effect of Eng is analyzed in the macrocirculation (*e.g.*, aorta and/or renal artery). In this study, we set 2 different biologic experiments to assess changes of Eng expression, regulation, and signaling with respect to endothelial and vascular dysfunction, both *in vivo* and *in vitro* under the cholesterol-hypercholesterolemia condition.

Nowadays, little is known about the possible relationship between Eng expression/signaling and endothelial/vascular dysfunction *in vivo* under hypercholesterolemia. Thus, we used young (2 mo old) ApoE^{-/-}/LDLR^{-/-} mice (23) without detectable atherogenic changes in the aorta in order to evaluate membrane Eng/Smad2/3/eNOS signaling with respect to the functional condition of the aorta. Our results showed that spontaneous hypercholesterolemia in ApoE^{-/-}/LDLR^{-/-} mice is accompanied by increased levels of the proinflammatory biomarker P-selectin, reduced urine and plasma concentration of

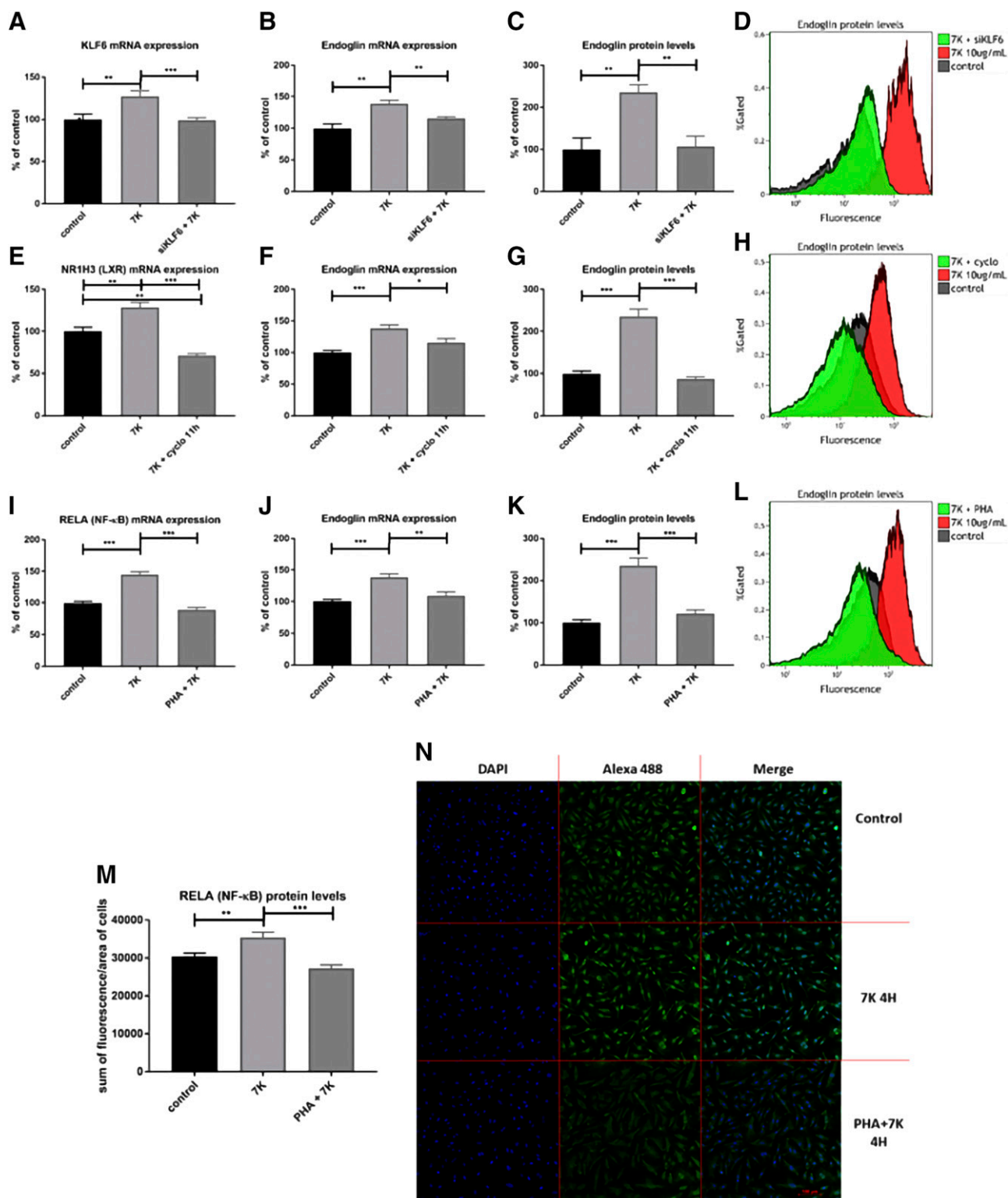


Figure 6. Effect of KLF6 silencing, cyclodextrins, or RELA (NF- κ B) inhibition on 7K-induced Eng expression in HAECs. Cells were untreated (control) or premedicated with 10 μ g/ml 7K for 12 h, as indicated. *A–D*) HAECs were transfected with siKLF6 mRNA prior to treatment with 7K, and expression of KLF6 mRNA (*A*), Eng mRNA (*B*), and Eng protein (*C, D*) was determined. *E–H*) HAECs were incubated with 10 mM 2-hydroxypropyl- β -cyclodextrin for 11 h prior to treatment with 7K, and expression of NR1H3 (LXR) mRNA (*E*), Eng mRNA (*F*), and Eng protein (*G, H*) was determined. *I–L*) HAECs were premedicated with 10 μ M PHA-408 for 10 min before addition of 7K, and expression of RELA (NF- κ B) mRNA (*I*), Eng mRNA (*J*), and Eng protein (*K, L*). *M, N*) RELA (NF- κ B) protein levels (*M*) were calculated from confocal microscopy photomicrographs (*N*) as described in Materials and Methods. DAPI (blue): nuclei; Alexa Fluor 488 (green): RELA (NF- κ B). Scale bar, 100 μ m. Data are shown as means \pm SEM, ANOVA followed by Bonferroni's multiple comparisons test ($n = 5$ –224 measurements from 3 independent cell stocks). * $P \leq 0.05$, ** $P \leq 0.01$, *** $P \leq 0.001$.

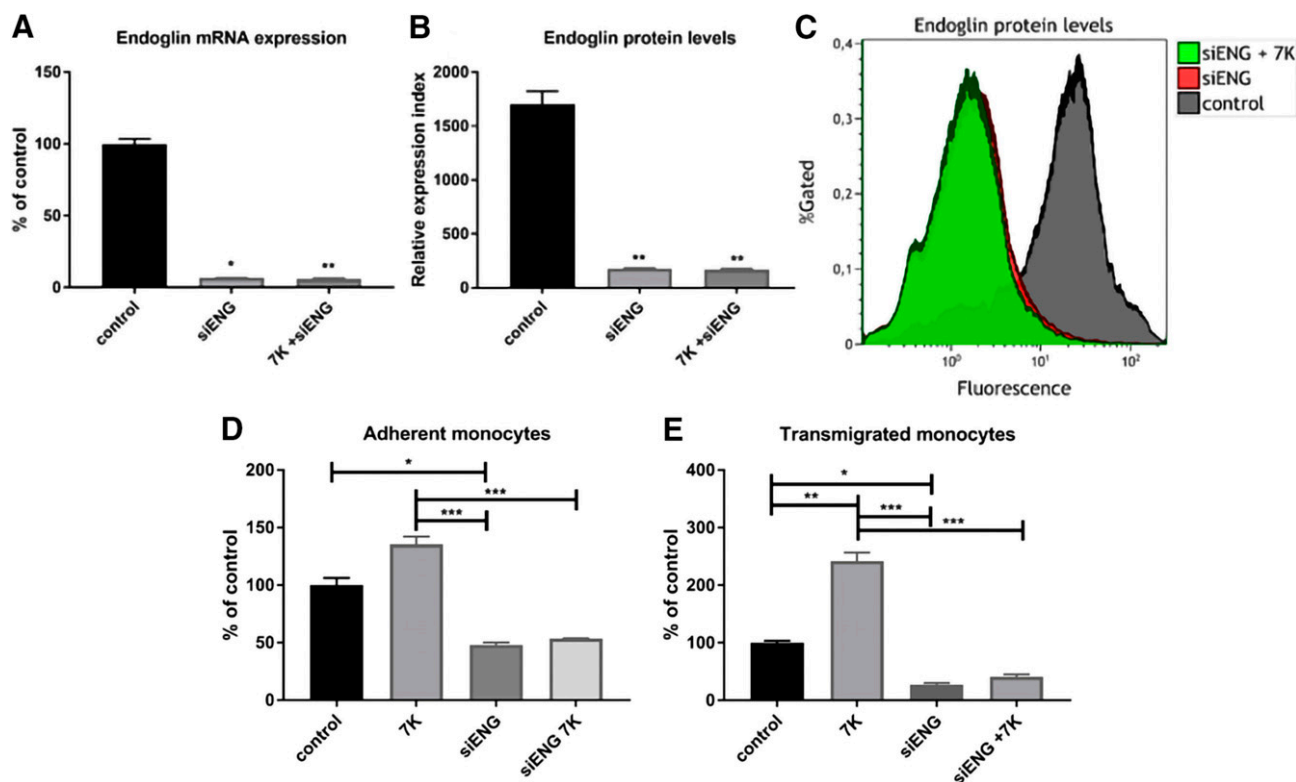


Figure 7. Effect of Eng silencing on adhesion and transmigration of THP-1 cells through HAECs monolayers. HAECs were transfected with Eng siRNAs or scRNA (control group) for 48 h and then premedicated with 10 $\mu\text{g}/\text{ml}$ of 7K for 12 h, as indicated. *A–C*) The expression of Eng mRNA (*A*) and Eng protein levels (*B*) was measured using flow cytometry (*C*). *D, E*) The number of adherent cells (*D*) was quantified using Kaluza software, and the number of transmigrated cells (*E*) was determined in 100 μl of culture media from the lower compartment of the transwell using flow cytometry. Data are shown as means \pm SEM, ANOVA with Kruskal-Wallis test followed Dunn's multiple comparisons test ($n = 6\text{--}12$ measurements from 3 independent cell stocks). * $P \leq 0.05$, ** $P \leq 0.01$, *** $P \leq 0.001$.

NO_3^- , and increased levels of sEng, suggesting the early development of endothelial dysfunction in these mice without detectable atherosclerosis.

High levels of sEng might be considered as a biomarker of early endothelial/vascular dysfunction/alteration and vascular damage in many cardiovascular disorders in clinical conditions. It was shown that sEng is generated by the cleavage from membrane-bound Eng by MMP-14, which was proposed to be the major Eng-shedding protease (3). Surprisingly, we found significantly reduced expression of MMP-14 in aortas of ApoE $^{-/-}$ /LDLR $^{-/-}$ mice, suggesting that MMP-14 is unlikely to be responsible for the cleavage of membrane Eng in the aortas in

these mice. Indeed, similar results were also shown by Brownfoot *et al.* (40), suggesting that other matrix metalloproteinases could be involved in the cleavage of membrane Eng. Moreover, it is unlikely that changes of sEng levels reflect changes of membrane Eng expression in only 1 vessel type (*e.g.*, the aorta). Instead, we propose that sEng is released from the whole vasculature in cardiovascular diseases. Indeed, we have demonstrated that hypercholesterolemia reduces membrane (aortic) Eng but increases the levels of circulating Eng (19). In addition, membrane Eng/Smad2/3/eNOS signaling was related to vascular reactivity and NO-dependent vasodilation (9, 10). We showed that membrane Eng/Smad2/3/eNOS

TABLE 1. Primary and secondary antibodies used for Western blot analysis

Mouse protein	Source	Catalog no.	Dilution	Secondary antibody dilution
Eng	Santa Cruz Biotechnology	sc-19793	1:200	1:5000
eNOS	Santa Cruz Biotechnology	sc-654	1:200	1:2000
GAPDH	MilliporeSigma	G8795	1:10,000	1:20,000
HO-1	Abcam	ab13243	1:2000	1:1000
MMP-14	Abcam	ab51074	1:2000	1:1000
p-eNOS Ser1177	Santa Cruz Biotechnology	sc-21871-R	1:500	1:2000
pMLC Thr18/Ser19	Cell Signaling Technology	3674	1:1000	1:2000
pSmad2/3	Cell Signaling Technology	88280	1:1000	1:2000

is altered and related to aggravation of endothelial dysfunction in mice exposed to high levels of sEng and mild hypercholesterolemia (28). Indeed, expression of membrane Eng, pSmad2/3, eNOS, and p-eNOS Ser1177 was reduced in hypercholesterolemic ApoE^{-/-}/LDLR^{-/-} mice when compared with normocholesterolemic mice in this paper. Noteworthy, reduced NO₃⁻ levels, as a stable end product of NO metabolism, is a hallmark of endothelial dysfunction (41, 42). In line with this, we observed a reduced expression of HO-1 in ApoE^{-/-}/LDLR^{-/-} mice aorta, which is involved in a vasodilatory mechanism based on an interaction with soluble guanylate cyclase and a subsequent release of NO (34). Taken together, these data suggest a lower production of NO in ApoE^{-/-}/LDLR^{-/-} mice when compared to control normocholesterolemic mice when Eng signaling is compromised.

In order to elucidate functional consequences of these changes, we evaluated vascular reactivity of aortic rings by wire myograph. The results showed no changes in Ach-induced relaxation but demonstrated reduced relaxation induced by SNP and increased relaxation response in ApoE^{-/-}/LDLR^{-/-} mice after L-NAME, suggesting an altered vascular function in these hypercholesterolemic mice. The response to L-NAME probably reflects an ongoing compensatory mechanism (generating NO) to maintain the physiologic relaxation in the aortas of ApoE^{-/-}/LDLR^{-/-} mice. We also observed a reduced expression of pMLC Thr18/Ser19 that is considered a major regulatory component in smooth muscle reactivity (43). Taken together, hypercholesterolemic mice have altered Eng expression and signaling in the aorta and reduced NO levels accompanied by alteration of vascular function in the aorta. Thus, we postulate that the reduced Eng levels are related to vascular dysfunction in the aorta prior to the formation of atherosclerotic lesion, suggesting an important role for Eng in cholesterol-induced endothelial/vascular dysfunction.

In the second part of the study, we aimed to elucidate Eng regulation/expression in endothelial cells *in vitro* when simulating hypercholesterolemia by 7K treatment. We were curious to know whether Eng is similarly regulated as *in vivo* in "atherogenesis/endothelial dysfunction" experiments.

Increased concentrations of oxLDL represent a major risk factor for the development of atherosclerosis (44, 45). Among the different oxysterols present in oxLDL, 7K has been shown to be more abundant in the circulation of patients with hypercholesterolemia (14) and in atherosclerotic lesions than any other oxysterol species (46). In addition, 7K potentiates inflammation (16) and foam cell formation (17), decreases eNOS activity, and impairs NO bioavailability in endothelium (47). Therefore, 7K was used to mimic hypercholesterolemic and proatherogenic condition of oxLDL in our *in vitro* experimental settings. Our results showed that 7K increased the expression of Eng (opposite to hypercholesterolemia in *in vivo* experiments), as well as biomarkers of endothelial dysfunction and inflammation ICAM-1 and P/E selectins in HAECs. These findings are in agreement with the active role of oxysterols in inflammatory diseases (48) and with the upregulated expression of Eng upon treatment with

22(R)-hydroxycholesterol and LXR agonists (36, 49). In addition, we demonstrated that the Eng/pSmad2/3/eNOS/p-eNOS-signaling cascade is activated in HAECs by 7K. These above results on Eng signaling suggest a completely opposite effect of cholesterol exposure *in vivo* and *in vitro*.

Moreover, 7K was able to increase the expression of transcription factors regulating Eng expression in our study, including KLF6 (4, 35), LXR (NR1H3) (49), and RELA (NFκB) (6, 7). Because 7K was able to up-regulate these 3 pathways responsible for regulating Eng expression, we aimed to evaluate whether they were also involved in the regulation of Eng expression under 7K exposure.

KLF6 is well known for its role in regulating Eng expression (4, 35), and we have shown that the silencing of KLF6 prevents 7K-mediated increase in both Eng mRNA and protein levels. Interestingly, cotransfection of RAW264.7 cells with KLF6 and NF-κB p65 showed an enhanced inflammatory reaction of cells after LPS treatment, suggesting an interplay between KLF6 and NF-κB p65 in inflammatory settings (50, 51). Of note, RELA (NF-κB p65) is key for the canonical pathway of inflammation (37) and production of HIF-1α (6, 7). In turn, HIF-1α, in combination with Sp1 and Smad3, is able to induce Eng expression (6), suggesting that an activation of RELA mRNA expression is indirectly responsible for the 7K-mediated increase in Eng mRNA expression and Eng protein levels observed in this study. Supporting this view, we interfered with RELA expression using the IκB kinase-2 inhibitor PHA-408 (38), leading to a decreased translocation of NF-κB to the nucleus and preventing the 7K-induced increase in Eng mRNA expression and Eng protein levels as well.

The oxysterol receptor LXR is able to bind LXR response elements in the Eng promoter and mediate the activation of Eng gene expression (36). To affect LXR mRNA expression, we used 2-hydroxypropyl-β-cyclodextrin. Cyclodextrins are known to extract cholesterol from cells (52) and increase activity of LXR in a time-dependent fashion; thus, they are able to increase LXR mRNA expression a few minutes or hours after administration (53). In our study, treatment with 2-hydroxypropyl-β-cyclodextrin for 11 h decreased LXR activity (52) and prevented 7K-induced increase in Eng expression. It is of interest to mention that cyclodextrin also disrupts caveolae on the cell surface of endothelial cells, and it is well known that Eng is present in caveolae (9), so the inhibitory effect on Eng expression could also be due to depletion of Eng-containing caveolae. Taken together, our results show that Eng expression in HAECs is regulated by 3 transcription factors (KLF6, NF-κB, and LXR) and that inhibition of each of these factors results in the prevention of 7K-induced Eng expression.

What are the functional consequences of changes in Eng expression with respect to potential atherogenesis? Transmigration of monocytes is one of the first steps in the development of endothelial dysfunction. Monocytes show hypercholesterolemia-associated trafficking through the endothelial monolayer, subendothelial accumulation, and differentiation, which results in formation of foam cells

(54–56); later, they participate in the progression of atherosclerosis. Therefore, we tried to evaluate a possible link between 7K-induced Eng expression and the adhesion/transmigration of monocytes across the HAECs monolayer. We showed that 7K-induced expression of Eng was accompanied by increased adhesion and transmigration of monocytes, whereas inhibition of Eng expression prevented the 7K-induced adhesion and transmigration. These data suggest that Eng plays a relevant role in oxysterol-induced trafficking of monocytes through the endothelial monolayer *in vitro*. This interpretation agrees with the reported role for Eng in integrin-mediated leukocyte adhesion and extravasation induced by inflammation (11).

Our current study shows differences in Eng expression after cholesterol exposure *in vivo* in aorta and *in vitro* in aortic endothelial cells. Several explanations may account for these apparent discrepancies. First, Eng is a part of TGF- β -signaling pathway, and it has been demonstrated that the role of TGF- β varies during atherogenesis. Thus, TGF- β is proatherogenic in the early phase (57) but antiatherogenic at later stages (58). In other words, Eng expression may vary during the different stages of atherogenic process and endothelial dysfunction as well. Second, *in vitro* experiments analyze changes of Eng expression and its consequences within hours, whereas *in vivo* experiments are carried out in 2-mo-old animals. This discrepancy deserves further investigation, especially focusing on timeline changes of Eng expression and functional consequences during the atherogenic process. Third, the animal model used in this study is deficient in LDL receptors; therefore, the uptake of cholesterol and oxysterols might be inhibited, and so it is the LXR intracellular pathway that triggers Eng expression. This point deserves further investigation as well. Moreover, not all the oxysterol types behave the same, and it is difficult to compare this *in vitro* result with the *in vivo* result with hypercholesterolemic mice. *In vivo*, a variety of oxysterol species are present, and they may act in concert or even in synergy, leading to a different outcome than the one induced by a single oxysterol species. Finally, the other significant difference between our *in vitro* and *in vivo* experiments is that LDL cholesterol in mice contains not only cholesterol but also apolipoprotein B 100-containing particles. Interestingly, several studies indicated that apolipoprotein B 100 seems to be at least a cofactor in endothelial dysfunction development besides cholesterol (59, 60), suggesting that the presence of complex lipoproteins in *in vivo* experiments might be responsible as well for different findings when compared to *in vitro* results. Thus, we will also focus on apoB effects on HAECs in our prospective experiments.

There are possible limitations in this study. First, we cannot confirm our *in vivo* results about the role of Eng in the development of endothelial or vascular dysfunction by using Eng knockout mice because these mice die *in utero* (61), and, to the best of our knowledge, no hypercholesterolemic Eng knockout animal model is available. The second potential limitation is related to our *in vitro* experiments. It is not feasible to use general oxLDL (that would mimic hypercholesterolemic conditions from our

mice experiments) in our *in vitro* experiments. Particles of oxLDL include different amounts of phospholipids, sphingolipids, free fatty acids, oxysterols, cholesteryl esters, apolipoproteins, and other biologically active compounds affecting the vascular cell wall. However, it is not possible to carry out *in vitro* experiments with these oxLDL particles due to their instability, autooxidation, aggregation, and fusion, among others (14). Thus, 7K, the most abundant oxysterol of oxLDL (62), was used in our *in vitro* experiments.

CONCLUSIONS

We showed for the first time that hypercholesterolemia altered Eng expression and signaling, followed by endothelial or vascular dysfunction before the formation of atherosclerotic lesions in ApoE^{-/-}/LDLR^{-/-} mice. By contrast, 7K increased Eng expression and induced inflammation in cultured HAECs, which was followed by an increase in adhesion and transmigration of monocytes *via* endothelium, that was prevented by Eng inhibition. Thus, we propose a relevant role for Eng in endothelial/vascular dysfunction/inflammation when exposed to cholesterol. Nevertheless, due to discrepancies between *in vivo* and *in vitro* results, we propose to be cautious when interpreting data about the role of Eng in endothelial/vascular dysfunction/inflammation from “acute” *in vitro* experiments or microcirculation studies when compared to long-term experiments in large atherosclerosis-prone blood vessels. FJ

ACKNOWLEDGMENTS

The authors thank Dr. Alena Mrkvicová and Milena Hajzlerová (both from the Department of Medical Biochemistry, Faculty of Medicine in Hradec Kralove, Charles University, Hradec Kralove, Czech Republic) for assistance during PCR analysis, Dr. Veronika Skarková (Department of Medical Biology and Genetics, Faculty of Medicine in Hradec Kralove, Charles University) for assistance during Elisa analysis and preparation of samples for Western blots, Drs. Soňa Cejková (Institute of Clinical and Experimental Medicine, Prague, Czech Republic) and Feroz Ahmad (Department of Biomedical Sciences, University of Reading, Reading, United Kingdom) for help with the human acute monocytic leukemia cell line, Dr. Petra Hiršová (Liver Pathobiology Laboratory, Mayo Clinic, Rochester, Minnesota) for information about immunocytochemistry, Dr. Hana Jansová (Department of Biochemical Sciences, Faculty of Pharmacy in Hradec Kralove, Charles University) for help with preparation of substances for cell treatments, Dr. Věra Králová (Department of Medical Biology and Genetics, Faculty of Medicine in Hradec Kralove, Charles University) for help with flow cytometry, and Pavlína Lukešová (Department of Biological and Medical Sciences, Faculty of Pharmacy in Hradec Kralove, Charles University) for help during chamber slide preparation. This work was supported by Project Efficiency and Safety Improvement of Current Drugs and Nutraceuticals: Advanced Methods–New Challenges (EFSA–CDN; CZ.02.1.01/0.0/0.0/16_019/0000841) cofunded by the European Regional Development Fund (ERDF), grants of Charles University Grant Agency (GAUK 1158413C and 1216217), Specific University Research (SVV260414), and Czech Health Research Council (AZV CR

17-31754A). C.B. was supported by grants from Consejo Superior de Investigaciones Científicas (201420E039) and Centro de Investigación Biomedica en Red de Enfermedades Raras (CIBERER; ISCIII-CB06/07/0038). CIBERER is an initiative of the Instituto de Salud Carlos III (ISCIII) of Spain supported by Fonds Européen de Développement Économique et Régional (FEDER) funds. The authors declare no conflicts of interest.

AUTHOR CONTRIBUTIONS

M. Vicen, B. Vitverova, and P. Nachtigal designed research and analyzed data; M. Vicen, B. Vitverova, R. Havelek, K. Blazickova, and M. Machacek performed research; and all authors wrote the manuscript.

REFERENCES

- Nachtigal, P., Zemankova Vecerova, L., Rathouska, J., and Strasky, Z. (2012) The role of endoglin in atherosclerosis. *Atherosclerosis* **224**, 4–11
- Venkatesha, S., Toporsian, M., Lam, C., Hanai, J., Mammoto, T., Kim, Y. M., Bdelah, Y., Lim, K. H., Yuan, H. T., Libermann, T. A., Stillman, I. E., Roberts, D., D'Amore, P. A., Epstein, F. H., Sellke, F. W., Romero, R., Sukhatme, V. P., Letarte, M., and Karumanchi, S. A. (2006) Soluble endoglin contributes to the pathogenesis of preeclampsia. *Nat. Med.* **12**, 642–649; erratum: 862
- Hawinkels, L. J., Kuiper, P., Wiercinska, E., Verspaget, H. W., Liu, Z., Pardali, E., Sier, C. F., and ten Dijke, P. (2010) Matrix metalloproteinase-14 (MT1-MMP)-mediated endoglin shedding inhibits tumor angiogenesis. *Cancer Res.* **70**, 4141–4150
- Botella, L. M., Sánchez-Elsner, T., Sanz-Rodríguez, F., Kojima, S., Shimada, J., Guerrero-Esteo, M., Cooremans, M. P., Ratziu, V., Langa, C., Vary, C. P., Ramirez, J. R., Friedman, S., and Bernabéu, C. (2002) Transcriptional activation of endoglin and transforming growth factor-beta signaling components by cooperative interaction between Sp1 and KLF6: their potential role in the response to vascular injury. *Blood* **100**, 4001–4010
- Ollauri-Ibáñez, C., López-Novoa, J. M., and Pericacho, M. (2017) Endoglin-based biological therapy in the treatment of angiogenesis-dependent pathologies. *Expert Opin. Biol. Ther.* **17**, 1053–1063
- Sánchez-Elsner, T., Botella, L. M., Velasco, B., Langa, C., and Bernabéu, C. (2002) Endoglin expression is regulated by transcriptional cooperation between the hypoxia and transforming growth factor-beta pathways. *J. Biol. Chem.* **277**, 43799–43808
- Van Uden, P., Kenneth, N. S., and Rocha, S. (2008) Regulation of hypoxia-inducible factor-1alpha by NF-kappaB. *Biochem. J.* **412**, 477–484
- Valbuena-Diez, A. C., Blanco, F. J., Oujo, B., Langa, C., Gonzalez-Núñez, M., Llano, E., Pendas, A. M., Díaz, M., Castrillo, A., Lopez-Novoa, J. M., and Bernabeu, C. (2012) Oxysterol-induced soluble endoglin release and its involvement in hypertension. *Circulation* **126**, 2612–2624
- Toporsian, M., Gros, R., Kabir, M. G., Vera, S., Govindaraju, K., Eidelman, D. H., Husain, M., and Letarte, M. (2005) A role for endoglin in coupling eNOS activity and regulating vascular tone revealed in hereditary hemorrhagic telangiectasia. *Circ. Res.* **96**, 684–692
- Jerkic, M., Rivas-Elena, J. V., Prieto, M., Carrón, R., Sanz-Rodríguez, F., Pérez-Barriocanal, F., Rodríguez-Barbero, A., Bernabéu, C., and López-Novoa, J. M. (2004) Endoglin regulates nitric oxide-dependent vasodilatation. *FASEB J.* **18**, 609–611
- Rossi, E., Sanz-Rodríguez, F., Eleno, N., Düwell, A., Blanco, F. J., Langa, C., Botella, L. M., Cabañas, C., Lopez-Novoa, J. M., and Bernabeu, C. (2013) Endothelial endoglin is involved in inflammation: role in leukocyte adhesion and transmigration. *Blood* **121**, 403–415
- Rossi, E., Pericacho, M., Bachelot-Loza, C., Pidard, D., Gaussem, P., Poirault-Chassac, S., Blanco, F. J., Langa, C., González-Manchón, C., Novoa, J. M. L., Smadja, D. M., and Bernabeu, C. (2018) Human endoglin as a potential new partner involved in platelet-endothelium interactions. *Cell. Mol. Life Sci.* **75**, 1269–1284
- Steinberg, D. (2002) Atherogenesis in perspective: hypercholesterolemia and inflammation as partners in crime. *Nat. Med.* **8**, 1211–1217
- Levitan, I., Volkov, S., and Subbiah, P. V. (2010) Oxidized LDL: diversity, patterns of recognition, and pathophysiology. *Antioxid. Redox Signal.* **13**, 39–75
- Chalubinski, M., Zemanek, K., Skowron, W., Wojdan, K., Gorzelak, P., and Broncel, M. (2013) The effect of 7-ketocholesterol and 25-hydroxycholesterol on the integrity of the human aortic endothelial and intestinal epithelial barriers. *Inflamm. Res.* **62**, 1015–1023
- Olkkonen, V. M., Béaslas, O., and Nissilä, E. (2012) Oxysterols and their cellular effectors. *Biomolecules* **2**, 76–103
- Hayden, J. M., Brachova, L., Higgins, K., Obermiller, L., Sevanian, A., Khandrika, S., and Reaven, P. D. (2002) Induction of monocyte differentiation and foam cell formation in vitro by 7-ketocholesterol. *J. Lipid Res.* **43**, 26–35
- Rathouska, J., Jezkova, K., Nemeckova, I., and Nachtigal, P. (2015) Soluble endoglin, hypercholesterolemia and endothelial dysfunction. *Atherosclerosis* **243**, 383–388
- Strasky, Z., Vecerova, L., Rathouska, J., Slanarova, M., Brcakova, E., Kudlackova, Z., Andrys, C., Micuda, S., and Nachtigal, P. (2011) Cholesterol effects on endoglin and its downstream pathways in ApoE/LDLR double knockout mice. *Circ. J.* **75**, 1747–1755
- Zemankova, L., Varejckova, M., Dolezalova, E., Fikrova, P., Jezkova, K., Rathouska, J., Cervený, L., Botella, L. M., Bernabeu, C., Nemeckova, I., and Nachtigal, P. (2015) Atorvastatin-induced endothelial nitric oxide synthase expression in endothelial cells is mediated by endoglin. *J. Physiol. Pharmacol.* **66**, 403–413
- Ruiz-Remolina, L., Ollauri-Ibáñez, C., Pérez-Roque, L., Núñez-Gómez, E., Pérez-Barriocanal, F., López-Novoa, J. M., Pericacho, M., and Rodríguez-Barbero, A. (2017) Circulating soluble endoglin modifies the inflammatory response in mice. *PLoS One* **12**, e0188204
- Ishibashi, S., Herz, J., Maeda, N., Goldstein, J. L., and Brown, M. S. (1994) The two-receptor model of lipoprotein clearance: tests of the hypothesis in “knockout” mice lacking the low density lipoprotein receptor, apolipoprotein E, or both proteins. *Proc. Natl. Acad. Sci. USA* **91**, 4431–4435
- Csányi, G., Gajda, M., Franczyk-Zarow, M., Kostogryz, R., Gwoźdź, P., Mateuszuk, L., Sternak, M., Wojcik, L., Zalewska, T., Walski, M., and Chlopicki, S. (2012) Functional alterations in endothelial NO, PGI₂ and EDHF pathways in aorta in ApoE/LDLR^{-/-} mice. *Prostaglandins Other Lipid Mediat.* **98**, 107–115
- Jawien, J., Csanyi, G., Gajda, M., Mateuszuk, L., Lomnicka, M., Korbut, R., and Chlopicki, S. (2007) Ticlopidine attenuates progression of atherosclerosis in apolipoprotein E and low density lipoprotein receptor double knockout mice. *Eur. J. Pharmacol.* **556**, 129–135
- Yamagata, K., Tanaka, N., and Suzuki, K. (2013) Epigallocatechin 3-gallate inhibits 7-ketocholesterol-induced monocyte-endothelial cell adhesion. *Microvasc. Res.* **88**, 25–31
- Kij, A., Mateuszuk, L., Sitek, B., Przyborowski, K., Zakrzewska, A., Wandzel, K., Walczak, M., and Chlopicki, S. (2016) Simultaneous quantification of PGI₂ and TXA₂ metabolites in plasma and urine in NO-deficient mice by a novel UHPLC/MS/MS method. *J. Pharm. Biomed. Anal.* **129**, 148–154
- Przyborowski, K., Wojewoda, M., Sitek, B., Zakrzewska, A., Kij, A., Wandzel, K., Zoladz, J. A., and Chlopicki, S. (2015) Effects of 1-methylnicotinamide (MNA) on exercise capacity and endothelial response in diabetic mice. *PLoS One* **10**, e0130908
- Vitverova, B., Blazickova, K., Najmanova, I., Vicen, M., Hyšpler, R., Dolezelova, E., Nemeckova, I., Tebbens, J. D., Bernabeu, C., Pericacho, M., and Nachtigal, P. (2018) Soluble endoglin and hypercholesterolemia aggravate endothelial and vessel wall dysfunction in mouse aorta. *Atherosclerosis* **271**, 15–25
- Nemeckova, I., Serwaczak, A., Oujo, B., Jezkova, K., Rathouska, J., Fikrova, P., Varejckova, M., Bernabeu, C., Lopez-Novoa, J. M., Chlopicki, S., and Nachtigal, P. (2015) High soluble endoglin levels do not induce endothelial dysfunction in mouse aorta. *PLoS One* **10**, e0119665
- Puig-Kröger, A., Rellosa, M., Fernández-Capetillo, O., Zubiaga, A., Silva, A., Bernabéu, C., and Corbí, A. L. (2001) Extracellular signal-regulated protein kinase signaling pathway negatively regulates the phenotypic and functional maturation of monocyte-derived human dendritic cells. *Blood* **98**, 2175–2182
- Dopico, A. M., Bukiya, A. N., and Jaggar, J. H. (2018) Calcium- and voltage-gated BK channels in vascular smooth muscle. *Pflügers Arch.* **470**, 1271–1289
- Santibañez, J. F., Letamendia, A., Perez-Barriocanal, F., Silvestri, C., Saura, M., Vary, C. P., Lopez-Novoa, J. M., Attisano, L., and Bernabeu, C.

- (2007) Endoglin increases eNOS expression by modulating Smad2 protein levels and Smad2-dependent TGF-beta signaling. *J. Cell. Physiol.* **210**, 456–468
33. Kaitu'u-Lino, T. J., Palmer, K. R., Whitehead, C. L., Williams, E., Lappas, M., and Tong, S. (2012) MMP-14 is expressed in preeclamptic placentas and mediates release of soluble endoglin. *Am. J. Pathol.* **180**, 888–894
 34. Kaczara, P., Proniewski, B., Lovejoy, C., Kus, K., Motterlini, R., Abramov, A. Y., and Chlopicki, S. (2018) CORM-401 induces calcium signalling, NO increase and activation of pentose phosphate pathway in endothelial cells. *FEBS J.* **285**, 1346–1358
 35. Gallardo-Vara, E., Blanco, F. J., Roqué, M., Friedman, S. L., Suzuki, T., Botella, L. M., and Bernabeu, C. (2016) Transcription factor KLF6 upregulates expression of metalloprotease MMP14 and subsequent release of soluble endoglin during vascular injury. *Angiogenesis* **19**, 155–171
 36. Henry-Berger, J., Mouzat, K., Baron, S., Bernabeu, C., Marceau, G., Saru, J. P., Sapin, V., Lobaccaro, J. M., and Caira, F. (2008) Endoglin (CD105) expression is regulated by the liver X receptor alpha (NR1H3) in human trophoblast cell line JAR. *Biol. Reprod.* **78**, 968–975
 37. Lawrence, T. (2009) The nuclear factor NF-kappaB pathway in inflammation. *Cold Spring Harb. Perspect. Biol.* **1**, a001651
 38. Mbalaviele, G., Sommers, C. D., Bonar, S. L., Mathialagan, S., Schindler, J. F., Guzova, J. A., Shaffer, A. F., Melton, M. A., Christine, L. J., Tripp, C. S., Chiang, P. C., Thompson, D. C., Hu, Y., and Kishore, N. (2009) A novel, highly selective, tight binding IkappaB kinase-2 (IKK-2) inhibitor: a tool to correlate IKK-2 activity to the fate and functions of the components of the nuclear factor-kappaB pathway in arthritis-relevant cells and animal models. *J. Pharmacol. Exp. Ther.* **329**, 14–25
 39. Vecerova, L., Strasky, Z., Rathouska, J., Slanarova, M., Brcakova, E., Micuda, S., and Nachtigal, P. (2012) Activation of TGF-beta receptors and Smad proteins by atorvastatin is related to reduced atherogenesis in ApoE/LDLR double knockout mice. *J. Atheroscler. Thromb.* **19**, 115–126
 40. Brownfoot, F. C., Hannan, N., Onda, K., Tong, S., and Kaitu'u-Lino, T. (2014) Soluble endoglin production is upregulated by oxysterols but not quenched by pravastatin in primary placental and endothelial cells. *Placenta* **35**, 724–731
 41. Heitzer, T., Schlinzig, T., Krohn, K., Meinertz, T., and Münzel, T. (2001) Endothelial dysfunction, oxidative stress, and risk of cardiovascular events in patients with coronary artery disease. *Circulation* **104**, 2673–2678
 42. Kleinbongard, P., Dejam, A., Lauer, T., Jax, T., Kerber, S., Gharini, P., Balzer, J., Zotz, R. B., Scharf, R. E., Willers, R., Schechter, A. N., Feelisch, M., and Kelm, M. (2006) Plasma nitrite concentrations reflect the degree of endothelial dysfunction in humans. *Free Radic. Biol. Med.* **40**, 295–302
 43. Somlyo, A. P., and Somlyo, A. V. (1994) Signal transduction and regulation in smooth muscle. *Nature* **372**, 231–236; erratum: 812
 44. Friedman, A., and Hao, W. (2015) A mathematical model of atherosclerosis with reverse cholesterol transport and associated risk factors. *Bull. Math. Biol.* **77**, 758–781
 45. Mitra, S., Goyal, T., and Mehta, J. L. (2011) Oxidized LDL, LOX-1 and atherosclerosis. *Cardiovasc. Drugs Ther.* **25**, 419–429
 46. Vaya, J., Aviram, M., Mahmood, S., Hayek, T., Grenadir, E., Hoffman, A., and Milo, S. (2001) Selective distribution of oxysterols in atherosclerotic lesions and human plasma lipoproteins. *Free Radic. Res.* **34**, 485–497
 47. Deckert, V., Perségol, L., Viens, L., Lizard, G., Athias, A., Lallemand, C., Gambert, P., and Lagrost, L. (1997) Inhibitors of arterial relaxation among components of human oxidized low-density lipoproteins. Cholesterol derivatives oxidized in position 7 are potent inhibitors of endothelium-dependent relaxation. *Circulation* **95**, 723–731
 48. Testa, G., Rossin, D., Poli, G., Biasi, F., and Leonarduzzi, G. (2018) Implication of oxysterols in chronic inflammatory human diseases. *Biochimie* **153**, 220–231
 49. Valbuena-Diez, A. C., Blanco, F. J., Oujo, B., Langa, C., Gonzalez-Núñez, M., Llano, E., Pendas, A. M., Díaz, M., Castrillo, A., Lopez-Novoa, J. M., and Bernabeu, C. (2012) Oxysterol-induced soluble endoglin release and its involvement in hypertension. *Circulation* **126**, 2612–2624
 50. Date, D., Das, R., Narla, G., Simon, D. I., Jain, M. K., and Mahabeleshwar, G. H. (2014) Kruppel-like transcription factor 6 regulates inflammatory macrophage polarization. *J. Biol. Chem.* **289**, 10318–10329
 51. Zhang, Y., Lei, C. Q., Hu, Y. H., Xia, T., Li, M., Zhong, B., and Shu, H. B. (2014) Kruppel-like factor 6 is a co-activator of NF-kB that mediates p65-dependent transcription of selected downstream genes. *J. Biol. Chem.* **289**, 12876–12885
 52. Coisne, C., Hallier-Vanuxeem, D., Boucau, M. C., Hachani, J., Tilloy, S., Bricout, H., Monflier, E., Wils, D., Serpelloni, M., Parissaux, X., Fenart, L., and Gosselet, F. (2016) beta-Cyclodextrins decrease cholesterol release and ABC-associated transporter expression in smooth muscle cells and aortic endothelial cells. *Front. Physiol.* **7**, 185
 53. Coisne, C., Tilloy, S., Monflier, E., Wils, D., Fenart, L., and Gosselet, F. (2016) Cyclodextrins as emerging therapeutic tools in the treatment of cholesterol-associated vascular and neurodegenerative diseases. *Molecules* **21**, e1748
 54. Carman, C. V. (2008) Teasing out monocyte trafficking mechanisms. *Blood* **112**, 929–930
 55. Mestas, J., and Ley, K. (2008) Monocyte-endothelial cell interactions in the development of atherosclerosis. *Trends Cardiovasc. Med.* **18**, 228–232
 56. Woollard, K. J., and Geissmann, F. (2010) Monocytes in atherosclerosis: subsets and functions. *Nat. Rev. Cardiol.* **7**, 77–86
 57. Majesky, M. W., Lindner, V., Twardzik, D. R., Schwartz, S. M., and Reidy, M. A. (1991) Production of transforming growth factor beta 1 during repair of arterial injury. *J. Clin. Invest.* **88**, 904–910
 58. Gojova, A., Brun, V., Esposito, B., Cottrez, F., Gourdy, P., Ardouin, P., Tedgui, A., Mallat, Z., and Groux, H. (2003) Specific abrogation of transforming growth factor-beta signaling in T cells alters atherosclerotic lesion size and composition in mice. *Blood* **102**, 4052–4058
 59. Yu, Q., Zhang, Y., and Xu, C. B. (2015) Apolipoprotein B, the villain in the drama? *Eur. J. Pharmacol.* **748**, 166–169
 60. Zhang, Y., Zhang, W., Edvinsson, L., and Xu, C. B. (2014) Apolipoprotein B of low-density lipoprotein impairs nitric oxide-mediated endothelium-dependent relaxation in rat mesenteric arteries. *Eur. J. Pharmacol.* **725**, 10–17
 61. Van Laake, L. W., van den Driesche, S., Post, S., Feijen, A., Jansen, M. A., Driessens, M. H., Mager, J. J., Snijder, R. J., Westermann, C. J., Doevendans, P. A., van Echteld, C. J., ten Dijke, P., Arthur, H. M., Goumans, M. J., Lebrin, F., and Mummery, C. L. (2006) Endoglin has a crucial role in blood cell-mediated vascular repair. *Circulation* **114**, 2288–2297
 62. Brown, A. J., Mander, E. L., Gelissen, I. C., Kritharides, L., Dean, R. T., and Jessup, W. (2000) Cholesterol and oxysterol metabolism and subcellular distribution in macrophage foam cells. Accumulation of oxidized esters in lysosomes. *J. Lipid Res.* **41**, 226–237

Received for publication October 18, 2018.
Accepted for publication January 15, 2019.